NASA TECHNICAL MEMORANDUM

PRESSURE LOSSES AND HEAT TRANSFER
IN NON-CIRCULAR CHANNELS WITH HYDRAULICALLY SMOOTH WALLS

J. Malak

NATIONAL AERONAUTICS AND SPACE ADMINISTRATION
WASHINGTON, D.C. 20546   FEBRUARY 1982

| 1. Report No.
NASA TM-76670	2. Government Accession No.	3. Recipient's Catalog No.
4. Title and Subtitle PRESSURE LOSSES AND HEAT TRANSFER IN NON-CIRCULAR CHANNELS WITH HYDRAULICALLY SMOOTH WALLS		5. Report Date
February 1982
		6. Performing Organization Code
7. Author(s)
J. Malak		8. Performing Organization Report No.
		10. Work Unit No.
9. Performing Organization Name and Address
Leo Kanner Associates,
Redwood City, California 94063 | | 11. Contract or Grant No.
NASw- 3101 3541 |
| | | 13. Type of Report and Period Covered
Translation |
| 12. Sponsoring Agency Name and Address
National Aeronautics and Space Administration, Washington, D.C. 20546 | | 14. Sponsoring Agency Code |

15. Supplementary Notes
Translation of "Tlakové ztráty a přestup tepla v kanálech nekruhových průřezů s hydraulicky hladkými stěnami," Československá akademie věd, Prague, Czechoslovakia, Ústav jaderného výzkumu, Informační středisko, Řež, ÚJV 2891-R, September 1972, 120 pages.

16 Abstract The influence of channel geometry on pressure losses and heat transfer in non-circular channels with hydraulically smooth walls was studied. As a basic assumption for the description of this influence, new integral geometrical criteria, selected according to experimental experience, were introduced. Using these new geometrical criteria, a large set of experimental data for pressure losses and heat transfer in circular and annular channels with longitudinal fins was evaluated. In this way it was empirically proved that the new criteria described channel geometry fairly well.

| 17. Key Words (Selected by Author(s)) | 18. Distribution Statement
Unlimited-Unclassified | | |
|---|---|---|---|
| 19. Security Classif. (of this report)
Unclassified | 20. Security Classif. (of this page)
Unclassified | 21. No. of Pages
92 + 8 | 22. |

N82-20464

ANNOTATION

The objective of this study was to determine the influence of the channel geometry on pressure losses and heat transfer in non-circular channels with hydraulically smooth walls. As a basic assumption for the description of this influence, new integral geometrical criteria, selected according to experimental experience, were introduced. Using these new geometrical criteria, a large set of experimental data for pressure losses and heat transfer in circular and annular channels with longitudinal fins was evaluated. (This research work had been performed in the Institute of Nuclear Research during the years 1967 through 1970.)

In this way it was empirically proved that the new criteria described channel geometry fairly unequivocally. Dimensionless relationships for the friction coefficient ξ and Nusselt number, Nu, expressed by means of these criteria have therefore universal validity. The universality of the new dimensionless relationship for ξ has then been confirmed by adequate transformation of all obtainable experimental results of similar studies done for all kinds of cross sections.

Detailed analysis and elaboration of experimental material mentioned above also made it possible to define with more precision the meaning of such concepts as flow development, transition regime, and non-isothermality influence in noncircular channels.

1. FOREWORD

Knowledge regarding pressure losses and heat transfer in channels with noncircular cross setions is for all practical purposes based to this day only on empirical findings and the key tool for its expansion is experimentation. Computation methods worked out over the past several years on the basis of rudimental experimental findings are still in no position by far to provide with a known degree of accuracy an answer to the query of what pressure losses and heat transfer would be likely to occur in a channel that had not been subjected to prior experimental investigation. The reason for this is constituted by the fact that empirical findings used in these methods as basic assumptions (e.g., configuration of velocity profiles, distribution of local tangential stress, etc.) have a narrowly limited range of validity and their generalization and application to a different geometry of channels can lead to entirely misleading results.

As a matter of fact, the situation in this field is such that experimental findings from each specific channel geometry or criterial relationships which describe the hydrodynamic and thermokinetic state in a given geometry still form an isolated point in the constantly expanding experimental materiel. Attempts to discover their mutual relationship have been unsuccessful. What we are after is not a completely generalized explanation, but a specific empirical method for approach to processing of experimental materiel which would make it possible to unite all extant materiel and discover criterial relationships of more general validity. In addition to their great practical importance, such criterial relationships -- in divergence to the enormous amount of scattered and diffuse experimental materiel -- would at the same time represent a basis of much better quality for studies oriented toward devising a theory of turbulent flow in channels with random cross sections and hydraulically smooth walls.

However, it ought to be pointed out that the by now relatively extensive experimental materiel has one basic shortcoming. Comparison of the results of measurements made by various authors on channels having an identical geometry shows in many cases that those results evince differences that are far from negligible and, at times, basic differences. As an example we can use a channel with a smooth annular cross section, which is the simplest geometry after a tube. So far, almost every author who investigated the state in annular rings, specifies a criterial relationship for the coefficient of friction losses that differs from that of other authors. A comparison of the results arrived at by various authors is shown in fig. 4 which was taken over from a study by Ort [4] and supplemented by results arrived at by Rybáček [3] and by the Institute of Nuclear Research. (The relative coefficient of friction losses in the diagram is related to the coefficient of friction losses in a circular channel with the same Reynold's criterion.) The situation is even worse in thermokinetics of annular channels. A detailed comparison of the results arrived at by studies of heat transfer in this type of channel was compiled by Quirrenbach [19]. The differences found between individual studies amount up to several tens of percent.

There can be a number of causes for such differences, and an objective assessment of all factors that affected the individual results is not possible without a detailed knowledge of the experimental conditions and methodology used in processing of experimental data, etc. Yet, it is specifically in regard to these points that most publications provide insufficiently detailed data.

As the first attempt at generalization of experimental data can be considered introduction of hydraulic diameter as the characteristic dimension of a channel together with the assumption that in defining channel geometry by means of d_h , criterial relations for a circular channel apply also to noncircular channels. However, it is clear by now that this method has a very limited area of application and that its indiscriminate use could lead to utterly wrong conclusions. At the same time it should be emphasized that the area of applicability of d_h has not been clearly defined.

The presented study represents another such attempt at generalization of experimental findings. It is based on a wealth of materiel obtained in the Institute of Nuclear Research during investigation of pressure losses and heat transfer in channels with a smooth annular cross section, annular cross section having a core with longitudinal fins and a tube with internal longitudinal fins. Approximately sixty channels with strongly varying geometry [1], [2] have been investigated in the course of these experiments. Detailed knowledge of the conditions under which the experimental findings were obtained, together with the amount of such findings, facilitated a detailed analysis of the results and assessment of individual factors that could have influenced those results. In this manner were laid the basic prerequisites for such an experiment.

The result of the study was discovery of integral geometrical characteristics which unambiguously define channels with a noncircular cross section with hydraulically smooth walls from the viewpoint of pressure losses and heat transfer. By means of these geometrical characteristics it became possible to process the experimental materiel into universally valid criterial relations for the coefficient of friction losses and Nusselt's criterion.

The term "universally valid" used for describing these relationships is to be interpreted as not confining their validity only to a certain geometry, as comparison of these relations with published experimental values has shown their suitability for use with channels of the most varied geometries that find application in technical practice.

The author considers it to be a delightful obligation and an expression of thanks for valuable cooperation to emphasize the significant contribution made by his collaborators to the presented study.

Engr Jaroslav Hejna closely collaborated on this entire study and contributed a number of valuable suggestions and critical comments to its final shape.

TABLE OF CONTENTS

2. LIST OF SYMBOLS

x	longitudinal coordinate	[m]
h	height of fin	[m]
δ	width of fin; rod spacing	[m]
n	number od fins; exponent	[1]
d	diameter of circular channel, rod diameter	[m]
$\mathcal{D}$	root diameter of finned tube	[m]
$\mathcal{D}_1, \mathcal{D}_2$	inner, outer annular diameter	[m]
ℓ	length of model; length of measured section	[m]
ℓ_T	length of heated section	[m]
ℓ_H	length of hydrodynamic	[m]
L_T	length of thermal	[m]
S	wetted circuit	[m]
F	cross-sectional area of flow	[m²]
S_z	fin circumference	[m]
d_h	hydraulic diameter	[m]
ζ	specific weight of gas	[kg/m^{-3}]
λ	thermal conductivity of gas	[W/m^{-1}/deg^{-1}]
λ_m	thermal conductivity of model tube material	[W/m^{-1}/deg^{-1}]
μ ν	dynamic, kinematic viscosity	[N/s/m^{-2}; m²/s^{-1}]
c_p	specific heat at constant pressure	[J/kg^{-1}/deg^{-1}]
p	static pressure	[N/m^{-2}]
t	local temperature; temp. at root circle	[deg]
Θ	median gas temperature	[deg]
ψ	thermal factor	[1]
u	velocity	[m/s^{-1}]
u^+	dimensionless velocity	[1]
y^+	dimensionless distance from wall	[1]
v^*	friction velocity	[m/s^{-1}]
G	flow-through weight	[kg/s^{-1}]
N	overall thermal output	[W]
q_L	thermal output per unit of length	[W/m^{-1}]
α	coefficient of heat transfer	[W/m^{-2}/deg^{-1}]
τ	tangential stress on wall	[N/m^{-2}]
n_z	fin efficiency	[1]
L	see relation in definition (29)	[m]

$\bar{L}$	see definition in equation (29)	[m]
$\bar{L_0}$	see definition in equation (31)	[m]
$L^* = \dfrac{\bar{L}}{\bar{L_0}}$	integral geometrical criterion	[1]
S_h, F_h, d_h	see para 6.2	
H	geometrical factor	[1]
ξ	coefficient of friction losses	[1]
Nu, Re, Pr	criteria of Nusselt, Reynolds and Prandtl	[1]
$\bar{N}$	median value of factor N along cross-sectional area of flow or along	
N_{max}	maximum value of factor N in channel	

PRESSURE LOSSES AND HEAT TRANSFER
IN NONCIRCULAR CHANNELS WITH HYDRAULICALLY SMOOTH WALLS

J. Malak

Czechoslovak Academy of Sciences, Prague, Czechoslovakia,
Institute of Nuclear Research - Information Center in Řež

3. Brief Description of Experiments Conducted at the Institute of Nu-/7*
clear Research; Method Used in Processing the Results

A detailed description of experimental research into pressure
losses and heat transfer in channels with a circular and annular cross
section having longitudinal fins, which was conducted at the Institute
of Nuclear Research in the years 1967-70, is provided in reports [1]
and [2]. These reports also list the results of measurements in the
form of relationships

$$\xi = \delta \ (Re) \text{ and } Nu = \delta \ (Re)$$

for the individual channels investigated. At this point we shall of-
fer only a brief outline of basic information essential for this study.

The first stage of research included experiments with annular
channels with longitudinal fins and a heated core. (This geometry
will be subsequently referred to as geometry A.) The fins were of
a rectangular cross section with a width of ~ 1.2 mm. Investigated
was a total of 27 variants which represented combinations of three
values of three basic geometrical parameters for which they were se-
lected: channel width (or cross section of outer tube D_2), number of
fins and height of fins. The length of channels was identical in all
cases and was equal to 1,200 mm. Inlet into the experimental channel
which could affect the results of measurements by its shape is shown
in fig. 1.

The second stage involved experiments with circular channels with
inner logitudinal fins. (This geometry will be referred to as geometry
B.) The fins were essentially the same as those in geometry A. Simi-
larly to geometry A, it was planned to examine 27 variants correspond-
ing to combinations of three values of inner diameter of tube, spacing
and height of fins. However, three variants were not investigated at
all, as finned tubes for those variants could not be produced with the
prescribed tolerances and with acceptable surface quality. The length
of channels in all variants was 2,050 mm. Configuration of the channel
inlet is shown in fig. 2.

These experiments were then supplemented by investigation of pres-
sure losses in six annular channels (1,200 mm long)which represented /8
limiting cases of geometry A at h→0.

---

* Numbers in the margin indicate pagination in the foreign text.

Detailed data regarding all of the investigated channel models are listed in appended tables.

All experiments were conducted in an open air line with a ventilator located behind the outlet from the experimental section. The models were heated by resistance heating at a constant thermal output per unit of length of the model.

The measurements included in all cases the flow-through weight of air, thermal output, distribution of static pressure along the channel, distribution of temperatures of the heat-exchange surface on the root circle along the length of the heated model and air temperature at the input and output of the experimental section.

Investigation of pressure losses was done in all cases at isothermal flow. The friction loss coefficient was computed with respecting the difference of the pulse at input and output of the measured sector according to the equation

$$\xi = 2 \, d_h \, \frac{\Delta p}{\ell} \, [\overline{\zeta}(\frac{F}{G})^2 - \frac{1}{\overline{p}}] \tag{1}$$

wherein Δp = pressure loss in channel sector of length 1

$\overline{p}, \overline{\zeta}$ = median values of pressure and specific weight of air in channel

G = flow-through weight

F = cross-sectional area of flow

Reynold's criterion is given by the relation

$$Re = \frac{G \cdot d_h}{F \cdot \mu} \tag{2}$$

For computation of the median value of the coefficient of heat transfer $\overline{\alpha}$ (centered along the heated circumference) was used equation

$$q_\ell = \overline{\alpha}(\pi.\mathcal{D} - n.\Delta + \eta_{\not z}.n.S_{\not z})(t - \Theta) \tag{3}$$

Derivation and analysis of the validity conditions for the equation/9 is contained in [1]. Of importance to us is the fact that in our experimental conditions this equation is valid irregardless of the actual distribution α along the heated surface.

The connotation of individual values in equation (3):

n, Δ = number and width of fins

$\mathcal{D}$ = root diameter of fins

$S_{\not z}$ = fin circumference

t = wall temperature at root circle

Θ = median temperature of gas

Efficiency of fins with a rectangular cross section was taken according to Gardner [16]:

$$\eta_{\not z} = \frac{tgh \; w}{w} \qquad \qquad w = h\sqrt{\frac{2\overline{\alpha}}{\lambda m}} \tag{4}$$

where λ_m is thermal conductivity of the fins' material.

In determination of the delivered thermal output from unit length of the model q_ℓ, in view of the structure of the used models (thick-walled tube with fins) consideration had to be given to axial heat sonductance. In view of the high thermal conductivity of the material of

the finned tubes and the structure of the heating system we can assume an automodel distribution of temperatures in radial cross cuts of the model. This can be put in the form of

$$q_L = \frac{N}{\ell_h} + F_m . \lambda_m \frac{\partial^2 t}{\partial x^2} \qquad (5)$$

The median temperature of gas at distance from input into the heated model at random distribution is determined by the relation

$$\Theta = \Theta_0 + \int_0^x \frac{q_L}{G . c_p} \, dx \qquad (6)$$

where N = overall thermal output

l_T = length of the heated model   /10

F_m = cross section of finned tube

Θ_0 = gas temperature at input into experimental section.

A program was compiled for analysis of experimental values on the computer GIER. To facilitate solution of the system of equations (3) ÷ (6), the experimentally determined distribution of temperatures along the length of the model was substituted for each regime by the method of least squares with a polynomial of the fifth order. At the same time, for the sake of comparison, was also determined the median coefficient of heat transfer without taking into consideration the effects of axial heat conductance. Results of thermokinetic research were processed in the form of the relation

$$Nu = \oint (Re)$$

where values of Reynold's and Nusset's criteria are counted with values of thermophysical properties of the coolant in relation to median temperature and gas pressure in the given radial cross cut of the experimental channel.

In addition to α, Nu and Re, in all cross cuts with measured surface temperature was also determined the thermal factor ψ

$$\psi = \frac{t}{\Theta} \qquad (7)$$

4. Effects Distorting Experimental Results   /11

The basic prerequisite for succeeding in out attempt to unify and generalize the experimental material was to base this study only on cases in which measurements were not subjected to distorting effects. Talking of factors that can distort experimental results, our natural premise was that the objective of our experiments was to measure pressure losses or heat transfer in the region with developed hydrodynamic conditions (distribution of velocity, distribution of tangential stress on channel walls)or, eventually, with developed thermal conditions (automodel thermal profile $(t-\Theta)$) in channels with hydraulically smooth walls.

Distorting factors can essentially be divided into two categories: The first category includes factors which in their essence are bound with the examined physical process and their distorting effect must be viewed as the consequence of our insufficient knowledge of the examined process. They are:

1. transitory region of flow   4. non-isothermity of flow
2. hydrodynamic entry-end sector   5. roughness of walls.
3. thermal entry-end sector

3

In addition to these factors, in individual cases come more-or-less into play factors of the second category which are a consequence of the selected experimental concept, failure to maintain the specified boundary conditions in its implementation, lack of suitability or inaccuracy of the used measuring methods, etc. Assessment of such distorting effects (which should rather be called experimental errors) and an eventual making of suitable corrections in processing of experimental data is, however, within the realm of possibility of only and solely of the author of any given experiment.

Let us have a closer look at the factors in the first category, which in our opinion are the key reason for a number of contradictory data found in experimental materiel. We attempted to cull from all accesible references the current state of knowledge regarding these problems and supplement them by our findings as well as by the results of an analysis of our own experimental materiel and that of others. Our objective was to redefine more accurately individual terms as well as to qualitatively assess the effects of individual /12 factors in the case of noncircular channels.

4.1 Transitory Region of Flow

The term "transitory region of flow" is used in hydrodynamics in two different connotations. In most cases we associate this term with that part of dependence of the coefficient of friction losses in a circular channel on the Reynold's criterion, in which ξ in transition from dependence on laminar flow to dependence on turbulent flow increases with increasing Re. For the sake of differentiation we shall refer to this region and the transitory region ξ.

We encounter this term in its second connotation in describing the velocity distribution in turbulent flow. This distribution is usually expressed in the form of the relation

$$
\left.
\begin{array}{c}
u^+ = \xi\,(y^+) \\[4pt]
u^+ = \dfrac{u}{v^*} \qquad\qquad y = \dfrac{y \cdot v^*}{v} \\[8pt]
v^* = \dfrac{\sqrt{\tau}}{\xi} = \text{friction velocity}
\end{array}
\right\} \qquad (8)
$$

Here u is local velocity ay distance y from channel wall and τ is tangential stress on the wall.

In the area of the laminar substratum applies that

$$u^+ = y^+ \qquad\qquad (9)$$

In turbulent core of flow in a circular channel -- and, according to a number of experimental results also in noncircular channels -- the distribution of velocity occurs in accordance with the relation

$$u^+ = a \cdot \log y^+ + b \qquad\qquad (10)$$

where constants a, b according to some authors have universal validity while, according to others, they depend of the geometry of a channel.

4

Between these two regions lies the region of transient flow -- /13
which we shall refer to as transient region u^+-- in which occurs a
laminar as well as a turbulent transfer of the momentum of motion.
However, according to the latest findings this process cannot be in-
terpreted as simultaneous effects of these two types of transfer, but
as an irregular alternation of laminar and turbulent flow. A factor
called coefficient of intermittence (discontinuity) γ -- which is de-
fined as the time component during which turbulent flow prevails at a
monitored point of the examined space -- is used due to its vividness
for description of transient flow. Thus, if applies that $\gamma = 0$, the
flow is purely laminar, while at $\gamma = 1$ the flow is completely turbu-
lent.

In a circular channel the extent of the transitory region ξ (ex-
pressed by the extent of Re) as well as its lower boundary depends on
a number of factors, the most important among them being geometrical
conditions and the degree of turbulance at entry into the channel.
In routine practice it is assumed that the transitory region lies at
$Re = (2,3 + 3,5) \cdot 10^3$. Nevertheless, during special conditions at en-
try, it became possible to maintain laminary flow into substantially
higher values of Re.

The best insight into the processes that occur in the transitory
region ξ in a circular channel from the viewpoint of velocity condi-
tions is provided by the results obtained by J. Rotta [15]. From de-
tailed measurements of velocity states and their chronological changes
he found out that in the transitory region ξ throughout the flowthrough
cross section the velocity distribution irregularly transfers from a
developed laminar profile into a developed turbulent profile and vice
versa. Hereby the coefficient of intermittence is not dependent only
on Re, but simultaneously undergoes strong changes with distance from
entry into the channel (fig. 5). Thus, in a cicular channel the tran-
sitory region ξ corresponds to velocity regimes during which the tran-
sient region u^+ affects practically the entire flow-through cross sec-
tion of the channel.

Velocity conditions in a noncircular channel will differ from
those in a circular channel in direct relation to the complexity of
channel configuration. As a measure of complexity of configuration we
can use the ratio of the maximum and median width of channel in the
direction of normals to the surface, or the ratio of the maximum and
median curvature of the wetted circuit. The most suitable and most
objective measure of the complex configuration of a channel is distri-
bution of tangential stress on the wall, or $(\tau_{max}/\bar{\tau})$.

In channels with complex configuration we do not deal any more with /1
a cross section represented by a single simple region as is the case in
a tube. In extreme cases we could rather talk of several regions that
strongly differ from the hydrodynamic viewpoint and that retain a cer-
tain measure of "autonomy". For better visualization in limiting cases
we can think of individual regions as independent channels connected in
parallel. The hydrodynamic conditions in each of them would then be
defined by its own Re.

In a tube during developed turbulent regimes the laminar substratum region as well as the transient region u^+ affects only a negligible part of the flow-through cross section. However, in channels with a highly complex configuration, laminar flow can be retained in some parts of the flow-through cross section up to relatively high values of Re, irregardless of the fact that in the remaining parts of the cross section prevails parallel turbulent flow, whereby the share of regions with laminar flow can be relatively high in regards to the overall flow-through cross section.

These regimes are vividly reflected in the results of measurements done by Eckert and Irvine [30] who investigated conditions in a channel with a cross section in the shape of an isosceles triangle with an apex angle of 11.5°. By means of visualization of flow and measuring of velocity profiles they delineated in the cross section the area of laminar flow and the dependence of its extent on Re (see fig. 51). At a still relatively high value of Re = 10^4, at the apex of the triangle, up to $\frac{1}{10}$ of its height prevails purely laminar flow.

The compounded structure of flow in a single channel, or simultaneous effects of laminar and turbulent transfer of motion necessarily must become reflected also in a loss of pressure. Under these conditions the dependence of the coefficient of friction losses on Re will be analogous in character to that of ξ in the transition area in a tube. Thus, from the viewpoint of local velocity conditions, the term "transitory region ξ" assumes a broader connotation in the case of channels with complex configuration than was the case with a tube. However, from the viewpoint of physical substance the connotation of this term is the same for all channel geometries. Thus, under the term transitory region ξ we shall subsequently understand that part of Re in which in a given channel the friction pressure loss is the result of the effects of laminar and turbulent transfer of motion.

On the basis of what was said about velocity conditions in non-circular channels it could be expected that the transitory region in noncircular channels will be wider than in a circular channel and that the lower boundary of the region of purely turbulent flow will be shifted toward higher values of Re. This assumption is fully confirmed by experimental results.   /15

From the hydrod-namic viewpoint, the noncircular channel closest to a circular channel is an annular channel. The results of our measurements of pressure losses in six annular channels with a curvature of $D_r/D_2 = 0.65$ to 0.95 show that great differences exist already between circular and annular channels. Our results are plotted in fig. 3 in the form $1/\sqrt{\xi} = \oint (Re\sqrt{\xi})$ supplemented by theoretical dependence of laminar flow in annular channels with $D_1/D_2 = 1$. For the sake of comparison the diagram also shows the corresponding dependences for a smooth tube. It is obvious that the transitory region in the case of an annular channel is substantially wider than that of a tube. When we attempt to estimate from the progression of the dependence $1/\sqrt{\xi} = \oint (Re\sqrt{\xi})$, interspaced by exp. points, the limits of the transitory region, we obtain the values

$$Re_D \approx 2 \cdot 10^3$$
$$Re_H \geqslant 2.4 \cdot 10^4$$

6

where indices D and H denote the lower and upper boundary, respectively. In determination of the upper boundary it is questionable whether the line interspersed with experimental points does really correspond to a purely turbulent regime, or whether at higher values of Re the actual progress might not resemble more closely, e.g., the relationship (21) which will be discussed in detail sub para 6 and 7. The fact that in annular channels the boundary between the transient and turbulent region is less conspicuously defined than in the case of a tube, is the logical consequence of the already mentioned difference in velocity conditions. Nevertheless, it is clear that the region of purely turbulent flow in annular channels lies roughly by 1 order of Re higher than in the case of a circular channel.

Results analogous to those for annular channels were also obtained in our measurements on channels of geometry A and B which represent channels with one of the most complex configurations that have been investigated so far. Among our results there are a number of cases with a significant share of the transitory region, or even completely dominated by the transitory region. Figures 11 and 12 show several /16 such typical cases for geometry A and B.

The effects of geometrical conditions at the entry into the channel on the extent and boundaries of the transitory region ξ can come to the fore very strongly even in channels with a complex configuration. Figures 7 and 8 show the plotted results of our measurements of four variants of geometry A at varying entry conditions. Each of the measurements was done using two models. In spite of the fact that these models were to be absolutely identical from the hydrodynamical viewpoint, measurements of pressure losses differed. Regretably, when we found out about these differences, the models II had already been destroyed and we could not undertake a detailed comparison of both models. However, supplementary verification of the production process turned up the fact that in some cases the edges of the model at its entry were rounded while in other cases their sharp edges were retained. Experiments with models I were therefore repeated under modified conditions at their entry, which we achieved by placing sheet-metal screens in front of the entry as is shown in fig. 1. In this manner we obtained a third group of results which, in some cases approximate more the original results obtained with model I, in other cases the results obtained with model II. For enhanced orientation and easier comparison the results have again been plotted in fig. 9 and 10 in the form $1/\overline{\xi} = \int (Re\overline{\xi})$. From the progress of individual measurements it can be deduced that with increasing value of Re these dependences transform into a single dependence.

Analysis of the results obtained by other authors in measurement of pressure losses in channels of the most varied geometries led us to the conclusion that a number of those results were obtained in the transitory region ξ without the authors of those studies being aware of it. It is a consequence of incorrect application of findings regarding the extent and boundaries of the transitory region ξ in circular channels to noncircular channels. That, as a result, leads to a number of incorrect conclusions deduced from experimental results affected by the transitory region.

In conclusion we ought to mention one more factor on the effects of which we were withdrawing comment for the time being. The results obtained by J. Rotta clearly show that stabilization of flux conditions in the transitory region ξ in the case of a tube calls for abnormally long channels (see fig. 5 and 6) on the order of several hundred d_h. The situation will be even worse in the case of noncircular /17 channels. As channels used in investigation of pressure losses never attain such lengths, the results of measurement in the transitory region will probably be distorted even more by the effects of the entry sector.

4.2 Hydrodynamic Entry Sector

The term "hydrodynamic entry sector" denotes that part of the channel beyond the entry in which occurs development of the velocity profile from the initial profile at entry up to a fully developed profile corresponding to the preset hydrodynamic regime. Connected with the development of the velocity profile is also development of tangential stress or its distribution along the wetted circuit, and development of transfer characteristics. The length of the entry sector depends on the hydrodynamic regime, the geometry of the channel, configuration of entry or, eventually, on defective flow prior to the experimental part.

Let us first examine the case of a tube. For laminar flow and a sharp-edged entry (i.e., with a balanced velocity profile of input velocity) we theoretically derived the relation

$$\frac{L_H}{d} = \cdot \ Re \tag{11}$$

The constant of proportionality differs from one author to another and ranges between 0.03 to 0.06 (see, e.g., [11]).

In the case of turbulent flow, the decisive effect on the length of the entry sector accrues to the shape of the channel entrance. It is this shape that determines whether the boundary layer in the development of the velocity profile will be turbulent from the start, or whether at the beginning part of the channel it will first be laminar and only after a certain distance from it transforms into a turbulent boundary layer. As a rule of thumb, the aerodynamically smoother the entrance, the longer the entry sector. From experimentation we know that an aerodynamically smooth entrance calls for a channel length of at least 50 d if we are to achieve a perfectly developed velocity profile. The effect of Re are for all practical reasons absent.

As we already mentioned, the situation in the transitory region ξ is entirely different, as is also shown by the results obtained by J. Rotta. Figure 5 shows the dependence of the coefficient of intermittence in the transitory region on the relative distance from the entrance into the channel, and fig. 6 shows change of velocity in the /18 axis of a tube with Re for 3 distances from the entrance. Both figures show that stabilization of the velocity profile in the transitory region calls for channel length on the order of hundreds of diameters.

8

In case of a geometry most closely resembling a tube, i.e., a smooth annular channel, the situation in the turbulent region is not clear. On the one hand, only very few experimental data are available and, on the other hand, these data show basic differences. In investigating pressure losses in annular channels in a range $\mathcal{D}_1/\mathcal{D}_2 =$ = 0.77 through 0.93, J. Ort [4] measured the values of the entry sector in a range of L_H/d_h = 7 through 21. In keeping with his results is also Dreissler's datum for a flat channel $L_H/d_h \doteq 10$ (quoted from Ort's study).

Results analogous to Ort's were also obtained in our experiments with models of geometry A and B. The values of L_H/d_h ranged between 5 through 30, whereby a majority of cases were at the lower limit of that range[1].

Extreme maximum values of L_H/d_h were determined for variants in which the investigated range of Re was completely or partially in the transitory region ξ.

We were assessing the length of the entry sector, similarly to Ort, from the progression of static pressure along the channel, or, to be more specific, from a comparison of the actual distribution of pressure with linear progression which was interspersed by experimental points in the region without apparent effects of the entry sector. The difference between actual and linear progression was in most cases very small. In view of the aforementioned and with a view to the relatively short length of the entry sector (and the resulting small number of experimental points in the entry region) this procedure does not appear to be very accurate and the quoted values of L_H/d_h must be regarded as only approximative information.

However, on the other hand, Rothfus with his collaborators [41] /19 in experimental investigation of annular channels in the range of $\mathcal{D}_1/\mathcal{D}_2$ = 0.12 through 0.35 came to the conclusion thatstabilization of hydrodynamic conditions calls for a channel length in excess of 200 d_h. They based it on direct measurement of tangential stress on the inner diameter and its changes with distance from the entrance into the channel.

From what was said about experimental techniques used in individual cases we get an explanation of the difference between our results and those of Ort on the one hand, and Rothfus' results on the other. While Rothfus based his approach on measurement of local values, our and Ort's measurements provide information only about the median value of tangential stress on the wetted circuit. And that is a substantial difference, the consequences of which we will best realize by a comparison of conditions in a circular and a noncircular channel.

---

[1]In keeping with these values are also the results of experiments on enlarged models of geometry A at $\mathcal{D}_1/\mathcal{D}_2$ = 1 that are currently conducted at the Institute of Nuclear Research. The accuracy of all measurements is at the same time substantially higher than was the case in experiments described in the report [1].

Let us start out with a tube. We assume the presence of balanced entry conditions at the entrance into the channel. Under this assumption the local tangential pressure on the wall is identical with its median value along the circumference of the channel. With increasing distance from the entrance the gradually balanced velocity profile transforms into a developed profile. In the region close to the wall the velocity decreases while, conversely, it increases in the central part of the channel. There is a drop in the radial gradient of velocity at the wall and, as a result, with increasing distance from the entrance there is also a monotonous decrease in tangential pressure on the wall.

The situation is substantially different in the case of a noncircular channel. Let us again assume a balanced velocity profile at the entrance, meaning that input velocity coincides with the median velocity in the channel. However, during development of the velocity profile the situation is not as unequivocal as was the case in a circular channel. In view of the configuration of the channel in some regions of the flow-through cross section the "median" velocity will decrease while the opposite will apply to other regions.. Tangential stress on the wall in individual regions will also change correspondingly. From our and Ort's experiments we can draw the conclusion that development of hydrodynamic conditions in channels with cross sections of a complex configuration (i.e., with $\tau_{max}/\overline{\tau} > 1$) progresses in such a manner so that -- with the exception of a small region beyond the entrance corresponding to values of L_H/d_h from our and Ort's experiments -- the development of local velocity conditions and local valus of τ has no effect on the median value of $\overline{\tau}$ and the latter, for all practical pur-/20 poses, does not change along the channel. According to our results, this conclusion should essentially apply also to the transitory region ξ.

4.3 Thermal entry sector

The term "thermal entry sector" or, also, "sector of thermal stabilization" denotes for us that part of the heated channel in which occurs the development of thermal conditions from the initial balanced thermal profile in coolant at the entrance to the heated section up to the region of automodel of thermal profile ($t - \theta$).

In implementing an experiment or the real thing there can occur two different cases:

1. The beginning of the heated section is identical with the entrance into the investigated channel. Development of velocity and thermal conditions progresses simultaneously.

2. Ahead of the heated section is an unheated channel of identical geometry and, as a result, at the beginning of the heated section the velocity profile is already fully developed in isothermal flow. Another relatively small change in hydrodynamic conditions occurs only in the flow ceasing to be isothermal.

10

As in actual practice in a majority of cases is encountered the first case, and because our experiments were also conducted under such conditions, we shall subsequently deal only with this arrangement. As the development of hydrodynamic and thermal conditions progresses in the entry sector simultaneously with mutual interaction, these two processes cannot be separated from each other. Thus, whenever we refer to the thermal entry sector we will be referring to that part of the channel where there occurs development of flow simultaneously with the development of thermal conditions.

According to experimental findings, the lengths of hydrodynamic and thermal entry sectors in a cicular channel are for all practical purposes approximately the same [11]. Most authors who have experimentally investigated this problem specify values of L_T/d_h ranging between 40 and 60. In the case of noncircular channels, same as was the case of local hydrodynamic conditions, substantially higher values can be expected to be encountered than was the case with a tube. A few experiments conducted in this respect fully confirm such an assumption. Thus, e.g., Eckert and Irvine in their already quoted study /21 [30] specify for the investigated triangular channel $L_T \geqslant 100\ d_h$. The effects of the entry sector together with those of the transitory region ξ also became strongly reflected in most published studies devoted to heat transfer in annular channels that used the method of constant temperature of the heat-exchange surface in determination of the median coefficient of heat transfer in the entire channel. Assessment of errors and limitations of this method from the viewpoint of determination of $\bar{\alpha}$ in the region with developed velocity and thermal conditions was done under the assumption applicable to a tube. This would also account for the great differences between the results of experiments conducted by various authors (see [19]).

We based our assessment of the effects of the thermal entry sector during our experiments with channels of geometry A and B on measurements of the progress of temperature of wall along the length of the model and the corresponding distribution of $\bar{\alpha}$. To enhance clarity and suppress the effects of Re the results were processed in the form

$$\frac{\bar{\alpha}}{\bar{\alpha}_r} = \oint (x)$$
(12)

For reference value $\bar{\alpha}_h$ was taken the value of $\bar{\alpha}$ in the last measured cross cut near the channel exit.

In assessment of the processed results, in the case of some variants there appeared certain errors and lack of logic in the distribution of $\bar{\alpha}/\bar{\alpha}_h$ that were caused by loss of heat at the end of the model. The method used for inclusion of the effects of axial heat conductance in the model on the distribution of q_L did not manage to eliminate the effects of heat losses in some cases. This calculation method -- described in para 3, is based on experimentally determined distribution of temperature in the wall of the model, which by the method of least squares it replaces by a polynomial of the fifth order. This polynomial, which described temperature distributions with a high degree of precision, did not suffice in some cases for the first and second derivation of temperature at the ends of the model. In such cases the assessed progress of $\bar{\alpha}$ at the end of the channel again rises. Then it

11

became necessary to carry out an analysis and comparison of progressions of $\bar{\alpha}$, evaluated with respecting as well as neglecting the effects of heat conductance, compare the progressions $\bar{\alpha}/\bar{\alpha}_\lambda$ for various values of Re and determine to what distance from the end the effects /22 of heat loss extend. Such an example can be seen, e.g., in fig. 14. To facilitate comparison, fig. 13 and 15 show cases when the effect of terminal losses failed to materialize.

We determined that the length of the thermal entry sector in our experiments ranged between $L_T = (17-80)$ d_h according to the type of the examined geometrical variant. As the length of the models ranged between 50-400 d_h, the region with developed velocity and thermal conditions was never reached in the case of some variants.

In assessment of the effects of the transitory region and of the entry sector, very effective proved comparison of the relations

$$\frac{1}{\sqrt{\xi}} = \delta(Re\sqrt{\xi})$$

(ξ)

$$\frac{\alpha}{\alpha_\lambda} = \delta(x)$$

(α)

$$Nu = \delta(Re)$$

(Nu)

Such a comparison and placement of the relationships (ξ), (α) and (Nu) into mutual connection provides a more comprehensive idea of the hydrodynamic and thermokinetic conditions in the channel and their change along the channel. Let us cite a few typical cases:

In variant 13 the relationship (ξ) (fig. 11) up to a value of Re equal to 8.10^3 has the character of a transitory region. At the same value of Re also the relationship (α) (fig. 13) shows a strong region of laminar heat transfer, and the relationship (Nu) (fig. 18), only at values of Re > 8.10^3 transforms into a relation of the type

$$Nu = .\ Re^{0.8}$$

Analogous facts could be found in the case of variant A 15.

In the case of variant A 25 (fig. 11, 16, 18) all three relationships lie clearly in the transitory region and closer to the laminar region. (Values of Nu in fig. 18 were assessed in the one-before-last measured cross cut only for illustration of the conditions.)

Variant B 18 represents a case in which there occurred a distortion of the relationship (α) (fig. 17) as a result of a terminal loss, primarily in the last cross cut. For the progression of the relation /23 (α) at various values of Re it is readily obvious that in the region Re < 3.10^4 practically the whole model lies in the entry sector. In view of the fact that relationship (ξ) (fig. 12) up to Re = 4.10^4 is in the transitory region, the great length of the entry sector is to be expected. The relationship (Nu) also behaves in keeping with these factors (fig. 19).

These several typical examples clearly show how interrelation of the relationships (α), (ξ) and (Nu) makes it possible to identify even the relatively weak effects of distorting factors.

12

In conclusion, the effects of the entry sector (or effects of the length of a model) on the relationship $Nu = \oint (Re)$ can be most vividly demonstrated in fig. 20 which shows the results of measurements on the variant B7 as a typical example. The points marked by circles are local values of Nu at varying distances from the entrance into the channel plotted in relation to the local value of Re. The almost vertical intermittent lines represent the progression of Nu along the length of the model at constant flow of coolant. Values of Nu decrease with increasing distance from the entry and at balanced conditions gradually attain a value corresponding to the sought after relation $Nu = \oint(Re)$. The second system of intermittent lines shows how would progress if we used models of varying length in our experiments. The resultant relation $Nu = \oint(Re)$ is then distorted by the effects of the entry sector not only in regards to absolute values, but also form. The resultant form of the relation $Nu = \oint(Re)$ for the variant B7, shown by the thick solid line throughout the investigated extent of Re, corresponds to the typical form of this relationship for a circular channel with inclusion of the transitory region of flow (see, e.g., [3]).

4.4 Effects of Nonisothermal Flow

In assessment of thermokinetic experiments we relate all thermophysical properties of the coolant to its median temperature, i.e., temperature computed from thermal balance. It appears, however, that with increasing difference between the temperature of the wall and the median temperature of the coolant (i.e., with increasing thermal flow) at otherwise identical conditions of the experiment, the value of the thermal coefficient decreases. This phenomenon is caused by a change in the thermophysical properties of the coolant in the region at the   /24 heated wall as a result of high temperature gradients. This means that median temperature of coolant is not suitable as the defining temperature for thermophysical properties and that the correct value is to be found somewhere in the region between t and Θ. This fact is respected in the criterial equation for Nusselt's criterion by a suitable function of the so-called temperature factor ψ which is defined as the ratio of wall temperature and the medium temperature of coolant (see equation (7)).

Kutateladze   12 derived on the basis of an analogy between transfer of motion and heat for gas-cooled circular channels the relation between the coefficients of heat transfer at isothermal and nonisothermal flow in the form

$$\frac{\alpha}{\alpha_0} = (\frac{2}{\sqrt{\psi} + 1})^2 \tag{13}$$

wherein α_0 is the coefficient at   = 1.
However, most empirical findings are expressed in the form

$$\frac{\alpha}{\alpha_0} = \psi^{-n} \tag{14}$$

Relation (13) can then be replaced by relation (14) with $n = 0.55$. The values of $\underline{n}$ from the experiments range between 0.3 to 0.55. However, we must realize that conducting an experiment that would facilitate direct assessment of the effects of the thermal factor is for all practical purposes impossible. In actual implementation of an experiment of

13

this kind a change in ψ is immediately accompanied by a change in and Re. As a result, assessment of the effects of ψ is always indirect and burdened with large errors.

Since we are unable to describe the effects of nonisothermal flow with any degree of accuracy even in a circular channel, then in regard to channels with a complex configuration, where temperature of the heat-exchange surface varies along the circumference, we know practically nothing about these effects. At the same time, the error caused by the thermal factor can be considerably large. In the case of a tube, e.g., change in ψ from a value of 1 to 1.3 corresponds to a change in Nu by approximately 13%.

For that reason, operational conditions in investigation of heat transfer in geometry A and B were selected so that the thermal factor in the region of balanced thermal conditions be as identical as possible for all regimes of all tested geometrical variants. The thermal factor in our experiments is related to the wall temperature on the root circle.

We also attempted at the same time (as we shall mention later) to experimentally determine this effect for at least several variants.

4.5 Effects of Wall Roughness

Another factor that can strongly affect measurement of pressure losses in roughness of walls. The effects of roughness are relatively well known in the case of circular channels, the so-called sand roughness. This involves a case when the density of unevennesses is high and when the effects of roughness depend only on a single parameter k/R (k = height of unevennesses). We know substantially less in regards to cases when the density of unevenesses is low and when the effects are produced by their geometrical configuration.

As was the case in para 4.4, we must state that we do not know anything about these effects in noncircular channels. Use of relations for a tube with sand roughness by means of the hydraulic diameter would in the case of channels with a complex configuration be illogical and make no sense. From what we know about circular channels it follows that we can regard a channel as hydraulically smooth (i.e., there is no manifestation of the effects of roughness) in a case when the height of unevennesses is smaller than the thickness of the laminar substratum. In view of the complex structure of flow in variegated channels the same absolute roughness will manifest itself in individual parts of the channel in a different manner.

We only know that, same as in case of a tube, manifestation of the effects of wall roughness increases with increasing Reynold's criterion. As soon as wall roughness starts to affect the flow conditions, the gradient of the relation $\xi = \mathscr{f}(Re)$ starts to drop and, in the end, this relation will transfer into the automodel region.

Rendering an objective decision whether the effects of roughness became manifested in a specific case -- with the exception of the

14

automodel region -- is impossible as long as we do not posses a detailed knowledge of circulation in noncircular channels. At the present time such assessment depends on the subjective explanation of the experiment's author or, more precisely, on the criteria selected by him for the assessment.

According to the criterion selected by us, no effects of roughness were encountered in our experiments.

5. Basic Findings and Assumptions

5.1 Pressure Losses

From a detailed processing and comparison of experimental data from our own as well as others' experiments, accompanied by a detailed analysis of experimental conditions, we reached the conclusion that in all cases, in which there is no manifestation of the formerly mentioned distorting effects, the coefficient of friction losses in the region of developed turbulent flow corresponds to the general equation

$$\frac{1}{\sqrt{\xi}} = C_1 . \log Re\sqrt{\xi} + C_2 \qquad (15)$$

wherein constants C_1 and C_2 are the function of channel geometry.

The empirically proven general validity of equation (15) thus narrows down the problem of finding a criterial relationship for the coefficient of friction losses to determination of the dependence of constants C_1 and C_2 on channel geometry. However, from this viewpoint, processing of experimental data in the form of the relation $1/\sqrt{\xi} = \oint (Re\sqrt{\xi})$ proved unsuitable. In this system the effects of experimental errors is reflected much stronger than in the system (ξ ; Re), resulting in a larger scattering of experimental points. In view of the fact that our experiments in individual cases did not cover even one whole order of Re, we found it very difficult and problematic to accurately determine constants C_1 and C_2 , which are very sensitive to interpolation of the relation (15). This applies primarily to constant C_2 .

Nevertheless, an informative assessment of constants C_1 and C_2 supplemented by an analysis of the the relationships $\xi = \oint (Re)$ resulted in another finding which simplified the whole task. By simple transformation, with a precision corresponding to the precision of the experiment, relation (15) can be transposed on Prandtl's known relation for a smooth tube. Such transformation corresponds to substitution of the hydraulic diameter by a more suitable characteristic geometrical dimension.

For given pressure losses and flow-through weight of coolant applies that

$$\xi = . \ d_h$$
$$Re = . \ d_h$$

15

If we designate a suitable characteristic dimension, which makes the mentioned transformation possible, as d_0 and the corresponsong values of the coefficient of friction losses and the Reynolds criterion as ξ_0 and Re_0, then it applies that

$$\frac{\xi_0}{\xi} = \frac{Re_0}{Re} = \frac{d_0}{d_h} \tag{16}$$

We denote

$$\frac{d_h}{d_0} = H \tag{17}$$

and call this value a geometrical factor.
The

$$\xi_0 = \frac{\xi}{H} \tag{18}$$

$$Re_0 = \frac{Re}{H} \tag{19}$$

and because the values ξ_0 and Re_0 apply to Prandtl's universal law of friction, i.e.,

$$\frac{1}{\sqrt{\xi_0}} = 2.\log Re_0 \sqrt{\xi_0} - 0.8 \tag{20}$$

we can put it in the form of

$$\frac{\sqrt{H}}{\xi} = 2.\log \frac{Re\sqrt{\xi}}{H^{3/2}} - 0.8 \tag{21}$$

5.2 Heat Transfer

Heat transfer into a channel with a variegated cross section can be described by means of a simple equation, such as, e.g., equation (3), only in certain cases and under certain conditions. Heat Transfer is generally described by equation

$$q_L = \int_S \alpha (t - \theta) \, dS \tag{22}$$

wherein

q_L = thermal output transferred from unit length
   of the heating element into the cooling gas

t = local temperature of heat-exchanging surface

θ = median temperature of gas

S = circumference of heat-exchanging surface

We can simplify this equation on the basis of the analogy between the transfer of motion and heat. We assume that distribution $\tau/\bar{\tau}$ is, as well as distribution $\alpha/\bar{\alpha}$, merely a function of channel geometry. Ergo

$$\frac{\alpha}{\bar{\alpha}} = \phi_1 (S) \tag{23}$$

In regions with stabilized thermal conditions we can further assume that the prerequisite of automodel distribution of wall temperature has been met

$$\frac{t - \theta}{\bar{t} - \theta} = \phi_2 (S) \tag{24}$$

16

Equation (22) can then be written in the form

$$q_L = \bar{\alpha}.(\bar{t}-\theta)._{\Delta}\int \delta_1 (S).\delta_2 (S).dS \tag{25}$$

The possibility for further simplification of equation (25) must always be considered in connection with the specific geometry of the channel and the specific design and material composition of the heated element. The justification for each simplification must be verified by preliminary calculations made under various assumptions and distributions of α along the heat-exchanging surface. Consideration in this case must be given to both internal as well as external factors (i.e., distribution of temperatures and thermal flows in the heated element). The objective of these calculations is to find out in what way use of simplifications could distort energy calculations or the information which the experiment is to provide.

Our subsequent comments involve only cases for which description of heat transfer could use an equation of the type

$$q_L = \bar{\alpha}(\bar{t}-\theta).S \tag{26} \quad /29$$

where centering is done along the circumference of the heat-exchanging surface.

Equation (3) used in assessment of thermokinetic experiments on geometry A and B represents application of equation (26) to our specific geometrical conditions. The suitability for use of equation (3) as well as its limitations for channels with longitudinal fins was proven by a theoretical analysis and a number of calculations using the computer GIER. Details are contained in report [1].

Similarly as was the case with hydrodynamics, we first concentrated on the form of dependence of Nusselt's criterion on Reynold's criterion. We undertook a detailed analysis of our own as well as accessible experimental materiel of others and eliminated all cases in which we reached the conclusion that measurement was not performed at balanced hydrodynamic and thermal conditions. In a great majority of cases we then determined the dependence of

$$Nu = const. \, Re^{0.8} \tag{27}$$

The constant is a function of channel geometry, thermophysical properties of coolant and the thermal factor. If we further assume that the effects of thermophysical properties of the gasseous coolant can be expressed in the same way as for a tube, then relation (27) can be put in the form

$$Nu = D \, . \, Pr^{0.4} \, . \, Re^{0.8} ..\psi^{-n} \tag{28}$$

where constant D is merely a function of geometry.

6. Integral Geometrical Characteristics

6.1 Pressure Losses

The relation (21) generalizes our old experience that in certain cases involving noncircular channels the relation for a smooth tube /30

can be used for determination of ξ provided that we use hydraulic diameter as a characteristic dimension of the channel, while in other instances this procedure could lead to misleading conclusions.

Some authors tried to apply this experience in such a manner that in specific cases, where use of d_h did not facilitate unification of experimental results, they made use of another dimension of the given geometry as the characteristic dimension. As an example we can cite triangular lattices of rods with longitudinal bypass flow. If we use as a characteristic dimension the diameter of a circle plotted onto the lattice, the results show good coincidence with a smooth tube. Such an approach -- if it produces results in the first place -- is always dependent on the author's estimate and cannot be used without prior knowledge of experimental results.

The kind of conclusions to which can lead an indiscriminate use of the hydraulic diameter and criterial relation for a tube can be illustrated on three typical cases.

Let us first consider a circular channel with very thin and deep internal radial slots. In such a case there is practically no difference in the flow-through diameter in comparison with a smooth tube, while the wetted circumference can increase by a number of times. The hydraulic diameter and the friction loss coefficient will decrease in the same ratio. But it is clear that hydrodynamic conditions will not substantially differ from those in a smooth tube[1].

As a converse case we can take the eccentric annulus. According/31 to the definition of d_h it should not be affected by accentricity and the latter should consequently also not affect pressure losses. However, we know from the experiment that pressure loss decreases with increasing eccentricity and that the difference in pressure loss between a concentric annulus and an annulus with eccentricity equal to 1 amounts to 30 to 40%. However, hydraulic diameter in not an unequivocal characteristic value even for such simple geometry as is a concentric annulus. Experiments have again proven that ξ depends fairly heavily on curvature $\mathcal{D}_1/\mathcal{D}_2$ which is not reflected in d_h.

The relation (21) formally reduces this problem to the question of what determines the geometrical factor H and what does it depend on. That means that we must find a factor that would be merely a function of channel geometry and which would respect in a correct manner the indicated extreme cases. This factor must in some suitable way "weigh" the effects of individual parts of the wetted diameter on flow in the channel. If such a factor is to unequivocally define channels of the most varied geometrical configurations from the viewpoint of hydrodynamics, this factor must be of an integral character.

---

[1] For simplification's sake we have so far neglected general conditions that some authors (e.g., [13]) refer to as limiting the use of d_h, i.e., that in all parts of the flow-through diameter the width of the channel in the direction of the normal must be higher than the thickness of the "boundary" layer in which occurs maximum change in velocity during turbulent flow.

18

These general requirements could be used to define an infinite number of factors. We therefore embarked upon a search for a factor that would have the simplest and logical definition which would be, relatively speaking, the easiest for assessment and which could be applied at least in part to some descriptions of turbulent flux. After various considerations and carrying out a number of auxiliary calculations and unsuccessful experiments which we will not describe here, we decided on a factor that some authors use as a local measure of turbulence and which in the case of a circular channel is interpreted essentially as the mixing length.

The dissipative effect of an element of channel wall on random interference with flow in the vicinity of point M is quantitatively bound to reciprocal value of the distance of point M from the given wall element. For that reason the characteristic distance L of point M from the channel wall is given by the integral

$$\frac{1}{L} = \frac{1}{2} \int_{2\pi} \frac{1}{\ell} \, d\varphi \qquad (29)$$

where ℓ is the distance of point M from the channel wall in the direc- /32 tion of φ. Relation (29) was used in his study [6] by Buleyev. According this relation the factor L very closely resembles the measure of turbulence derived under assumption of resemblance of turbulent processes in various regions of liquid flux by A. M. Obukhov [40]. If we use relation (29) to assess the distribution of L in a circular channel we find out that

$$\ell = 0.44 \ L$$

The factor ℓ in this case is the mixing path of Prandtl's semi-empirical theory of turbulent flow, arrived at by Nikuradze from experimental values of velocity distribution in a circular channel with respecting the actual distribution of tangential stress in the tube cross section.

The factor L, even though it respects the shape of the channel, is merely a local factor. However, the maximum value of L (L_{max}) in the given cross section, or -- what we deem more suitable -- the median value of L in the given cross section could be taken as a value characterizing the channel.

$$\bar{L} = \frac{1}{F} \int_F L \ dF \qquad (30)$$

This factor which has the dimension of width is not only a function of channel configuration, but is at the same time a function of its absolute size. We therefore used as channel characteristic the factor

$$L^* = \frac{\bar{L}}{\bar{L}_0} \qquad (31)$$

which we shall refer to as the integral geometrical criterion or characteristic.

The factor $\bar{L}_0$ in relation (30) denotes the median characteristic distance $\bar{L}$ for an equivalent tube:

$$\bar{L}_0 = 0.0887 \ . \ d_h \qquad (32)$$

19

6.2 Heat Transfer

The flow-through cross section of noncircular channels can form an n-times coherent region bounded by n closed curves. Each of these curves corresponds to a part of the wetted circuit that can be individually heated. If in processing the values from investigation of pressure losses we could define channel geometry by a single geometrical characteristic, similar approach is not possible when dealing with heat transfer in a region with multiple connections. In such a case we must respect the distribution of α in the individual parts of the wetted circuit. (However, from the viewpoint of individual parts of the circuit, we again work with the median value of $\overline{\alpha}$ in the given part -- see equation (26)). Thus, we need one more geometrical factor which would respect distribution of α. We undertook selection of this factor on the basis of the following simple contemplation:

If we assume the validity of Reynold's analogy between transfer of motion and heat, then applies that

$$\frac{\overline{\alpha}_i}{\overline{\alpha}} = \oint \left(\frac{\overline{\tau}_i}{\overline{\tau}}\right)$$

where factor with the index "i" are related to the i-th part of the wetted circuit. We further assume that no transfer in motion occurs accross the orthogonal trajectory to isotachs which intersects the relative maxima of velocity. This line is then plotted in approximation of the corresponding line in field L.[1]

If we now designate the area bounded by this trajectory and the /34 heated circuit as F_T and the heated circuit S_T we can formulate

$$\frac{\overline{\alpha}_i}{\overline{\alpha}} = \oint \left(\frac{d_{T_i}}{d_h}\right) \qquad\qquad d_T = \frac{4\ F_T}{S_T}$$

We then used the factor d_T/d_h together with the factor L^* in processing experimental data regarding heat transfer in channels the flow-through cross section of which represents a doubly connected region.

For a simply connected region it applies that

$$d_T \equiv d_h \qquad\qquad\qquad\qquad (34)$$

Computation of both integral geometrical characteristics L^* and d_h/d_T in the case of more complex geometries is practically impossible without a computer. Programs and calculations for our needs were provided by Engr J. Schmid, CSc. Detailed methodology is in report [17].

---

[1] We verified this assumption for the case of a smooth annulus, it being the only one for which experimental documentation is available. A part of the authors stipulates that the position of maximum velocity arrived at through assessment of the experiment conforms to the theoretical relation for laminar flow also in the region of turbulent flow. Roberts in his theoretical study [18] uses for turbulent flow a relation derived from experiments, one that differs from laminar flow. The relative position of maximum velocity in relation to the curvature of the annulus according to both relations is shown in fig. 26. The relative position of L_{max} lies between these two progressions.

7. Universal Criterial Relations

7.1 Universal Criterial Relation for ξ

In assessment of the geometrical factor for the individual types of channels investigated we used the experimental relation $1/\sqrt{\xi} = \mathcal{f}(Re\sqrt{\xi})$ as a guide for determining whether the entire measurement or its part was affected by the transitory region ξ. Actual assessment of H was done graphically from experimental relations $\xi = \mathcal{f}(Re)$. With the use of a simple mechanical device (template) it was easy to perform transformation to Prandtl's universally valid law of friction and directly read off the value of H.

In our search for the dependence of H on channel geometry, the experimental values of H were plotted consecutively in relation to L^*, L_{max}/d_h and a combination of the two in the form $(L_{max}^2/L.d_h)$. The results are shown in fig. 21 through 24 in such a manner that the individual investigated variants can be identified by markings of experimental points. (The used symbols are shown in tables for geometry A and B.) Figures 21 and 22 are practically identical, however the latter figure shows only differentiation of geometry A and B and also includes results obtained by Rybáček [3].

Smooth annulus is represented by a single point with indicated dispersion which includes the results obtained by the Institute of Nuclear Research, by Rybáček [3] and Ort [4], as shown in fig. 27. The factor L^* does not depend on it practically at all in the case of small annuli from a curvature of $\mathcal{D}_1/\mathcal{D}_2 \approx 0.4$ and up (see fig. 53) and has a value of 0.934. This value of L^* represents the absolute minimum of L^*. There is no geometry that could have a lower L^*.

Comparison of fig. 21, 23 and 24 clearly shows that the relation $H = f(L^*)$ results in a substantially smaller dispersion of experimental points than is dependence of on two other factors. Thus, we are of the opinion that the integral geometrical criterion L^* defines channel geometry better than factors (L_{max}/d_h) and $(L_{max}^2/L.d_h)$.

The dependence of on channel geometry can be now expressed by the relation

$$H = 0.268 \text{ to } 0.842 \ (L^*)^{-1.2} \tag{35}$$

Nevertheless, the exception in this relation is formed specifical- ly by a smooth tube, the law of turbulent friction of which we used as the basis for our processing. Relation (35) yield for a tube the value of $H = 1.1$ instead of the correct value $H = 1$.

We have failed so far in finding a satisfactory explanation for this contradiction. The simplest and most probable explanation might be that the used method, to include the integral geometrical characteristic, represents only a certain degree of approximation of actual conditions and, as such, cannot be in agreement with all empirical findings.

However, we must realize at the same time that a circular channel represents from the viewpoint of all other types of channels a certain extreme in two directions:

1. It is the only channel in which the local value of tangential stress on the wall is identical with the median value of τ.

2. Of substantially more importance is the fact that for all practical purposes purely longitudinal flow exists solely in circular channels. In all other types of channels that were subjected to experimental investigation, there was evidence of a secondary transverse flow which strongly affects the distribution of τ along the wetted circuit and which necessarily must also become reflected in the extent of pressure losses. A possible exception from this allegation might be formed by annular channels. However, the results of measurements made so far still show enough divergence to preclude formation of an unequivocal conclusion.

An answer to these problems could be provided only by a well-founded theory of turbulent flow in channels with a random cross section -- if it can be formulated.

Finally, plotted in fig. 25 are all our experimental results processed in the form of relation (21) with theoretical values of H according to relation (35). The median error in comparison with relation (20) is less than 10%, which in view of the overall accuracy of the experiments can be considered to be a very good result.

In this manner the relation (21) in connection with relation (35) represents a criterial equation for the coefficient of friction losses the validity of which is not limited to merely a certain channel geometry. We will prove its potential application to all types of channels sub para 8.

7.2 Universal Criterial Relation for Nusselt's Criterion

All of our experiments were conducted in such a manner as to have the thermal factor in the region of balanced thermal conditions range between ψ = 1.2 to 1.3; median temperature $\overline{\psi}$ = 1.27. As the characteristic thermokinetic factor for individual geometrical variants was selected and computed from experiments the value of nusselt's criterion for Re = 5.10^4. We then gradually verified whether this value can be brought into an unequivocal dependence on some of the simple combinations of factors L^*, L_{max} and d_h/d_T, which can be arrived on the basis of certain clear concepts of the transfer conditions in a channel. In this manner we have proven that this requirement can be met only by the geometrical criterion $L^* \frac{d_h}{d_T}$. The dependence of the values Nu_5 on the geometrical criterion $L^* \frac{d_h}{d_T}$ is shown in fig. 28. Marking of the experimental points again facilitates identification of the individual variants being investigated.

Figure 29 shows the same dependence, but point markings serve only to differentiate geometry A and B. Experimental results arrived at by

22

K. Rybáček [3] are also included. His experiments were carried out
at other values of ψ than were our experiments. As much as facili-
tated by data in [3], we computed the thermal conditions for the ex-
periments done by Rybáček and converted his results to our conditions
by means of Kutateladze's relation (13). In spite of the fact that
the chosen approach can be considered to be only a rough approximation
of actual conditions, the coincidence between those values and our own
results is good.

The interpolated relation in fig. 28 could be expressed by

$$Nu = 97. \left(L^* \frac{dh}{dT} \right)^{-0.91} \tag{36}$$

If we assume that even in the case of channels with a complex
cinfiguration the effects of termophysical properties of the coolant
can be expressed by means of the factor $Pr^{0.4}$ and the effect of the
thermal factor by Kutateladze's relation, than from relation (36) we
obtain a modified known relation for a circular channel:

$$Nu = 0.022 . Pr^{0.4}. Re^{0.8}. \left(L^* \frac{dh}{dT} \right)^{-0.91}. \psi^{-0.55} \tag{37}$$

Thus, relation (36) precisely intersects the point which corres- /38
ponds tothe value Nu_5 for an air-cooled circular channel.

Let us return one more time to the diagrams in figures 28 and 29.
In comparison with investigation of pressure losses, the results on-
tained in experimental investigation of heat transfer with a view to
the number and type of measured factors always burdened by larger er-
rors. At the same time, investigation of heat transfer is more sub-
jected to the distorting effects of the transitory region ξ and of
the entry sector. If we become aware of this fact, we can assess the
dispersion of experimental points on these diagrams as relatively
small.

Figures 30 and 31 show plotting of all experimental relations
$Nu = \int (Re)$ adapted in the form

$$\frac{Nu. \left(L^* \frac{dh}{dT} \right)^{0.91}}{97} = \int (Re) \tag{38}$$

Points which lie beyond the region of ± 10% in comparison to the
relation (37) belong for their major part to a few geometrical config-
urations for which it was not possible to unequivocally determine
whether the measurement was affected by one of the mantioned factors
or not.

Equation (37) can again be regarded as a criterial relation for
Nusselt's number, which is not bound to a single specific geometry.
Nevertheless, in comparison with the criterial relation for ξ, the use
of this equation is limited by several conditions:

1. The basic condition, which we pointed out already sub para 5,
is suitability of equation (26) for computation of heat transfer in a
specific case. Otherwise this condition may be defined so that heat
transfer must be dependent on the actual distribution of the local co-
efficient of heat transfer along the heat-exchanging surface.

23

2.   Relation (37) was derived from experimental values measured in channels with a flow-through cross section represented by a singly of doubly connected region. No experimental documentation aws available for multiple connected regions and suitability of relation (37) for such cases would first have to be established.

3.   Contrary to relation (21), it was not possible to compare equation (37) with a larger number of other authors' experimental findings regarding various channel geometries.

7.3   Thermal Entry Sector

In an effort to make widest possible use of experimental materiel and to obtain as many specifically formulated findings, I attempted to derive from the experimental progressions of $\frac{\alpha}{\alpha_h} = \delta\ (x)$ the dependence of length L_T on channel geometry. We were interested in finding out whether integral geometrical characteristics could also be used in this case as an unequivocal geometrical criterion. We were aware at the same time of the fact that experimental documentation, in view of the overall concept of our experiments and accuracy of measurements, was not exactly the most suitable for this purpose. For that reason we regard our results to be merely the first bit of information offered about this problem and an incentive showing the approach to this particular problem. Thus, we shall limit our comments to a mere listing of our conclusions:

Distribution of the coefficient of heat transfer along the model can be described by equation

$$\frac{\bar{\alpha}}{\alpha_\infty} = 1 + 0.1\ \frac{L_{T\ 1.1}}{x} \tag{39}$$

This equation formally coincides with the equation for distribution of α in a circular channel, which -- with reference to the study of Boelter, Young and Iverson -- is quoted in study [11].

The factor $L_{T1.1}$ is an x-th section coordinate with $\frac{\bar{\alpha}}{\alpha_\infty} = 1.1$. This factor is a function of channel geometry and of Reynold's criterion, whereby dependency on Re is substantially weaker. In most variants, the experimental results of which could be used for this purpose, $L_{T\ 1.1}$ increases with the Reynold's criterion up to values of Re = 2 to 3.10. For higher values of Re the value $L_{T1.1}$ remains constant. For these cases and for the region Re > 3.10^4 we devised the relations

$$\frac{L_{T\ 1.1}}{d_h} = \delta\ (L^*) \tag{40}$$

$$\frac{L_{T\ 1.1}}{d_h} = \delta\ (L^* \frac{d_h}{d_T} \tag{41}$$

The results are plotted in fig. 32 and 33. The geometrical characteristic L^* even in this case is not an unequivocal characteristic of the channel. As a result, relation (40) has one form for geometry A and another form for geometry B.

24

Relation (41) in comparison with the preceding relation is rela- /40
tively unequivocal, but experimental points show considerable scatter-
ing. From interpolation of experimental points we can express this
relation by the equation

$$\frac{L_{T\ 1.1}}{d_h} = 25\ (L^*\frac{d_h}{d_T}) - 22 \tag{42}$$

For illustration we computed the experimental progress of $\frac{\overline{\alpha}}{\alpha_\infty}$ in
the form of relation

$$\frac{\overline{\alpha}}{\alpha_\infty} - 1 = \delta\ (\frac{x}{L_{T\ 1.1}})$$

The value $L_{T\ 1.1}$ was for this purpose computed for individual var-
iants from relation (42). The results are shown in fig. 34, which is
being introduced without comment.

7.4 Effects of Thermal Factor ψ

For some variants of geometry A we conducted experiments design-
ed to produce results that would offer more accurate information about
the effects of thermal factor ψ in channels with complex configuration.
Wall temperatures of the model were measured at a constant flow-through
weight of coolant and at vaying values of thermal output and we deter-
mined the coefficient of heat transfer in the region of developed
thermal conditions. This approach was designed to suppress the effects
of Reynold's criterion as much as possible.

The results were processed in two ways:

1. The first approach did not take into consideration any change
in the Reynold's criterion in the investigated cross section as a re-
sult of varying values of median gas temperature in individual regimes.
Thus, effects in changes of Re on the Nusselt criterion were also dis-
regarded. The results obtained through this approach are shown in fig.
35 in the form of the relation

$$\frac{Nu}{Nu(\psi=1.1)} = \delta\ (\psi) \tag{43}$$

To prevent an eventual distortion of the results as a consequence
of an erroneous extrapolation of the relation $Nu = \delta(\psi)$ into $= 1$, we
related the relative value of Nusselt's criterion to the value of Nu at
$\psi = 1.2$. This value lies for all variants in the investigated range of
ψ.

It stands to reason that this approach is neither correct nor is /41
it logical. Nevertheless, it is interesting that the experimental re-
sults can be well described by Kutateladze's relation (13).

2. The second approach did take into consideration the effects
of changes in gas temperature on the value of Re and the effects of
the change on the value of Nu.

25

The results are shown in fig. 36. Their analysis showed that for all the investigated variants the effects of the thermal factor can be expressed by the relation

$$\frac{Nu}{Nu(\psi = 1)} = \psi^{-n} \tag{44}$$

but that the exponent n is again a function of geometry. The dependence of n on channel geometry is expressed in two ways in fig. 37 and 38. One makes use of factor L^*, the other $(L^* \frac{dh}{dT})$ as the geometrical criterion.

In view of the conduct and precision of experiments and the used methodology for processing the results, point dispersion is not excessive in either case. However, there were entirely too few experimental points to warrant drawing of any conclusions from these results.

As these experiments were conducted only on models of the geometry A_1, it is not possible to judge which geometrical criterion would be more suitable for this purpose. However, it can be assumed that same as was the case with the thermal entry sector, the most unequivocal geometrical characteristic will turn out to be the criterion $(L^* \frac{dh}{dT})$.

8. Comparison of the Universal Criterial Relation for ξ With Exper- /42
   imental Results Obtained by Other Authors

To prove the universal applicability of the criterial relations (21) and (35) for the coefficient of friction losses in a wide range of channel geometries, we undertook a comparison of this relation with experimental values for all types of channels for which we could find credible documentation in technical literature.

8.1 Triangular and Square Lattices of Parallel Rods

A sheaf of parallel rods arranged into a triangular or square lattice may be regarded as one of the key geometries of channels from the viewpoint of nuclear power engineering. There is also a relatively large volume of experimental materiel available for this geometry. For these reasons, sheaves of rods with parallel by-pass flow received the greatest amount of our attention.

Documentation for computation of H in both types of an infinite lattice represents the dependence of the grometrical criterion L^* or of the geometrical factor H on lattice density δ/d. The graphic form of these dependencies processed on computer GIER is shown in fig. 39. Comparison of experimental and computed values can be most vividly performed by comparing the relations

$$\frac{\xi}{\xi_0} = f (\delta/d) \tag{45}$$

wherein ξ_0 is the coefficient of friction losses in a circular channel at a given Re. The relation (45) can be substantially simplified for computation. The criterial relation for the coefficient of friction

26

losses (21) can be substituted in the region Re < 10^5 by the relation

$$\frac{\xi}{H} = 0.316 \ (\frac{Re}{H})^{-0.25} \tag{46}$$

After substitution from equation (46) into the relation (45) we obtain

$$\frac{\xi}{\xi_0} = H^{1.25} \tag{47}$$

wherein $H = \oint (\Delta/d)$.

A comparison of this relation with experimental values for a tri- /43
angular lattice is shown in fig. 41. It can be stated that there is a
congruence of almost 100%.

Investigations of velocity fields and of the distribution of tan-
gential stress in an infinite triangulat lattice routinely make use of
models with a configuration shown in fig. 42. However, due to their
infinite dimensions these models are not suited for investigation of
pressure losses, as has been experimentally shown a number of times
already. Fig. 42 shows a comparison of experimental and computed
values for this type of channel. For the sake of comparison, the same
figure shows the theoretical dependence for an infinite lattice. The
deviations of experimental values from theoretical dependence are
smaller than is the dispersion of experimental points. Figures 43 and
44 show a comparison of the experimental dependence of $\xi = \oint (Re)$ with
theoretical dependence for various types of lattice density. Their
coincidence is outstanding in all cases. Figure 44 also shows the
potential extent of effects on overall losses that can be caused by
inert draughts between sheaves of rods and the channel proper.

The same conclusions, in regards to congruence between theoretic-
al dependence and experimental results, can be drawn from diagrams 45,
46 and 47, which show a comparison for the elements of a square lat-
tice and an inifinite square lattice.

Into this group of channels we could also include the channel in
fig. 54. Three rods are placed in a triangular channel with rounded
corners. Study [33] investigated the dependence of pressure losses
in relation to the relative separation of rods. The forms of theoret-
ical and experimental dependence are very similar in spite of the fact
that dependence $\xi = \oint (S/d)$ is not monotonous. However, with decreas-
ing value of S/d the differences between the two progresses increase.
Nevertheless, it is difficult to reach any conclusions from this com-
parison. Experimental values were obtained for small values and a
narrow range of Reynold's number. Figure 55 shows experimental re-
sults recomputed into the relationship $1/\sqrt{\xi} = \oint (Re\sqrt{\xi})$. It is very
difficult to determine from these progressions whether the measurement
was affected by the transitory region of ξ. However, that possibility
should not be excluded.

8.2 Channels With a Triangular Cross Section

Comparison of theoretical dependence with experimental values for
channels with a cross section in the shape of an isosceles triangle
turned out to go less in favor of theoretical dependence than was the /44

27

case in the preceding instance. Comparison of theory and experiment at varying values of the apex angle β of a channel is shown in fig. 49 which has been essentially taken over from study [32].. In regard to form, theoretical and experimental dependence is mutually similar and at a value of β = 60° they coincide also as to their absolute value. However, with decreasing β the difference between the two dependencies increases up to 12%. The progress of both dependences is interesting in the region β→0. We originally mistakenly assumed that this limiting case corresponds to parallel plates. Only computation of the geometrical criterion L^* for a uniform trapezoid with varying values of the apex angle and varying ratio of height to base (fig. 52) showed how strongly changes the character of the dependence $L^* = \int (t/H)$ in the region β→0, $t/h→0$.

The small divergence between theoretical and experimental progress could be explained on the basis of the results obtained in the previously cited study [30]. The latter does not exclude the possibility that in the region of Re, in which the triangular channels were investigated, in a part of the channel could occur laminar flow. In that case the measurement results would be affected by the transitory region ξ.

8.3 Sheaf of Rods With LongitudinalFins

We undertook a comparison of the theoretical relation with experimental results obtained by V. Krett [37] for a sheaf of rods, each with three longitudinal fins. The channel diagram and the measurement results are shown in fig. 56. Theoretical dependence is very well centered on experimental results obtained for isothermal and nonisothermal flow.

8.4 Eccentric Annulus

Eccentric annulus represents a typical example of a channel in which use of hydraulic diameter as a characteristic dimension fails. The more we were interested to find out how well would apply the criterial relation (21) with relation (35). As we did not have at our disposal any studies providing experimental values, we used for comparison the relation

$$\frac{\xi}{\xi_{\varepsilon=0}} = (1 - \varepsilon)^{0.178} \tag{48}$$

(where is eccentricity) which was used in study [34] and was assess- /45
ed on the basis of experimental findings in studies [35] and [36]. This relation does not take into consideration the experimentally detected weak effects of curvature. Its validity is also limited in the direction of an increase in ε.

In fig. 57 this relation is compared to two theoretical dependences for D_1/D_2 = 0.5; 0.95. Congruence is again very good.

28

1. An analysis of our and other authors' experimental findings in the measurement of friction and pressure losses in noncircular channels with hydraulically smooth walls showed that in all cases in which the results have not been affected by distorting factors, the dependence $\xi = \int (Re)$ can be applied by simple transformation to the Prandtlian universal law of friction in a smooth tube. The transformation relation is hereby merely a function of channel geometry.

2. On the basis of empirical findings we formulated general requirements for selection of geometrical characteristics factors which could play at a higher level a role similar to that played by hydraulic diameter at the outset of research into flux in noncircular channels. On the basis of these requirements we defined integral geometrical characteristics (criteria) and it was empirically proven that these criteria relatively unequivocally define the geometry of noncircular channels from the viewpoint of pressure losses and transfer of heat.

3. We used these geometrical criteria to process experimental materiel from research of pressure losses and of heat transfer in circular and annular channels with longitudinal fins. In this manner we obtained universal criterial relations for the coefficient of pressure losses and the Nusselt criterion. (Validity of the relation for Nu is of course milited to gaseous media with $Pr \sim 1.$)

4. Comparison of the criterial relation for ξ with published experimental values for noncircular channels showed applicability of this relation for channels with the most varied configuration with hydraulically smooth walls.

5. Unification and generalization of experimental materiel which is facilitated by these criterial relations make it possible to expand our knowledge in regards to flux conditions in noncircular channels as regards integral characteristics and provide an improved basis for the study of turbulent flow theory than was offered previously by the widely splintered experimental materiel.

10. REFERENCES

1. Malák, J., Řezníček, M., Červenka J. and J. Hejna, "Hydrodynamics and Thermokinetics in Annular Channels With Longitudinal Fins," Institute of Nuclear Research, Report 2187/R,T/1969.

2. Červenka, J., Hejna, J. Malák, J. and M. Řezníček, "Hydrodynamics and Thermokinetics in Circular Channels With Longitudinal Fins," Institute of Nuclear Research, Report 2501/R,T/1970.

3. Rybáček, K., "Selected Cases of Heat Transmission During Longitudinal By-Pass Flow of Elements, Particularly Those With an Expanded Transfer Surface," State Research Institute of Thermal Engineering, Report 63-05033.

4. Ort, J., "Experimental Research of Turbulent Flow and Heat Transfer in Annular Joints Flown-through by a Gaseous Medium," State Research Institute of Thermal Engineering, Report 64-08004.

5. Gotovskiy, M.A. and E.V. Firsova, "Heat Transfer and Hydrodynamics in Elements of Power Systems," Trudy CKTI, 73, 1966.

6. Buleyev, N.I., "Heat Transfer," Compendium, Moscow 1962.

7. Ibragimov, M.Ch., Isupoc, Y.A., Kobzar, L.L. and V.I. Subbotin, Atomnaya energiya 21, 1966.

8. Subbotin, V.I., Ushakov, P.A., Levchenko, Y.D. and A.M. Aleksandrov, "Modelling of Thermodynamic Phenomena in the Active Zone of Fast Reactors," Paper presented at Czecho-Soviet Conference in CSSR, February 1970.

9. Shlykov, Y.P. and S.N. Tsarevskiy-Dyakin, Teploenergetika, 12.

10. Schlichting, H., "Boundary-Layer Theory," 6th edition, McGraw-Hill Book Company 1968.

11. Knudsen, J.G. and D.L. Katz, "Fluid Dynamics and Heat Transfer," McGraw-Hill Book Company 1958.

12. Kutateladze Ts.Ts., "Theory of Heat Exchange," Mashgiz 1962.

13. Novikov, Y.Y. and K.D. Voskresenskiy, "Applied Thermodynamics and Heat Transfer," Moscow 1961.

14. Mikheyev, M.A., "Basics of Heat Transmission," 2nd ed., Prague 1953.

15. Rotta, J., Ingenieur-Archiv, 24, 1956.

16. Gardner, K.A., Trans. ASME, November 1945.

17. Hejna, J., Malák, J., Pecha, P. and J. Schmid,, "Energy Optimization of Channel Geometry With Longitudinal Fins," Institute of Nuclear Research, Report 2544/R/1970.

30

18. Roberts, A., _Int. J. of H. and M. Transfer,_ 10/5, 1967.

19. Guirrenbach, F.J., "Heat Transfer During Turbulent Flow in Circular Channels," _Allg. Wärmetechnik,_ 9/13.

20. Sheynina, A.V., "Liquid Metals," (Compendium), Moscow 1967.

21. Levchenko, S.D., Subbotin, V.I., Ushakov, P.A. and A.V. Sheynina, "Liquid Metals," (Compendium), Moscow 1967.

22. Subbotin, V.I. et al., _Atomnaya energiya,_ 9/4, 1960.

23. Firsova, E.V., _Inzh. fiz. zhurnal,_ 15, 1963.

24. Miller P., et al., _A.I.Ch.E. Journal,_ 2/2, 1956.

25. Eifler, W. and R. Nijsing, _Nuclear Engineering and Design_ 5/1, 1967.

26. Tourneau, B.Le, at al., _Trans. ASME_ 79/8, 1957.

27. Gunn, D.J. and C.W.W. Darling, _Trans. Inst. Chem. Engrs._ 41, 1963.

28. Ushakov, P.A. et al, _Atomnaya energiya_ 13/2, 1962.

29. Schiller, L., _Zeitschrift f. angw. M. und M._ 3/1, 1925.

30. Eckert, E.R.G. and T.F. Irvine,Jr, _Trans. ASME_ 78, 1956.

31. Eckert, E.R.G. and T.F. Irvine,Jr, _Trans. ASME, Journal of Heat Transfer,_ May 1960.

32. Carlson, L.W. and T.F. Irvine,Jr., _Trans. ASME, Journal of Heat Transfer,_ November 1961.

33. Ibragimov, M. Kh., Isupov, I.A. and V.I. Subbotin, "Liquid Metals," (Compendium), Moscow 1967.

34. Yu, Wen-Shi and Orrington E. Dwyer, _Nuclear Science and Engineering,_ 24, 1966.

35. Diskind, T., Matos, C.A. and R.P. Stein, "Initial Experiments On Pressure Drop for Flow-through Eccentric Annuli," Columbia Univ., TID-5670, 1959.

36. Diskind, T., Leo, D., Lummis, R. and J. Vohr, "Basic Studies in Heat Transfer and Fluid Flow," NYO-9646 (1961). Columbia Univ. Quarterly Progress Report to the AEC.

37. Krett, V., "Research into Heat Transfer and Hydraulic Losses in a Sheaf of Finned Rods,", ŠKODA Plant Report no. Ae 1126/Concl.

38. Wantland, J.L., "Reactor Heat Transfer Conference of 1956," AEC Report TID, 7529, 525 (1957).

39. Gelin, P, _Comptes - rendus de l'Académie des Sciences_ 243, 1956.

40. Obukhov, A.M., _Prikladnaya matematika i mekhanika_ VI, 1942.

41. Rothfus, R.R., Monrad, C.C., Sikchi, K.G. and W.J. Heideger, _Ind. and Eng. Chemistry_ 47/5, May 1955.

11. List of Diagrams and Tables

Fig. 22 - Experimental dependence of $H = \delta(L^*)$ - results for geometries A and B and results obtained by K. Rybáček [3].

23 - Dependence of geometrical factor on geometrical criterion (L_{max}/d_h).

24 - Dependence of geometrical factor on geometrical criterion $(L^2_{max}/L.d_h)$.

25 - Processing of experimental results in the form of the relation $\frac{\xi}{H} = \delta(\frac{Re}{H})$ with geometrical factor value acc. to equation (35).

26 - Comparison of maximum velocity in laminar and turbulent flow through smooth annuli with maximum value of L.

27 - Values of the geometrical factor for varying curvatures of an annular channel derived from experiments and progress of $H = \delta(D_1/D_2)$ according to the relation (35).

28 - Experimental values of Nusselt's criterion for $Re\ 5.10^4$ and $\overline{\Psi} = 1.27$ and their dependence on the geometrical criterion $(L^* \frac{d_h}{d_T})$.

29 - Experimental values of Nusselt's criterion for $Re = 5.10^4$ and $\overline{\Psi} = 1.27$ and their dependence on the geometrical criterion $(L^* \frac{d_h}{d_T})$; differentiation between geometry A and B, including results obtained by K. Rybáček [3].

30 - Processing of the results of thermokinetic experiments on geometry A into the dependence form $\frac{1}{97}(L^* \frac{d_h}{d_T})^{0.91}$. $Nu = \delta(Re)$

31 - Processing of the results of thermokinetic experiments on geometry B into the dependence form $\frac{1}{97}(L^* \frac{d_h}{d_T})^{0.91}$. $Nu = \delta(Re)$

32 - Experimental values of $\frac{L_{T\ 1.1}}{d_h}$ and their dependence on L^*.

33 - Experimental values of $\frac{L_{T\ 1.1}}{d_h}$ and their dependence on $(L^* \frac{d_h}{d_T})$.

34 - Distribution of $\overline{\alpha}$ along the length of the model in the form of dependence $\frac{\alpha}{\alpha_\infty} - 1 = \delta(\frac{x}{L_{T\ 1.1}})$. Values of $L_{T\ 1.1}$ for individual variants computed from equation (42).

35 - Effects of the thermal factor on Nusselt's criterion at constant flow-through (no consideration given to change in Reynold's number due to thermal effects and effects of this change on Nu).

36 - Effects of the thermal factor on Nusselt's criterion at constant values of Re.

37 - Experimental values of exponent n as a function of criterion $(L^* \frac{d_h}{d_T})$.

38 - Experimental values of exponent n as a function of criterion L^*.

39 - Dependence of the geometrical criterion L^* and the geometrical factor H on the density of triangular and square lattices.

34

Fig. 1. Geometrical conditions at entry into investigated channel - geometry A.

CONICAL JUNCTION

$\phi\ 65.5$

15°

TUBE WITH INTERNAL FINS

FEED TUBE

Fig. 2. Geometrical conditions at entry into investigated channel - geometry B.

Fig. 3. Coefficient of friction losses in a smooth annulus.
Results of measurements by the Institute of Nuclear Research.

Fig. 4. Dependence of the coefficient of friction losses in a smooth annulus on channel curvature according to various authors. (Taken over from study [4].) For key to this figure see table on next page.

OUTLINE OF STUDIES REGARDING PRESSURE LOSSES IN SMOOTH ANNULI, THE RESILTS OF WHICH ARE COMPARED IN Fig. 4.

Ser.#	Author	Title	Re	Range D_1/D_2
1			$< 2,3 . 10^3$	$0 \div 1,0$
2	IDĚLČIK	Spravočnik po gidravličeskom soprotivleniju fassonych i prjamych	7.10^6	$0 \div 0,6; 1,0$
3	-"-	častij truboprovodov. Moskva 1960	3.10^6	$0 \div 0,6; 1,0$
4	-"-		$1,6.10^6$	$0 \div 0,6; 1,0$
5	BRAUER	Wärmeübergang in Ringspalten bei erzwungener Konvektion und örtlichen Sieden; Atomkernenergie, č.1, 1963	$2.10^3 \div 10^5$	$0 \div 0,8$
6	ROTHFUS	Fluid friction in noncircular ducts, Jour. AICHE Dec.1957	$3.10^3 \div 4.10^4$	$0 \div 0,6; 1,0$
7	ORT	Report SVÚTT č.64-08004	1.10^5	$0,77 - 0,93$
8	ORT	-"-	1.10^4	$0,77 \div 0,93$
9	WALKER-BIRD	Turbulent Newtonian flow in annuli. AICHE Journal 7/1961	5.10^3	$0 \div 0,5; 1,0$
10	-"-		$3,5.10^3 \div 2.10^4$	$0 \div 0,5; 1,0$
11	-"-		2.10^4	$0 \div 0,5; 1,0$
12	PYRÁČEK	Report SVÚTT č.63-05o33	3.10^4	$0,42 \div 0,84$
13	PYRÁČEK	-"-	10^5	$0,42 \div 0,84$
+		Institute of Nuclear Research	3.10^4	$0,625 \div 0,861$
15		Institute of Nuclear Research	10^5	$0,625 \div 0,861$
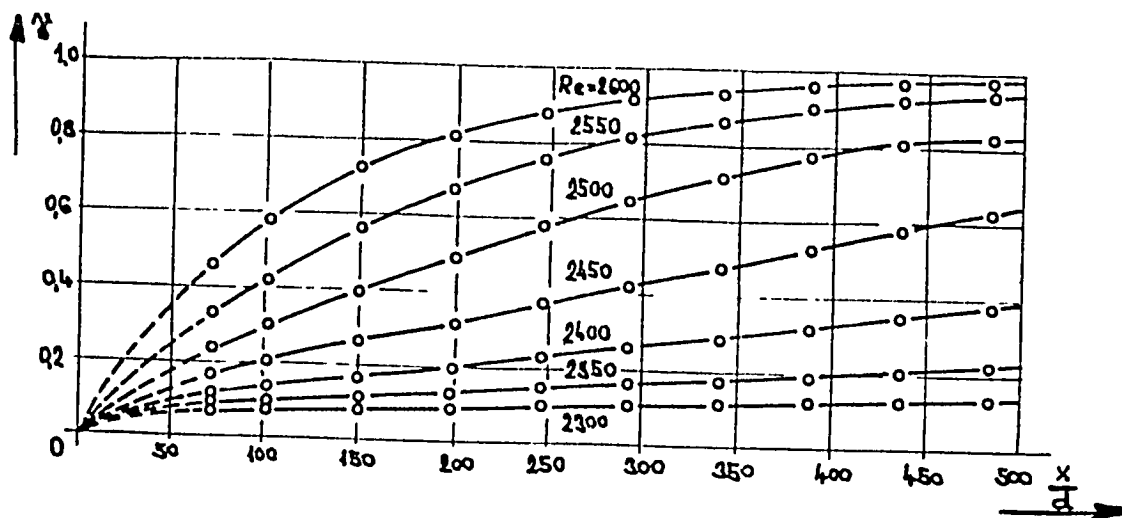
Fig. 5. Dependence of the coefficient of intermittency in a smooth tube on the distance from entry and the Reynold's criterion according to J. Rotta [15].
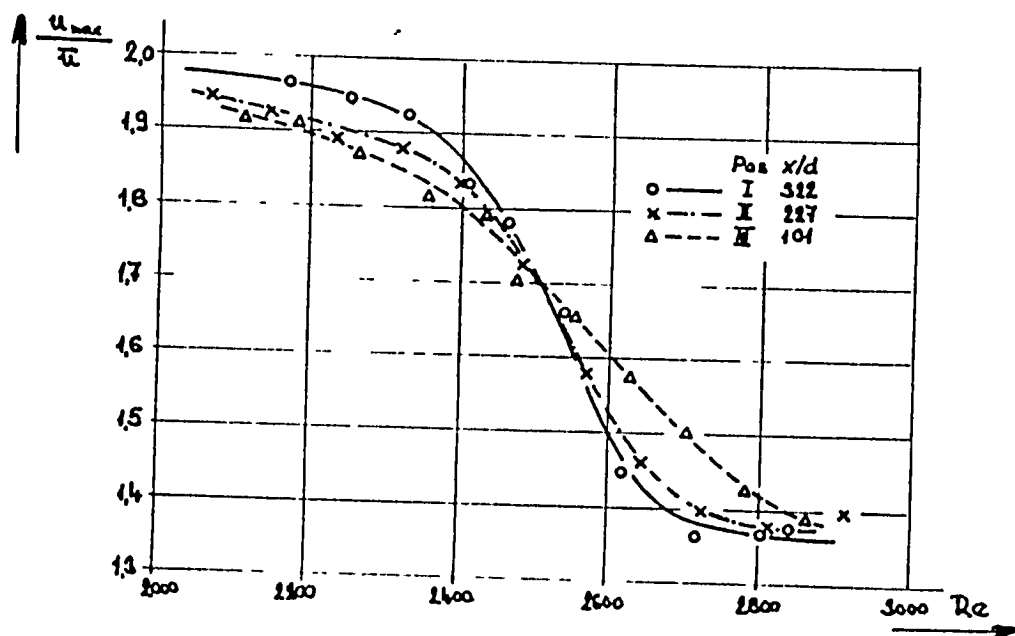
Fig. 6. Velocity changes along tube axis with the Reynold's number for three distances from entry [15].
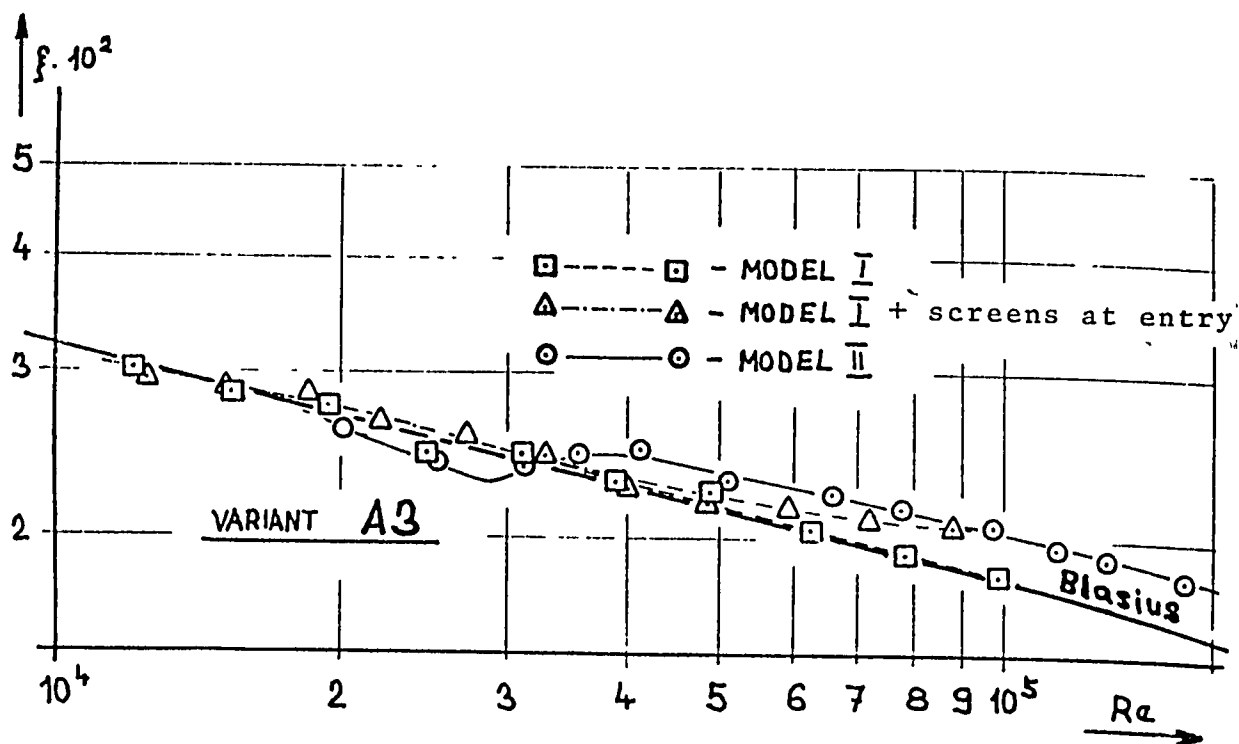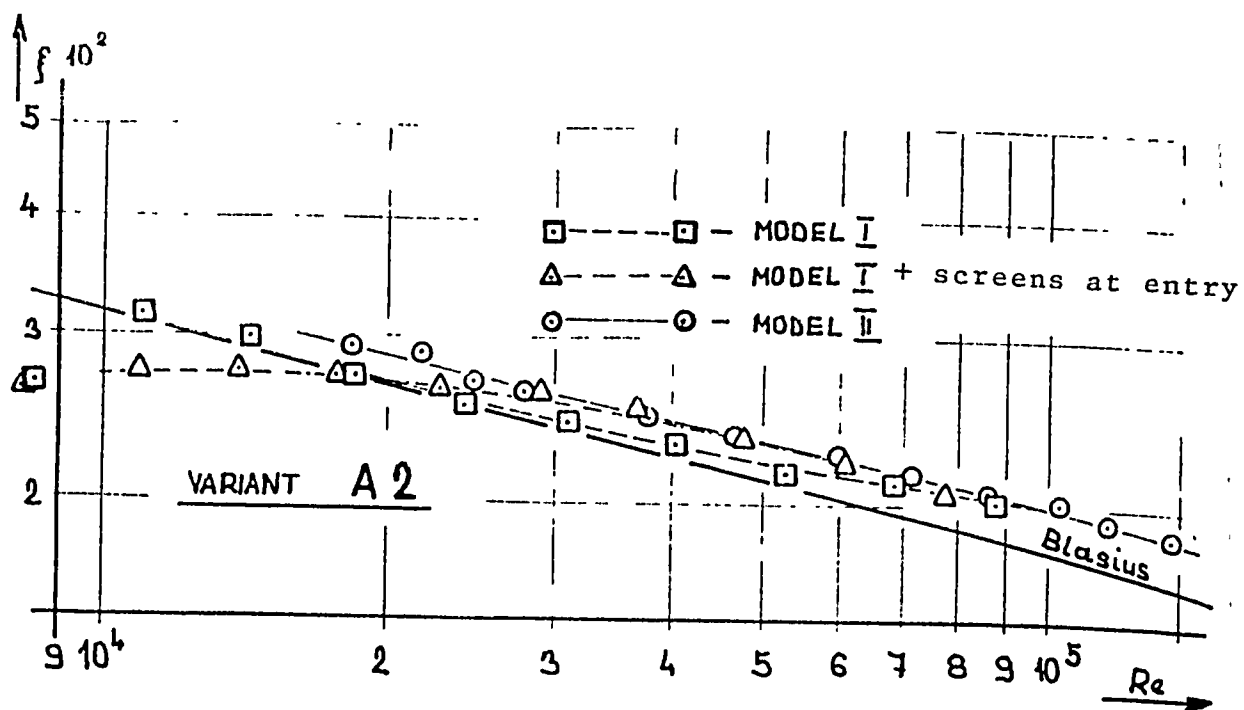
Fig. 7. Dependence of $\xi = \oint (Re)$ at varying conditions at entry into channels A2 and A3.
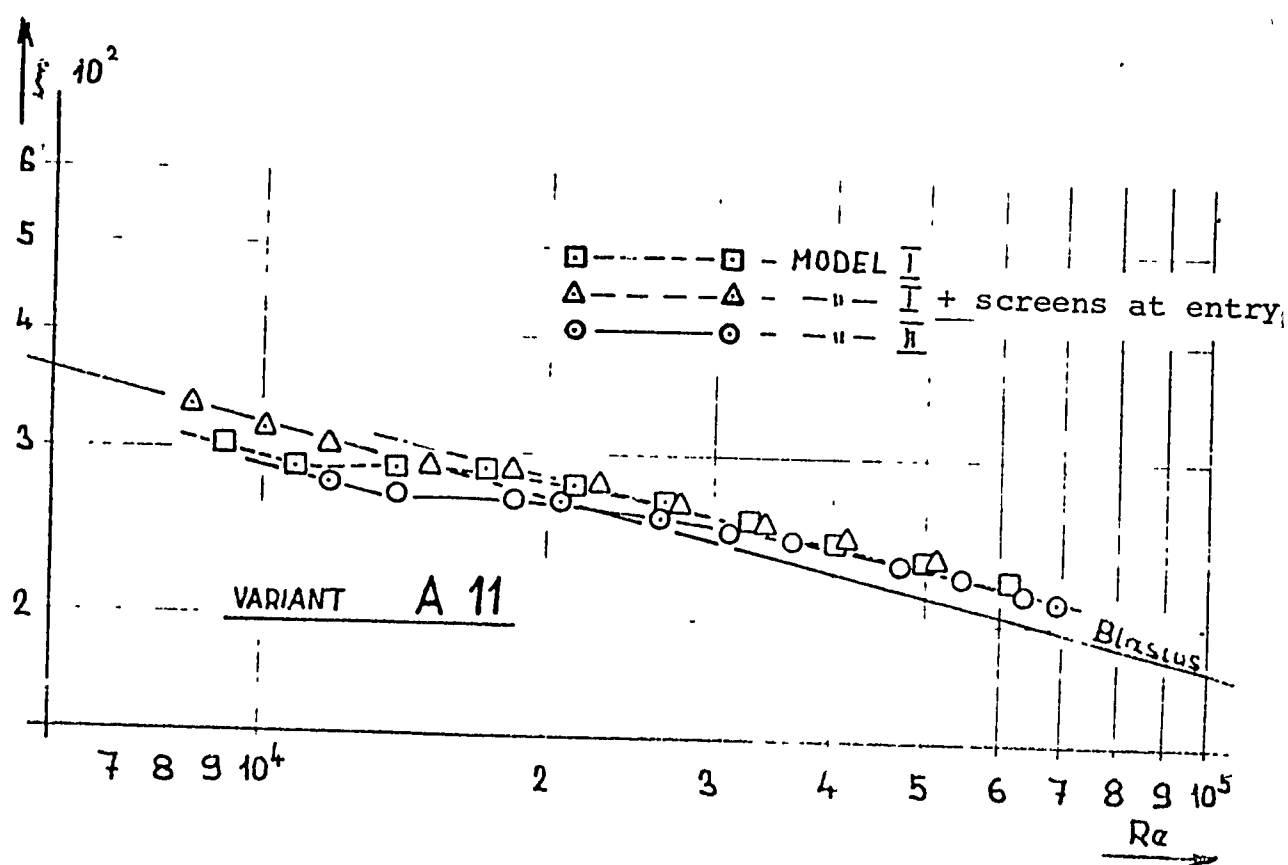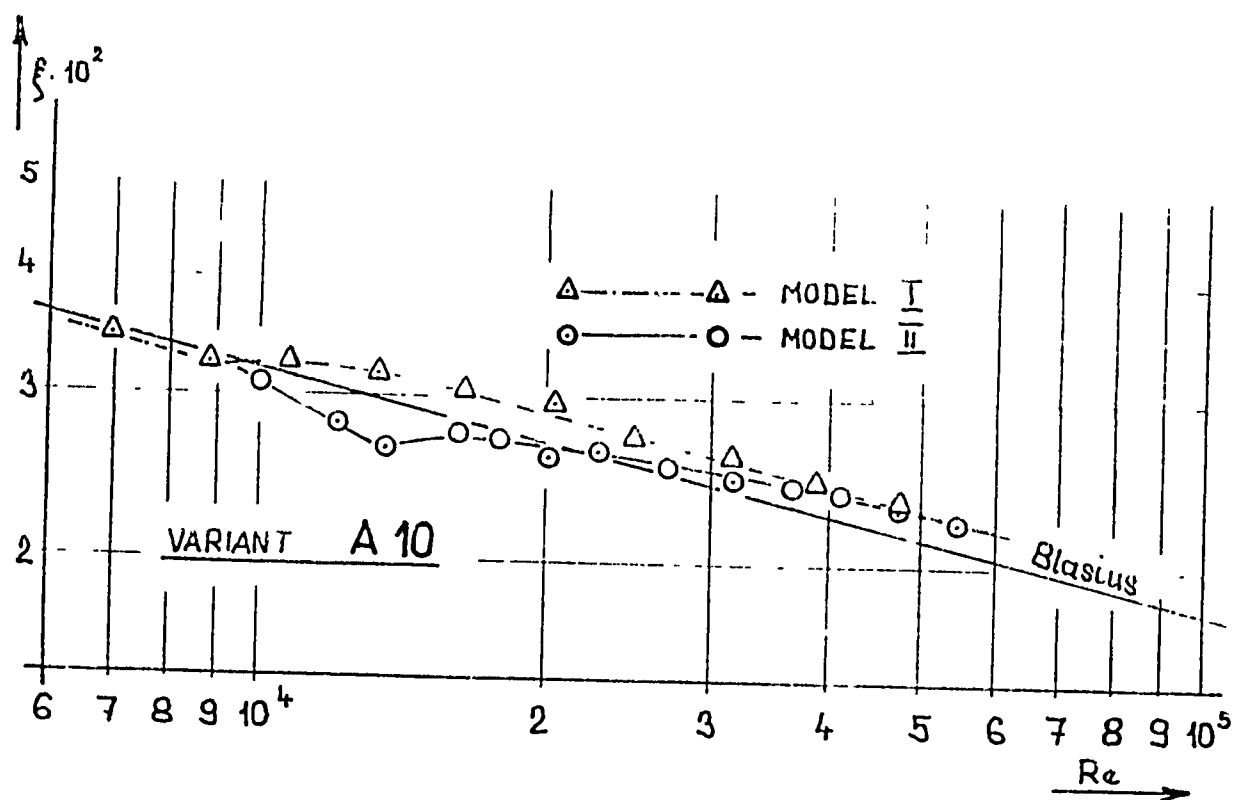
Fig. 8. Dependence of $\xi = \delta$ (Re) during varying conditions at entry into channels A10 and A11.

43
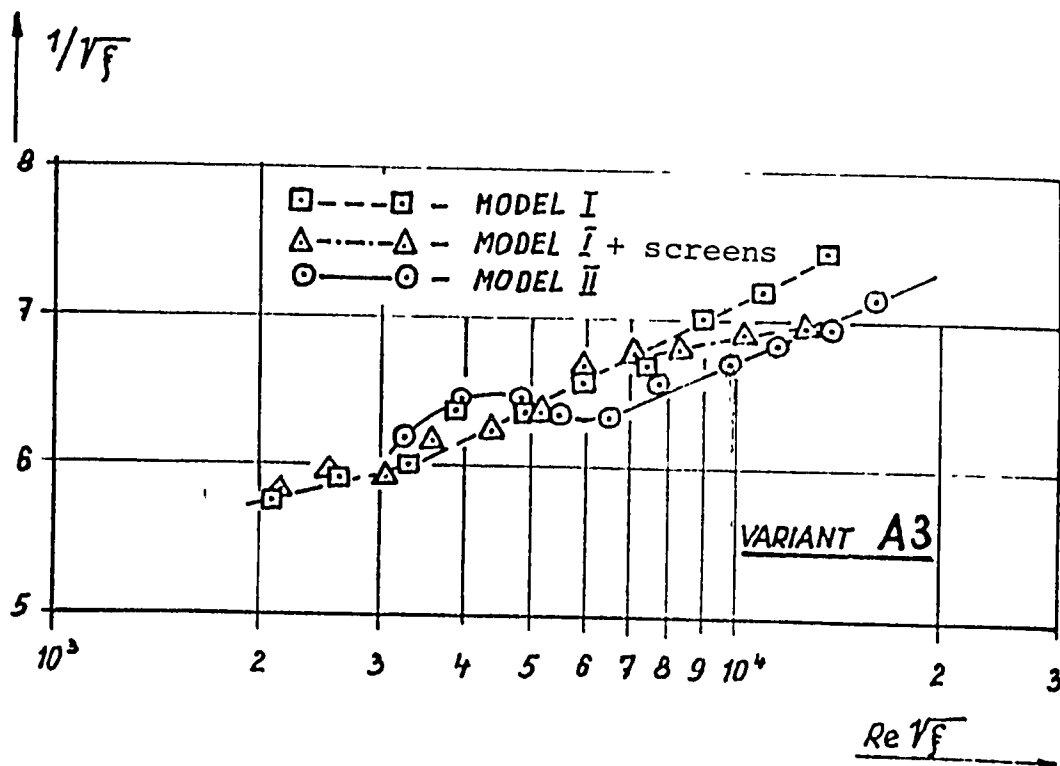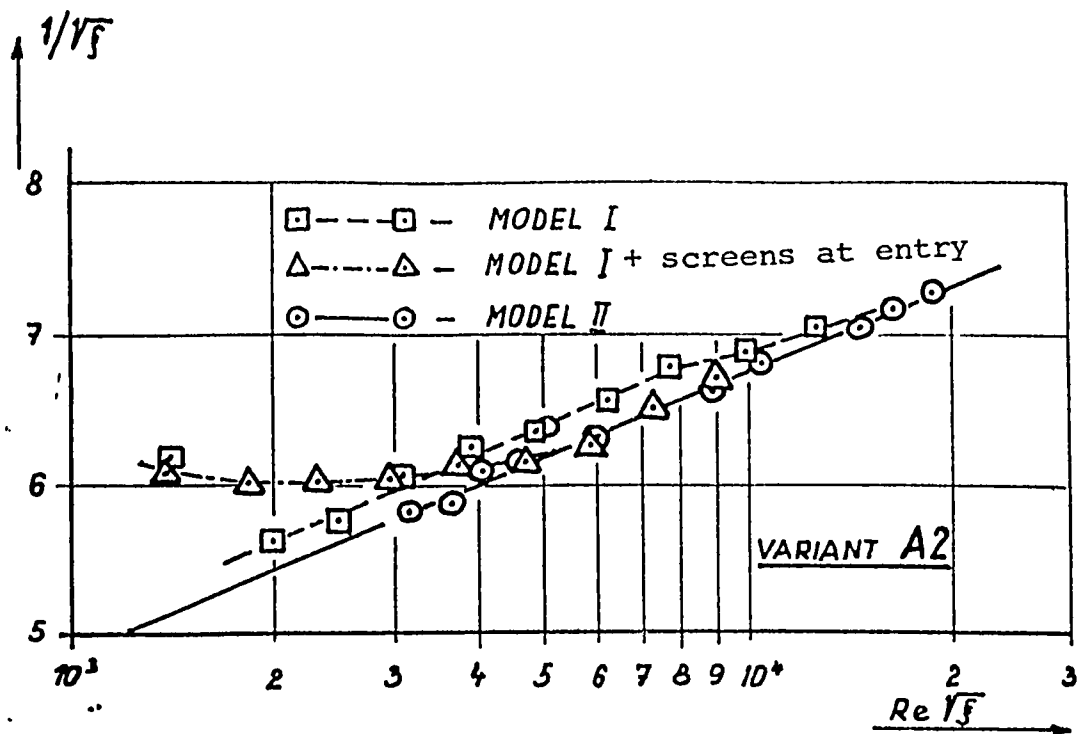
Fig. 9. Dependence of $1/\sqrt{\xi} = \int (Re\sqrt{\xi})$ during varying conditions at entry into channels A2 and A3.

44
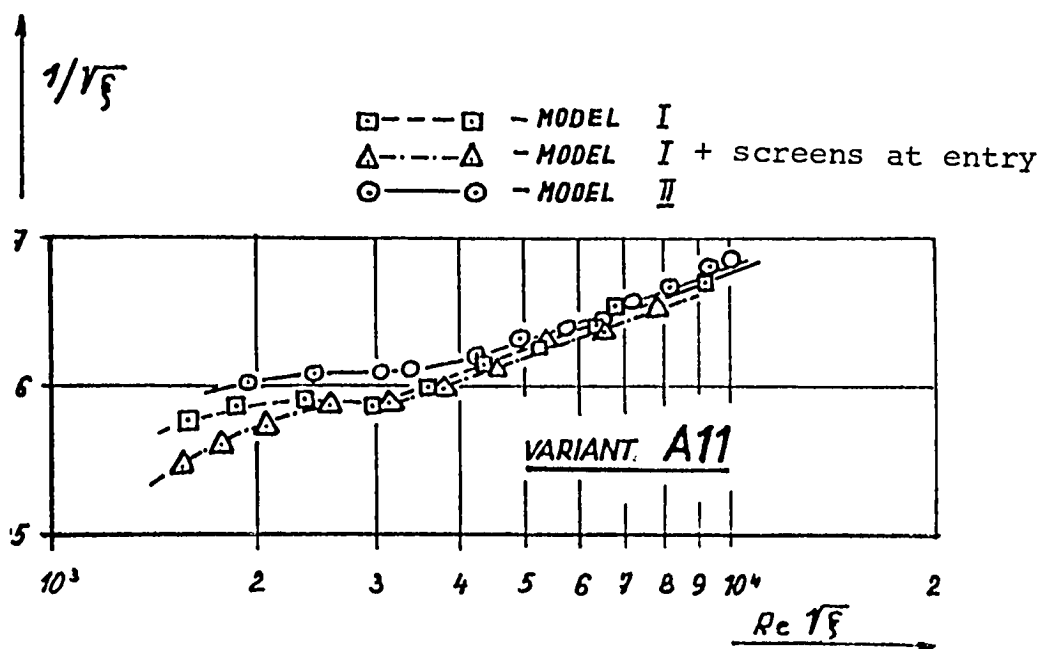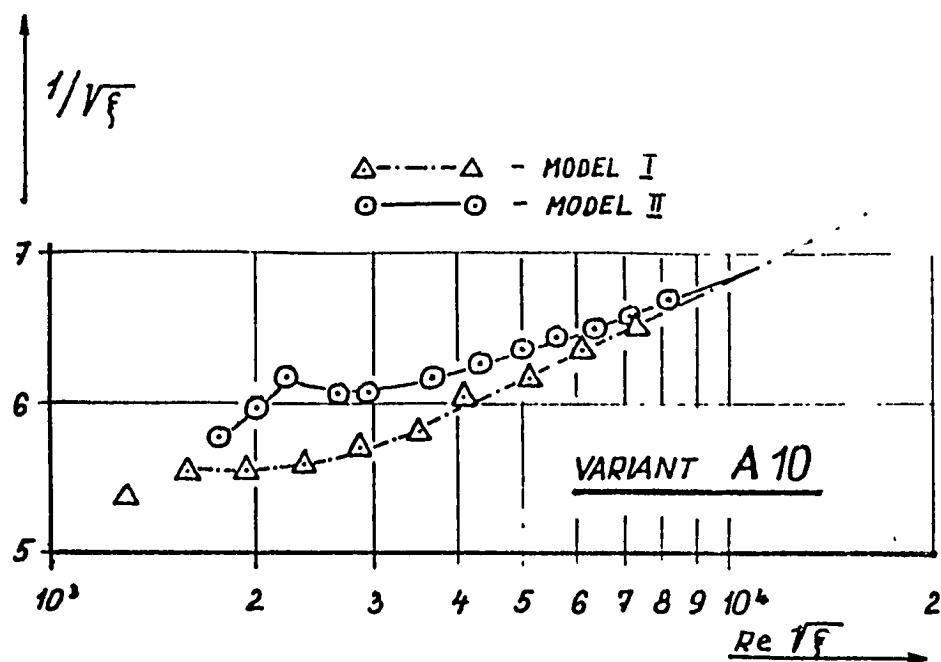
Fig. 10. Dependence of $1/\sqrt{\xi} = \oint (Re\sqrt{\xi})$ during varying conditions at entry into channels A10 and A11.
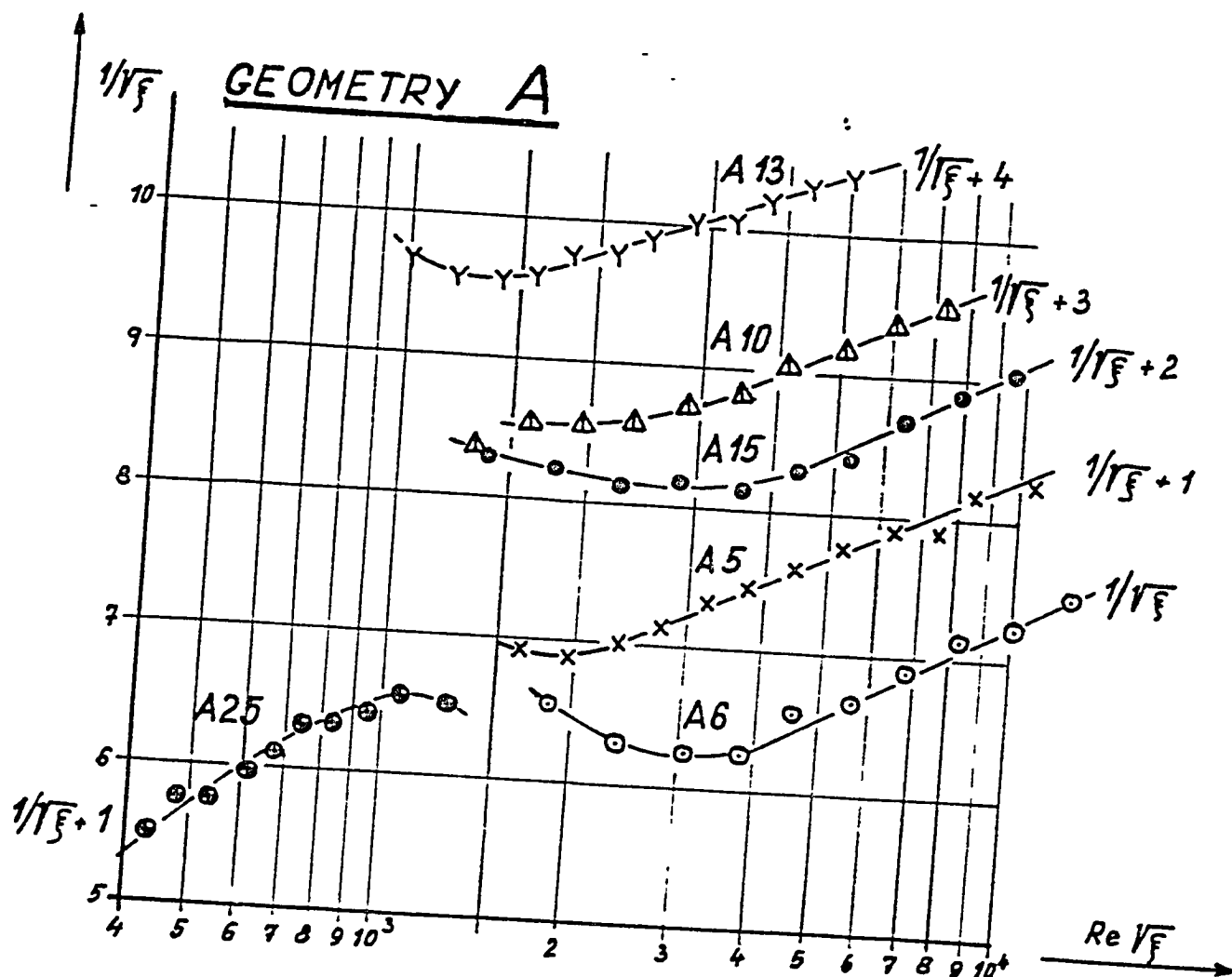
Fig. 11. Several examples of the form of experimental dependence of $1/\sqrt{\xi} = \oint (Re\sqrt{\xi})$ for geometry A.
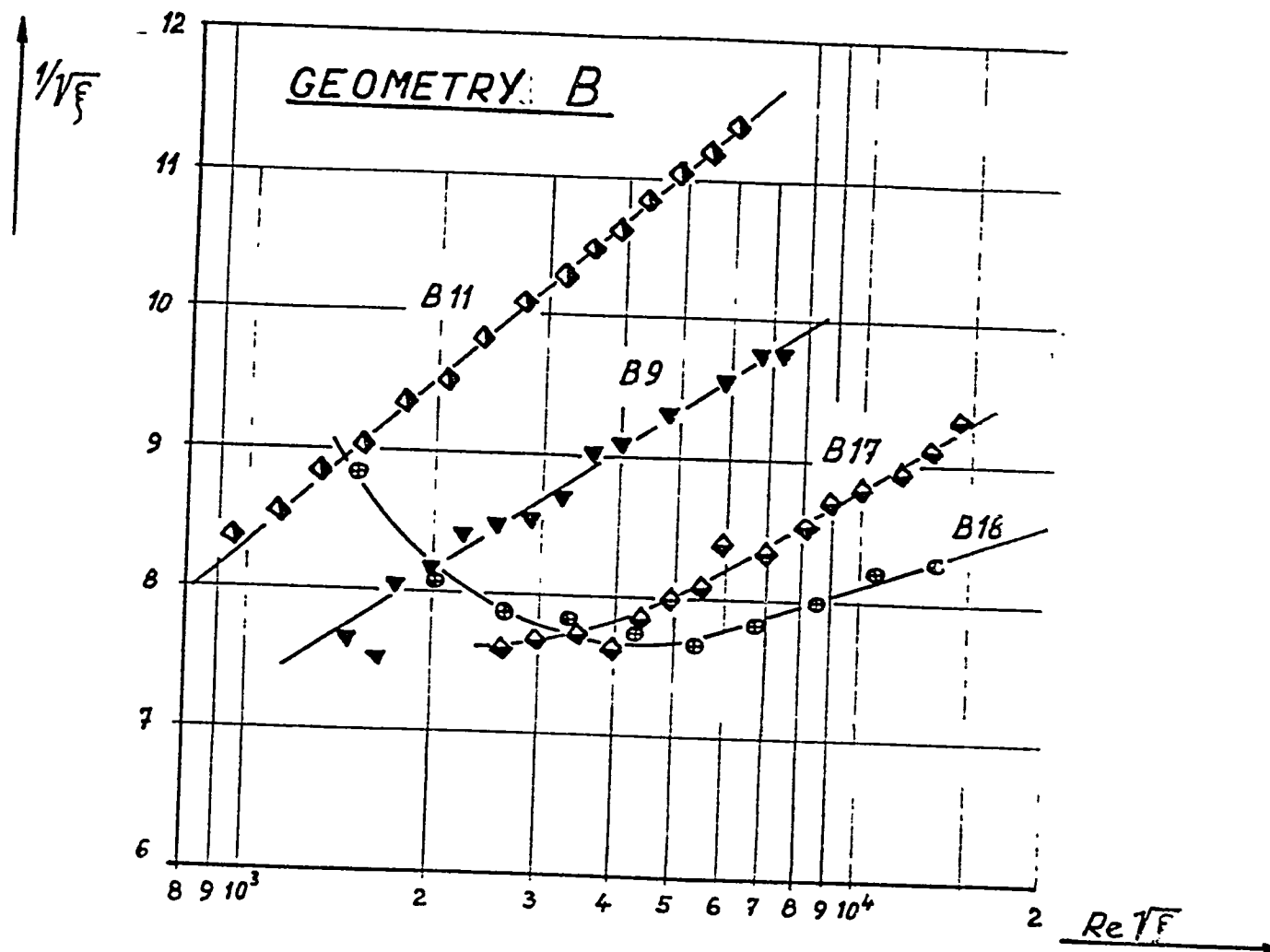
Fig. 12. Several examples of the form of experimental dependence of $1/\sqrt{\xi} = \delta \ (Re\sqrt{\xi})$ for geometry B.
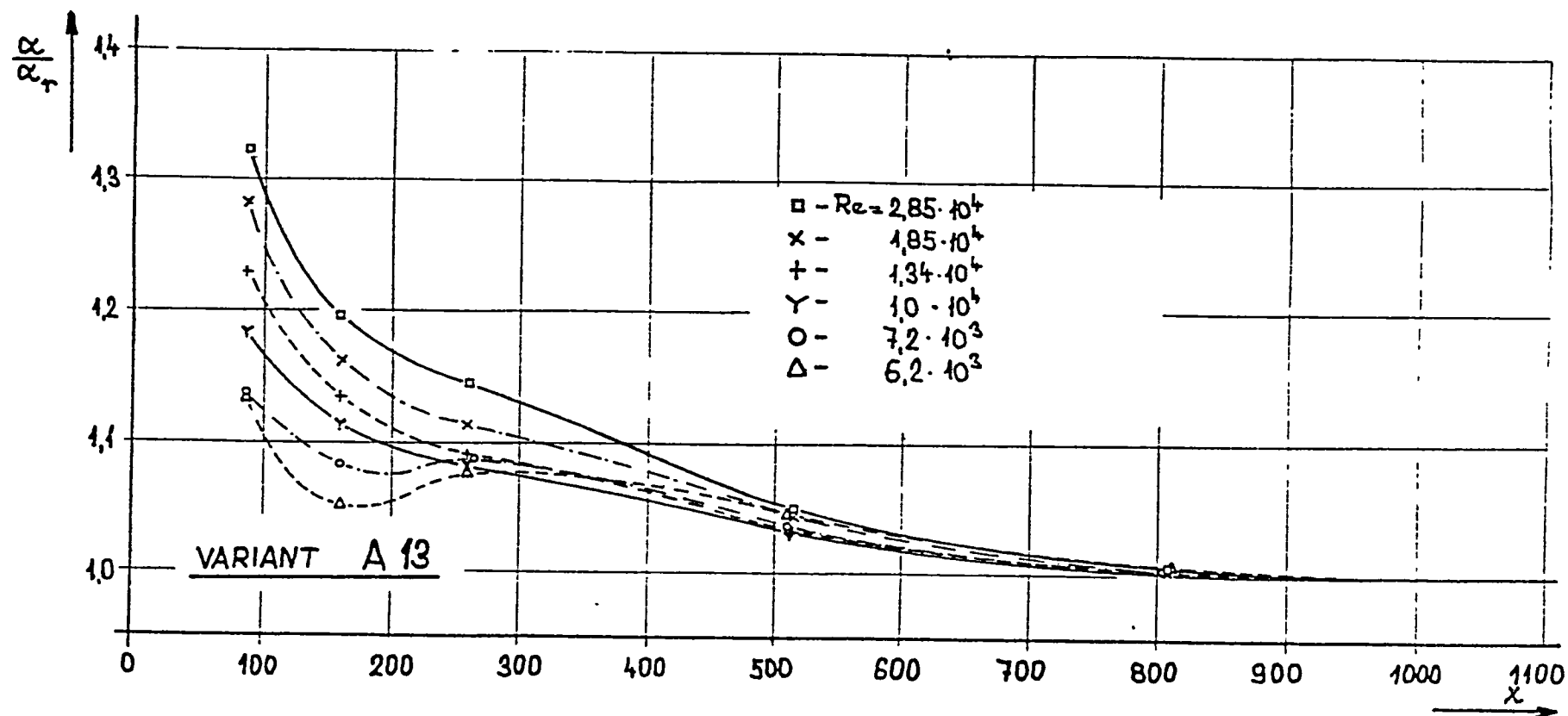
Fig. 13. Progress of α along the length of the model at varying Re.
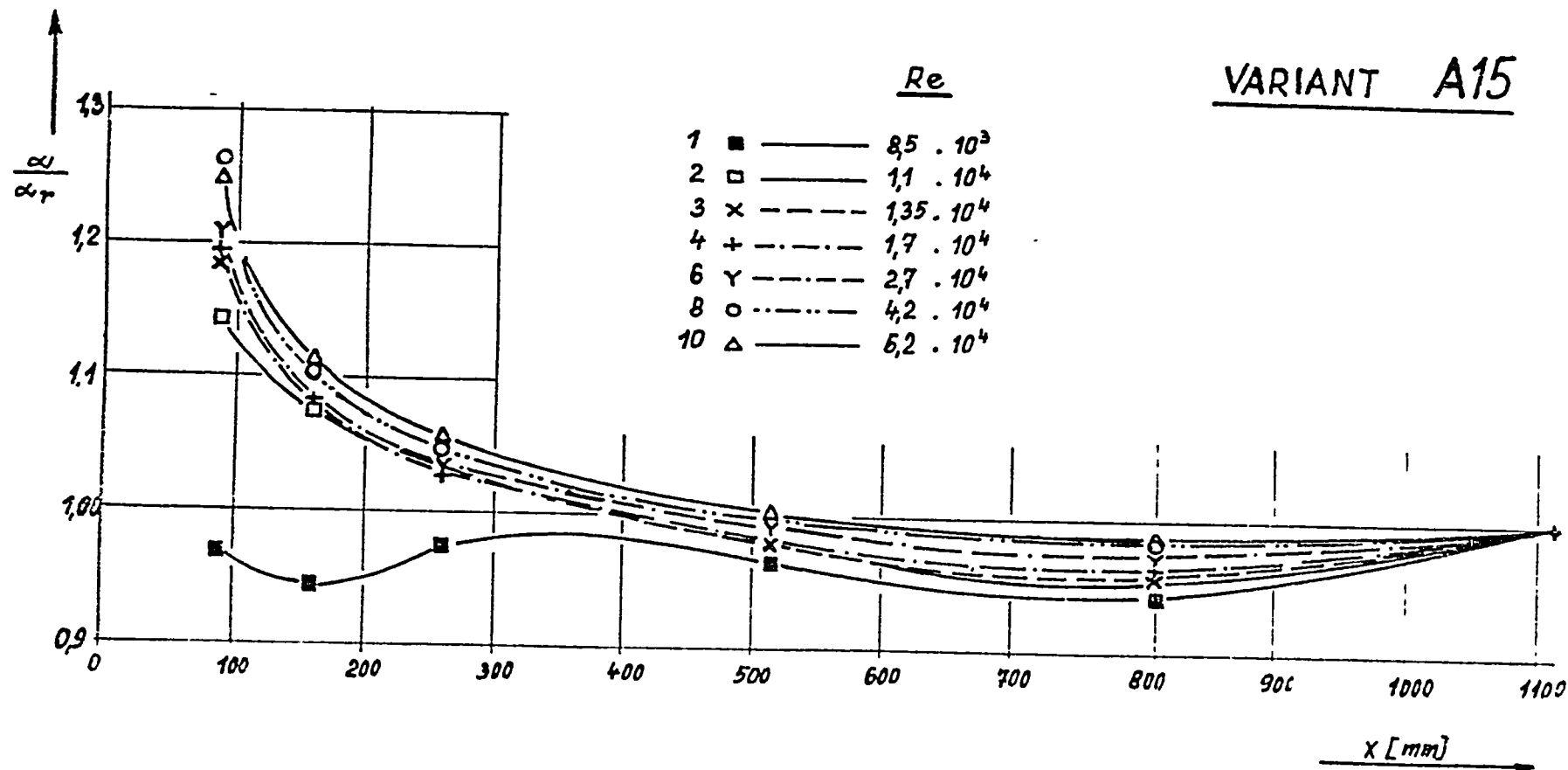
Fig. 14. Progress of α along the length of the model at varying Re.
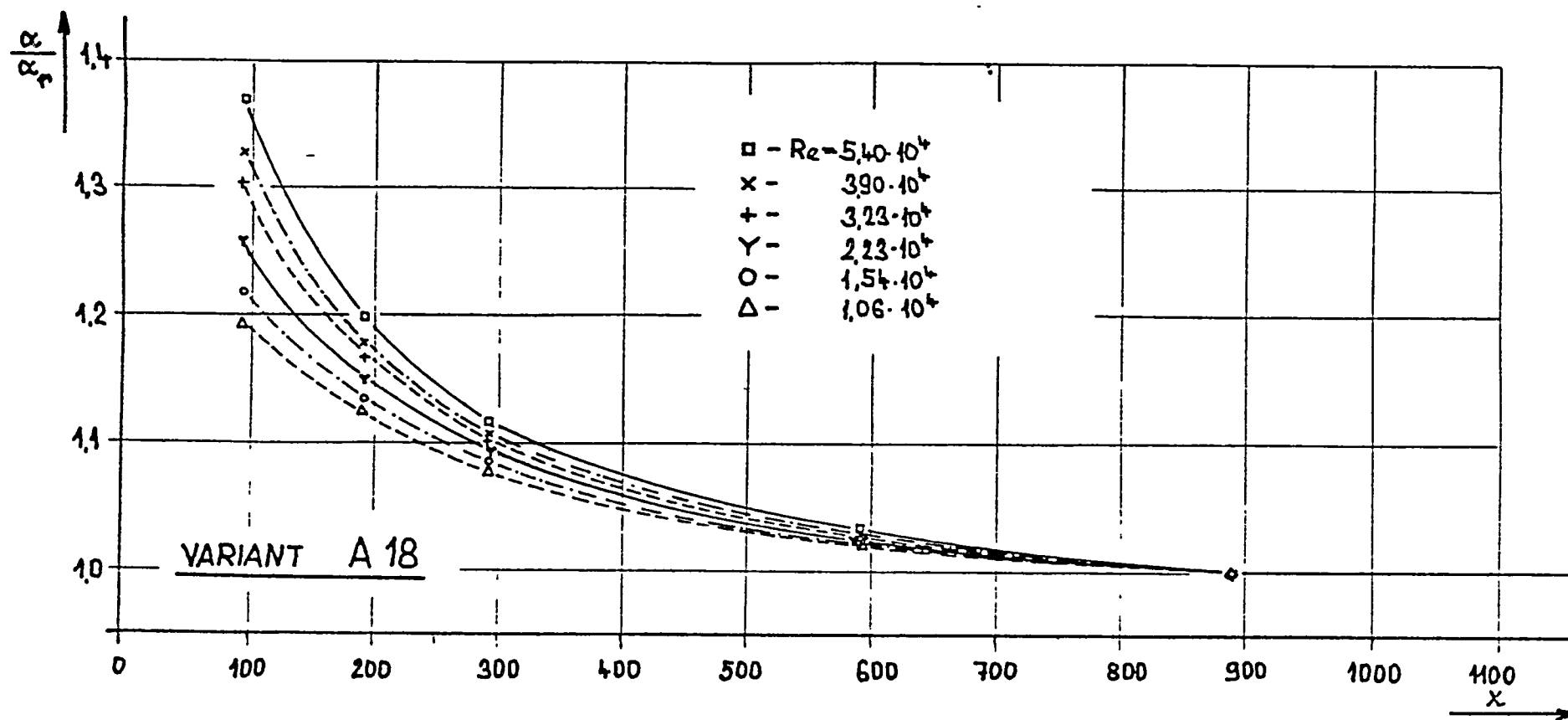
Fig. 15. Progress of α along the length of the model at varying Re.
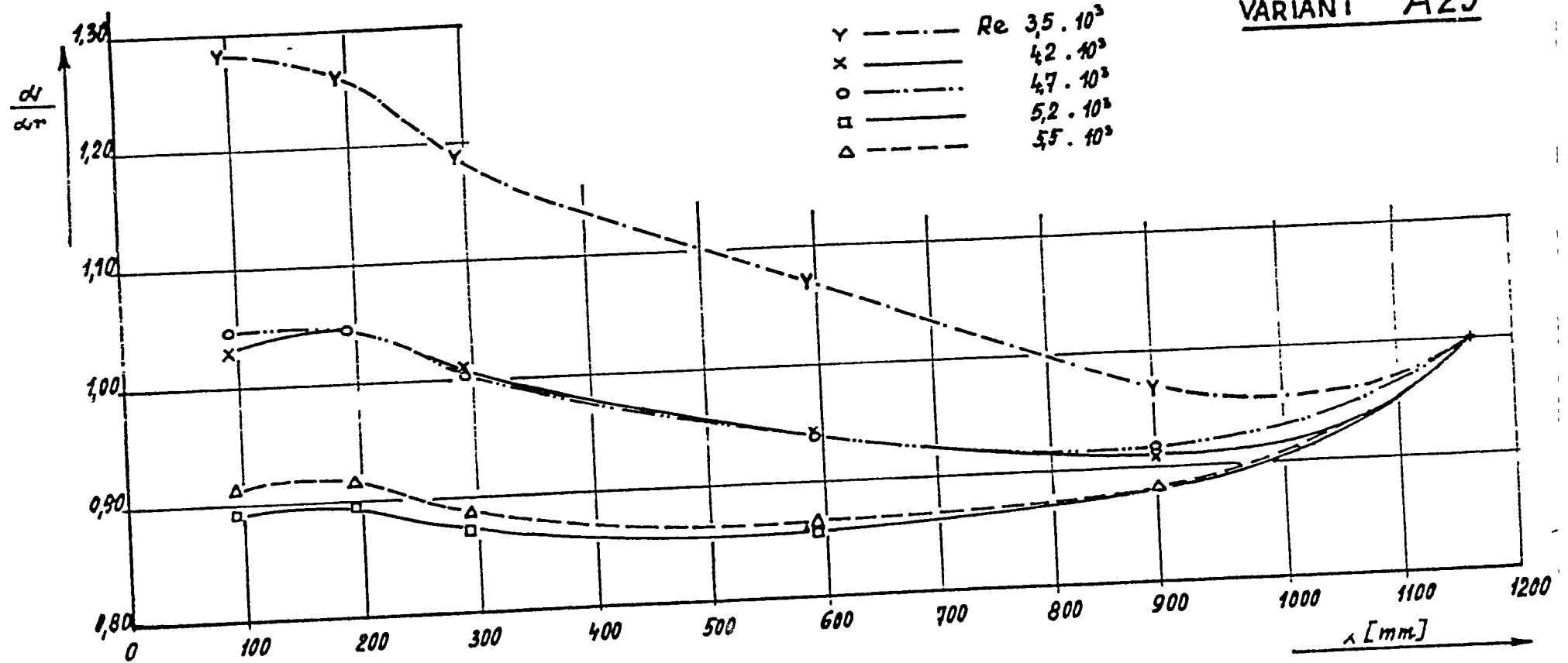
Figure 16. Progress of α along the length of the model at varying Re.
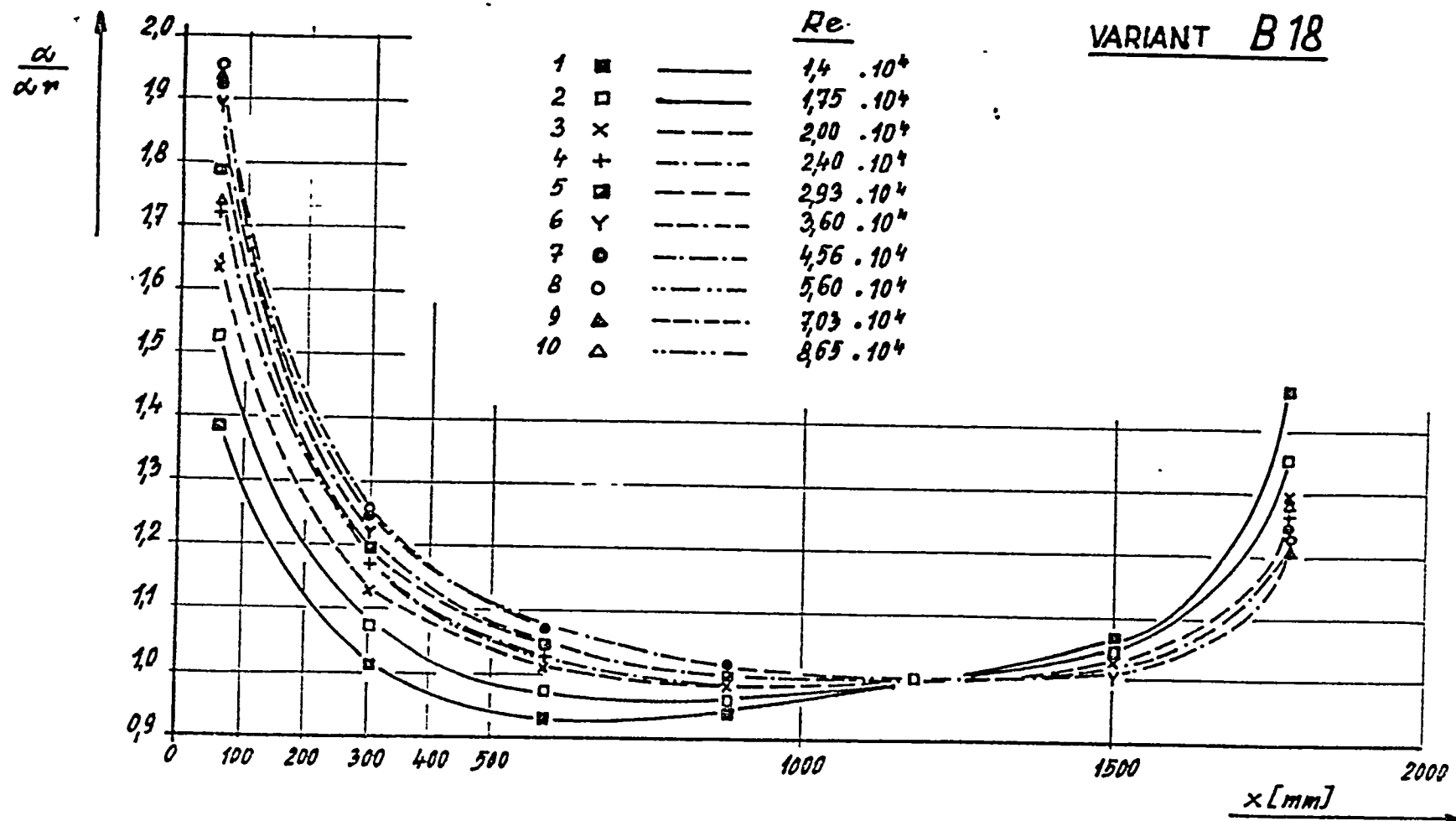
Fig. 17. Progress of α along the length of the model at varying Re.
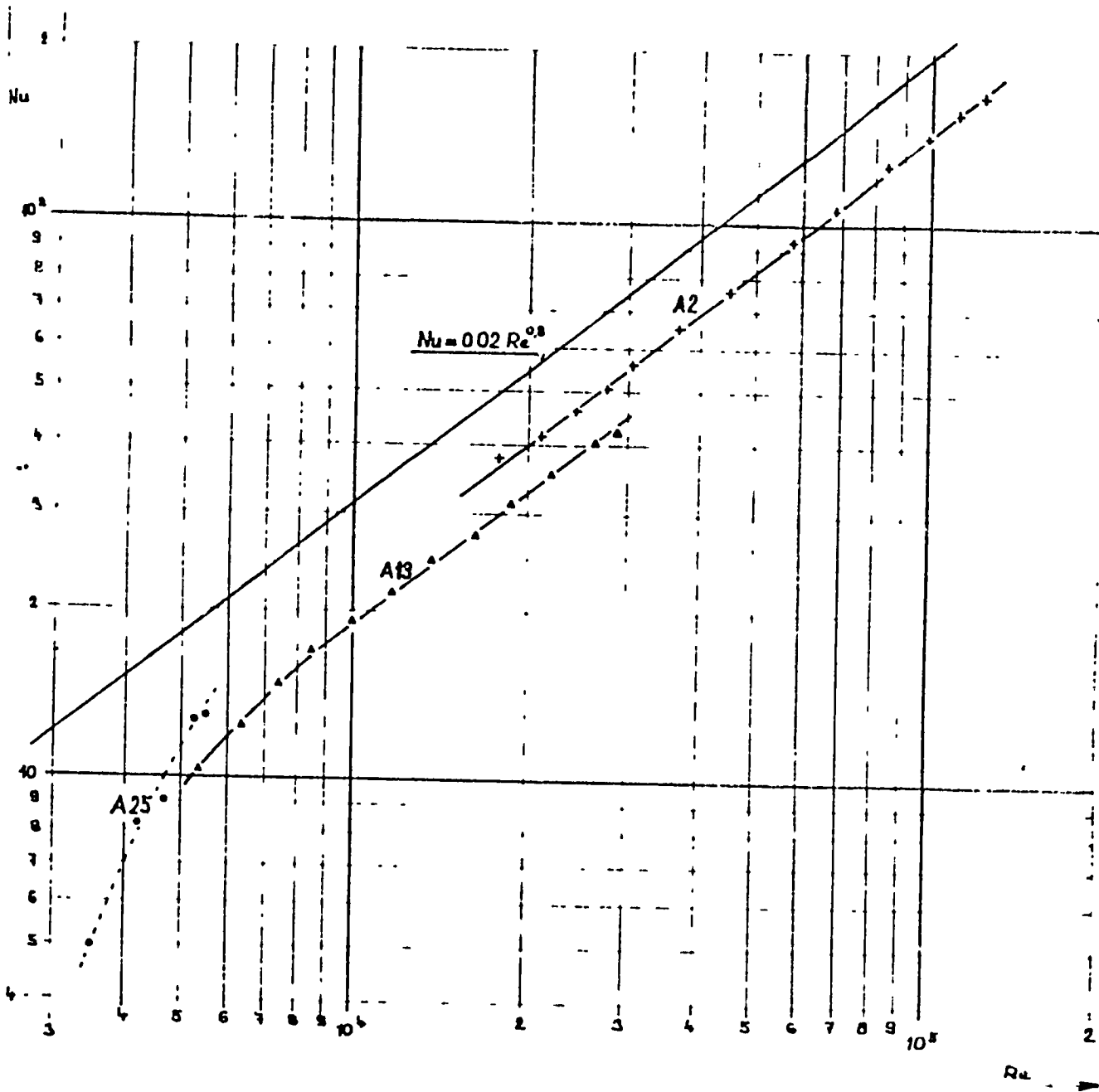
Fig. 18. Several examples of experimental dependence of $Nu = \oint (Re)$ for geometry A.

$$Nu = 0.02\, Re^{0.8}$$

Fig. 19. Several examples od experimental dependence of $Nu = f(Re)$ for geometry B.
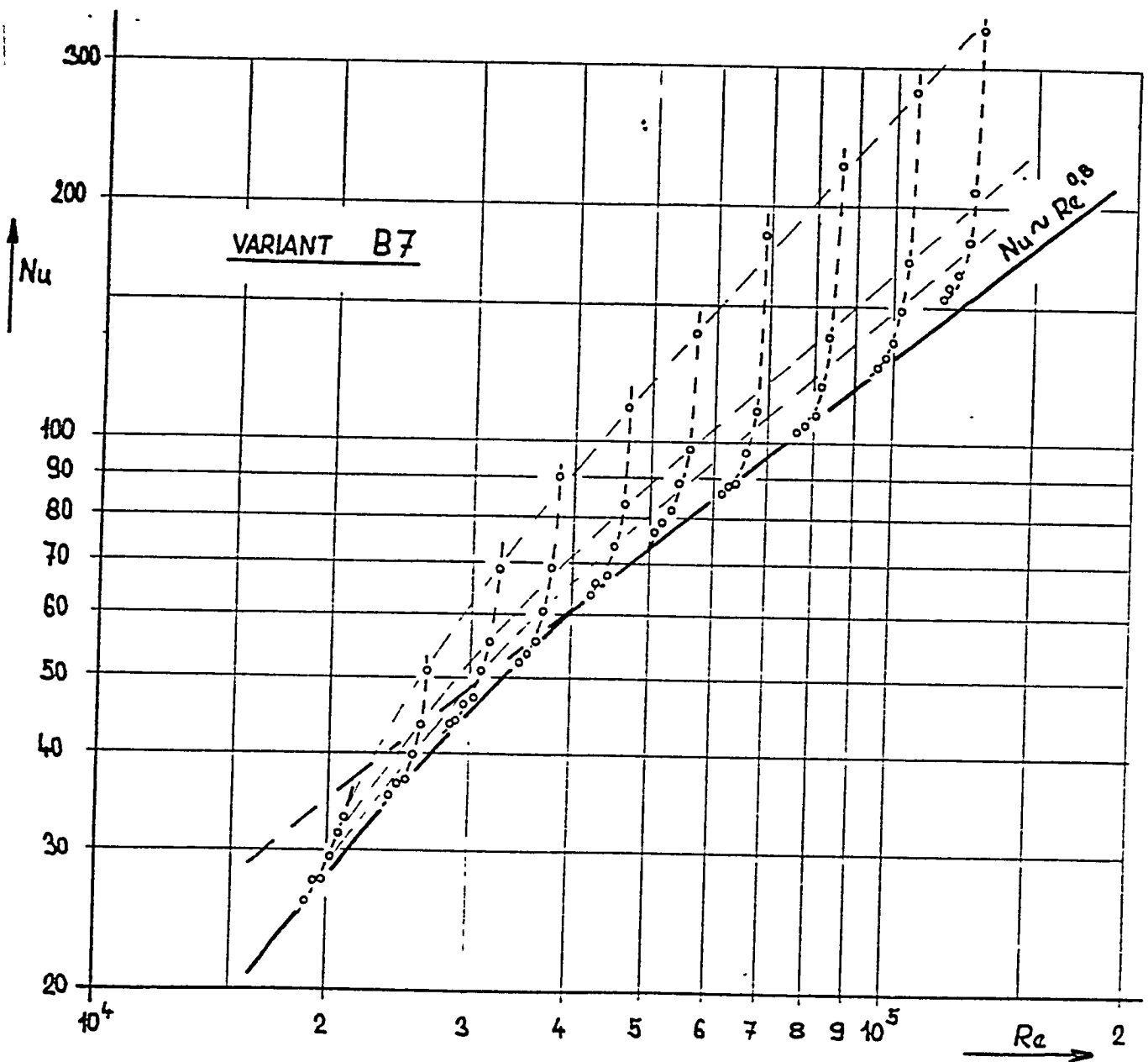
Fig. 20 Effects of the length of a heated model on the accuracy of determination of the dependence of $Nu = f$ (Re).
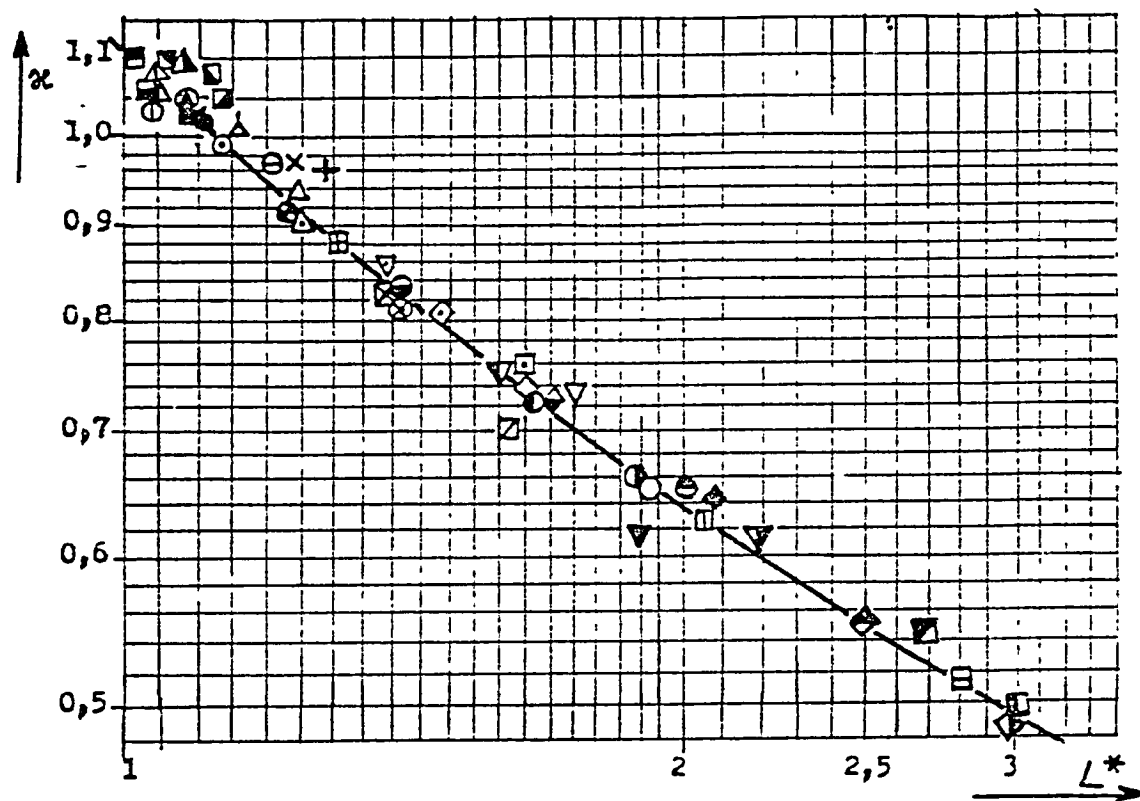
Fig. 21. Assessment of the dependence of the geometrical factor on the geometrical criterion L^* from the experiments conducted by the Institute of Nuclear Research.
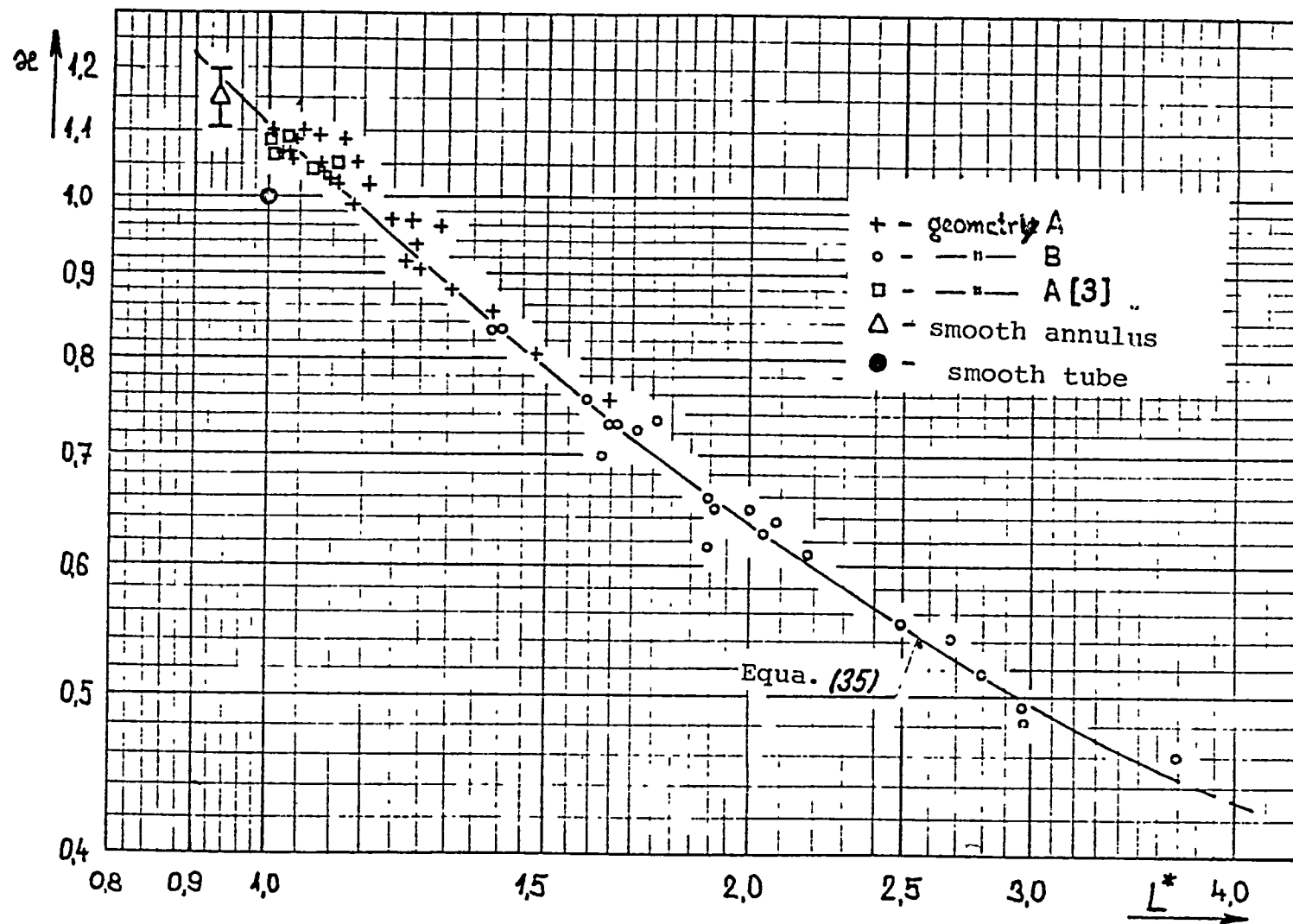
Fig. 22. Experimental dependence of $H = \oint(L^*)$ - results for geometries A and B and results obtained by K. Rybáček [3].
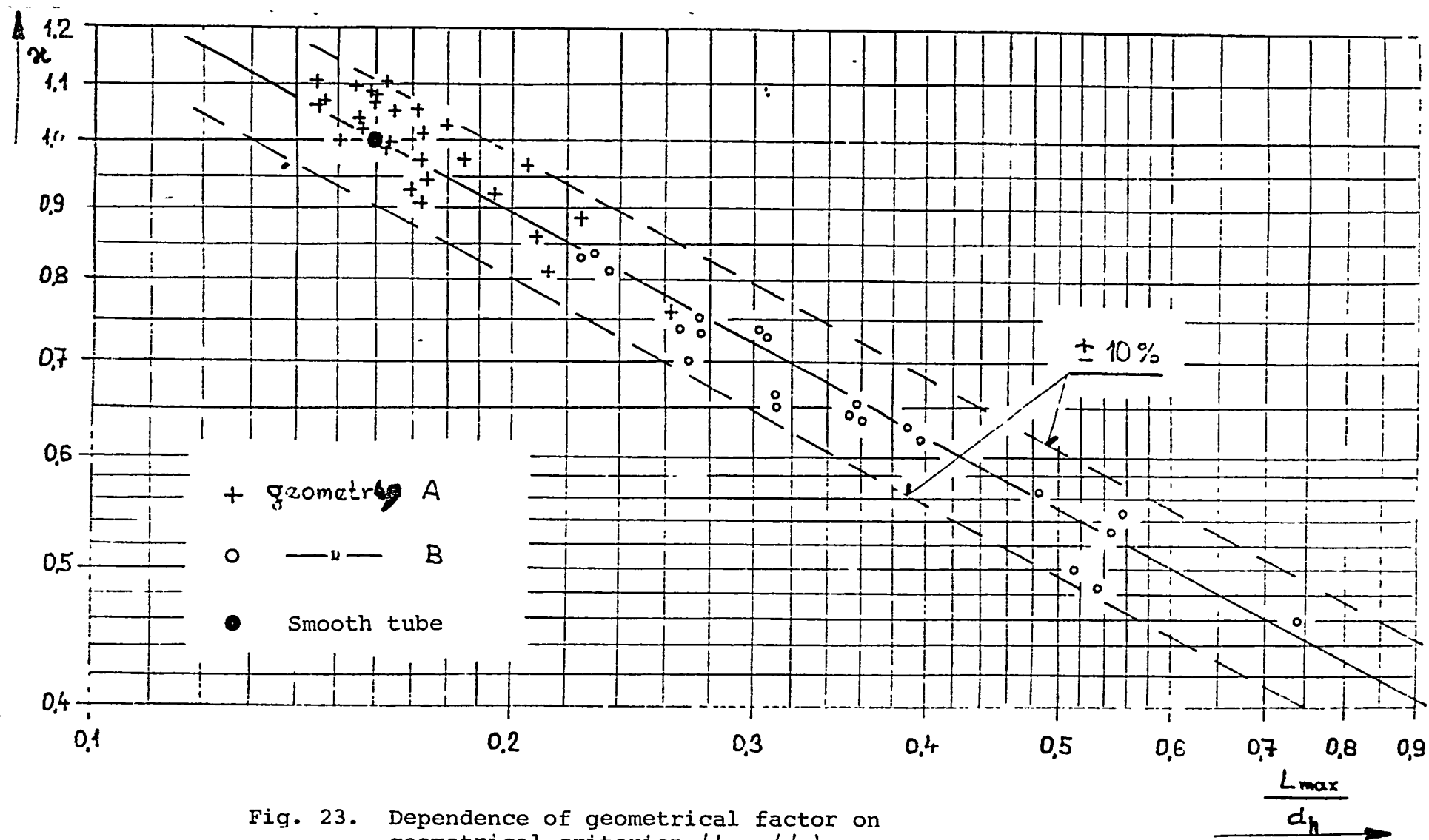
Fig. 23. Dependence of geometrical factor on
          geometrical criterion (L_{max}/d_h).
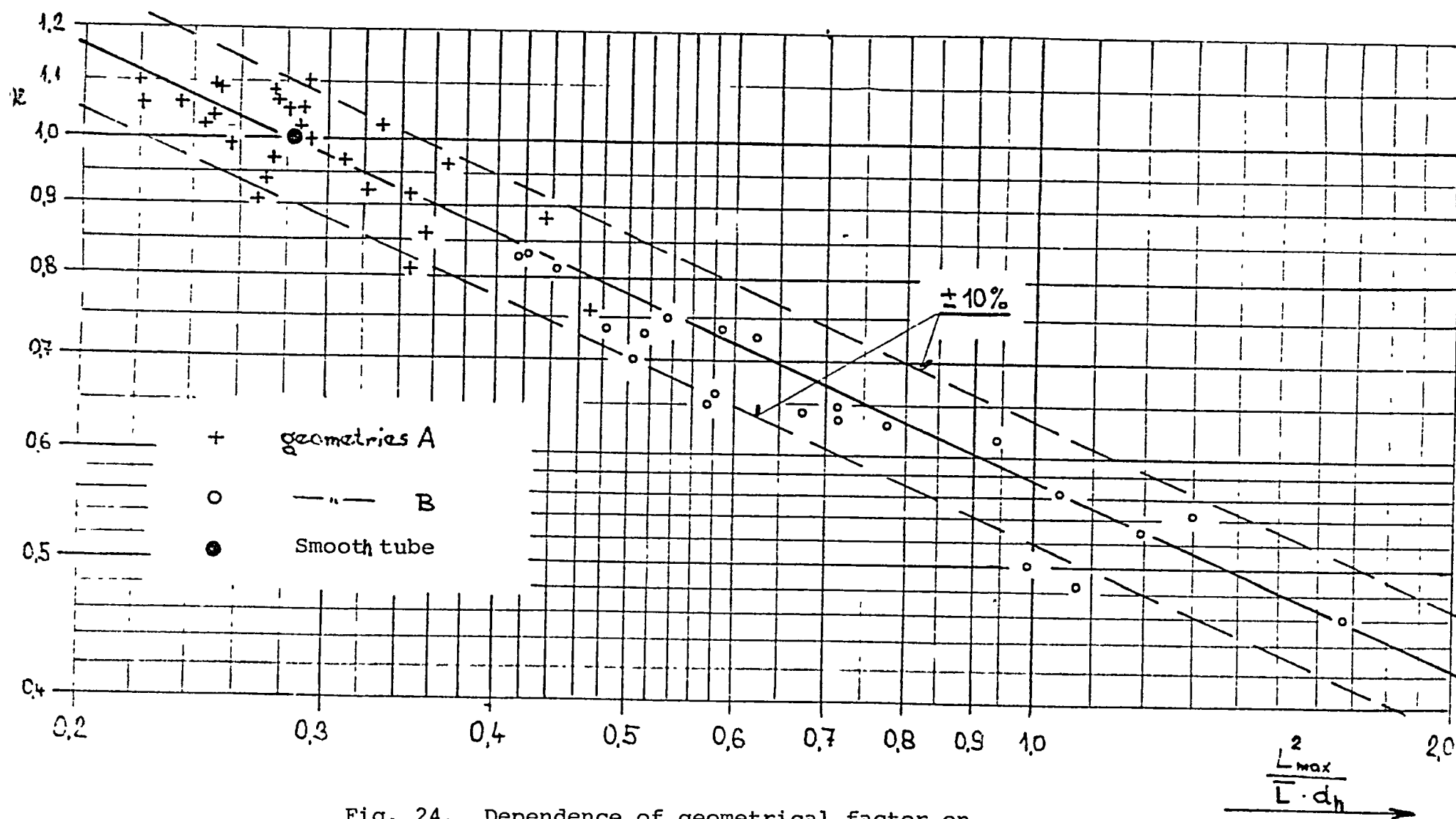
Fig. 24. Dependence of geometrical factor on geometrical criterion $(L^2_{max}/\overline{L} \cdot d_h)$.
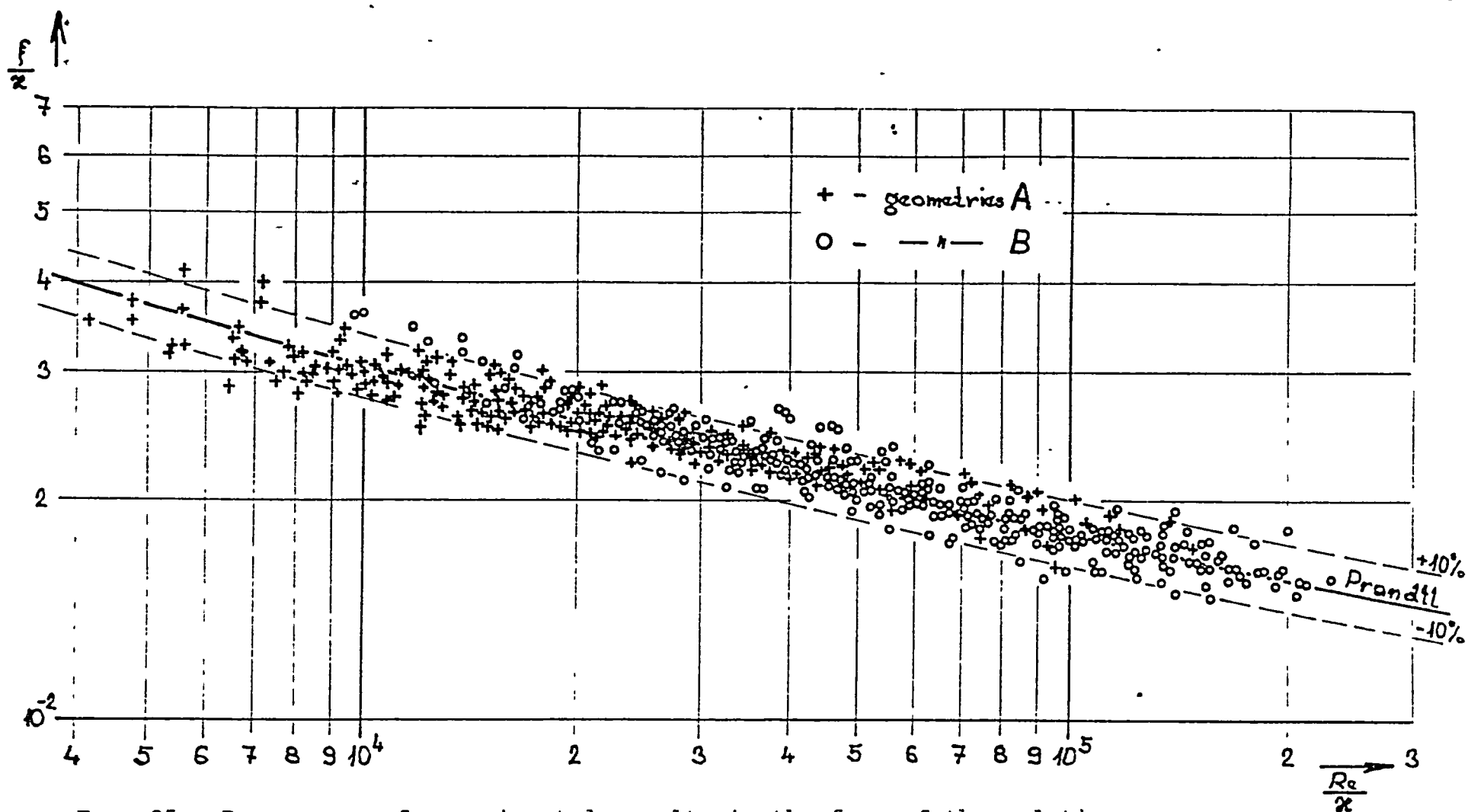
Fig. 25. Processing of experimental results in the form of the relation $\frac{\xi}{H} = \delta \ (\frac{Re}{H})$ with geometrical factor value acc. to equation (35).
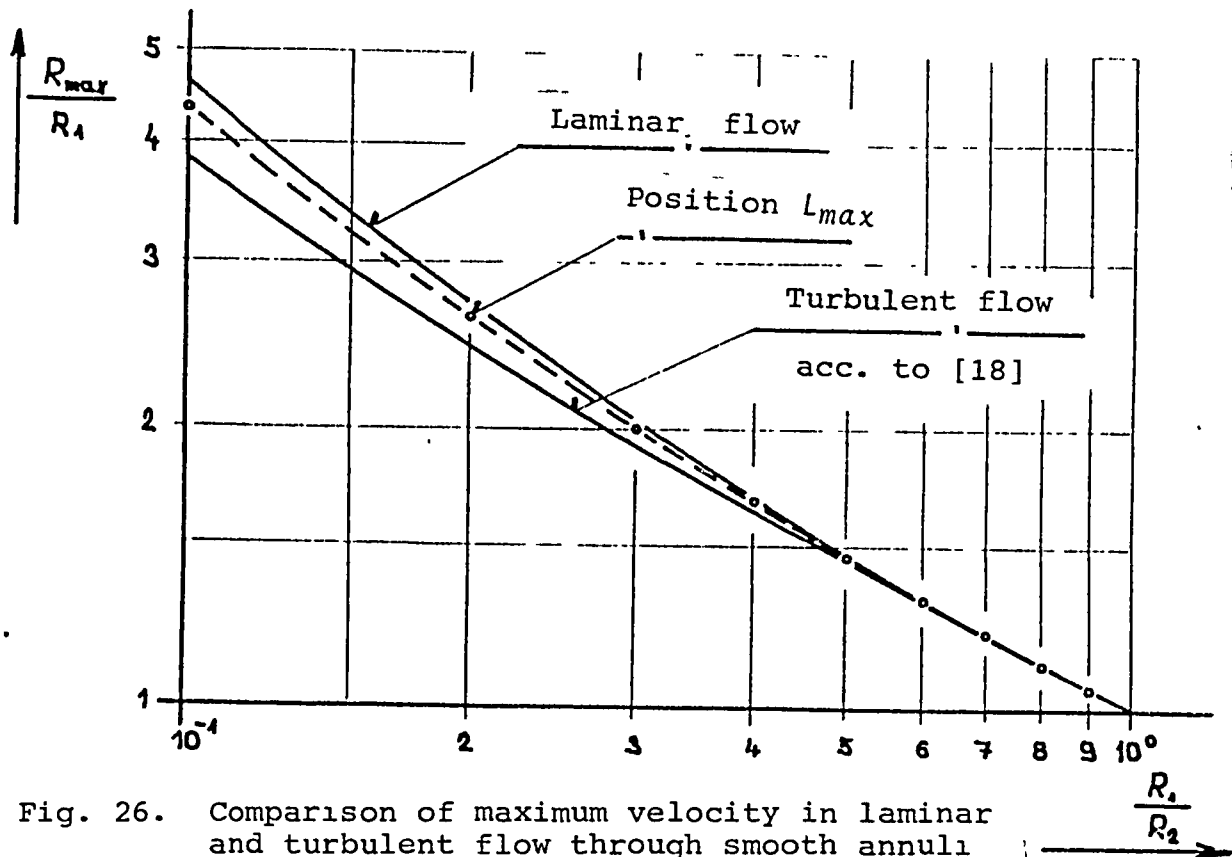
Fig. 26. Comparison of maximum velocity in laminar
and turbulent flow through smooth annuli
with maximum value of L.
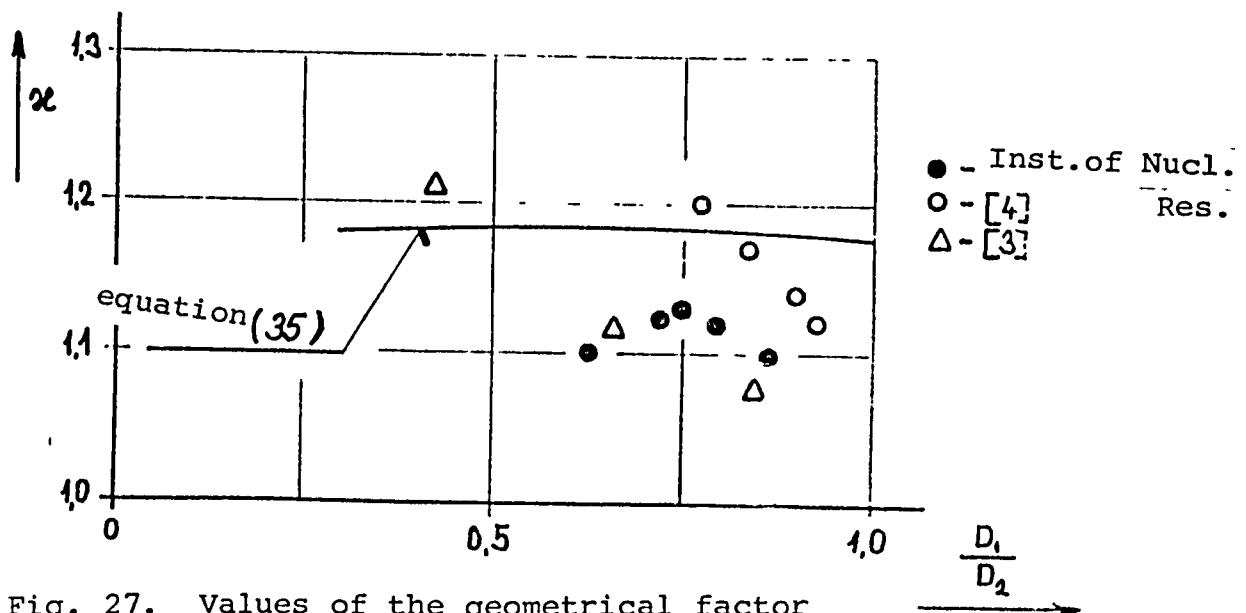
Fig. 27. Values of the geometrical factor
for varying curvatures of annular
channels derived from experiments,
and progress of $H = \mathcal{f}(D_1/D_2)$ ac-
cording to relation (35).
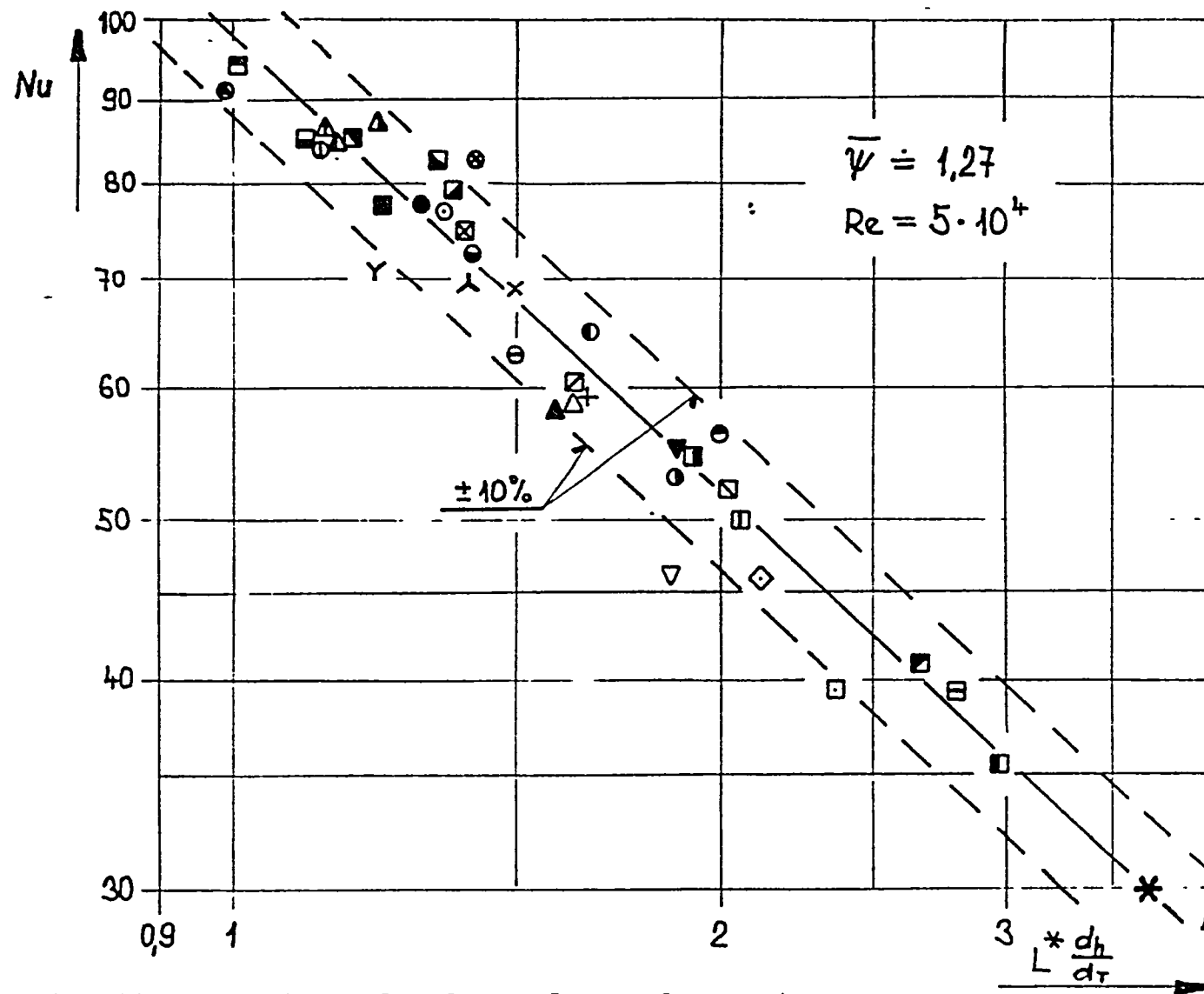
Fig. 28. Experimental values of Nusselt's criterion
for Re 5.10^4 and $\bar{\psi}$ = 1.27 and their depend-
ence on the geometrical criterion $(L^* \frac{d_h}{d_T})$.
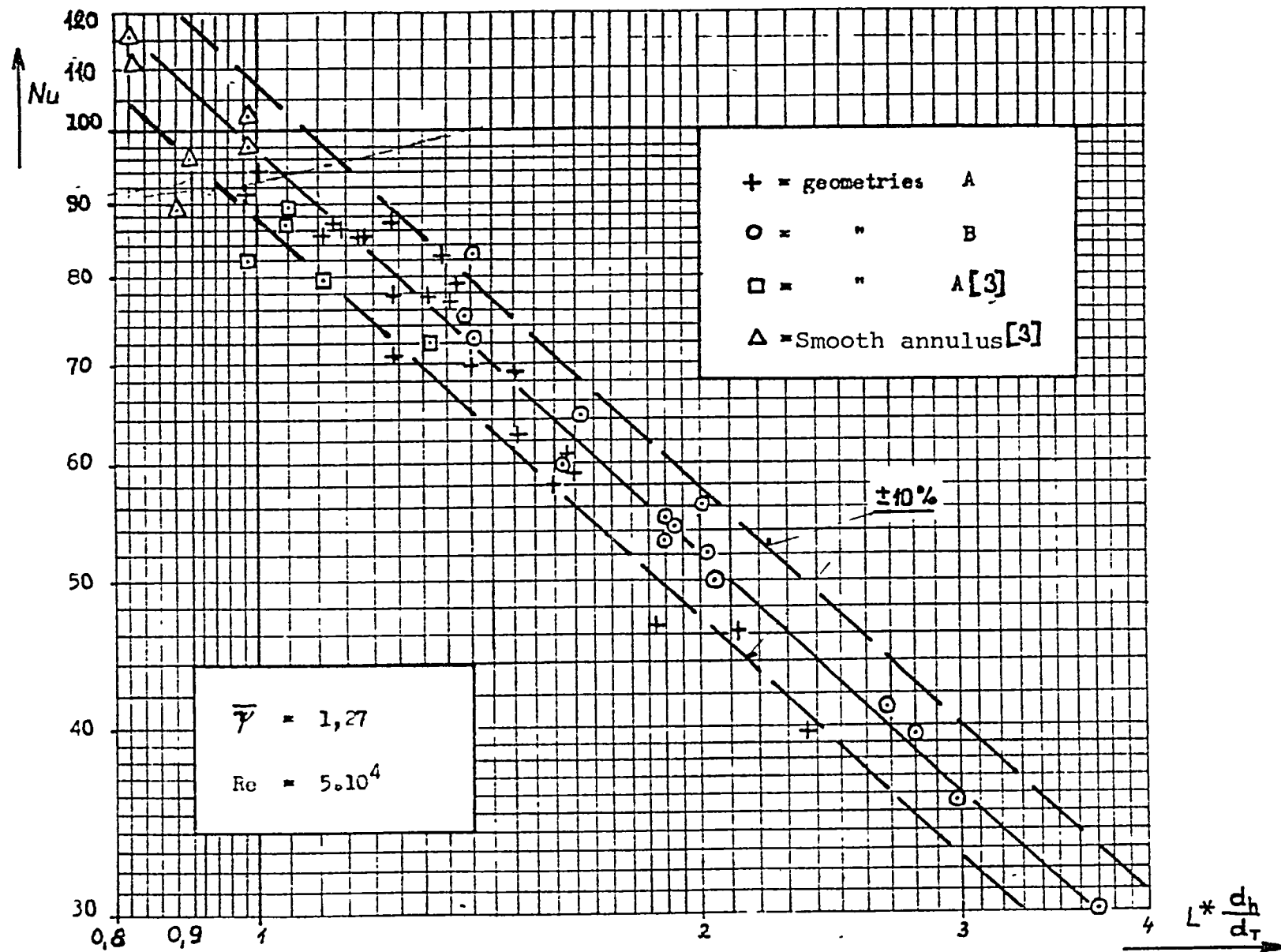
Fig. 29. Experimental values of Nusselt's criterion for $Re = 5.10^4$ and $\bar{\psi} = 1.27$ and their dependence on the geometrical criterion $(L^* \frac{d_h}{d_T})$; differentiation between geometry A and B, including results obtained by K. Rybáček [3].
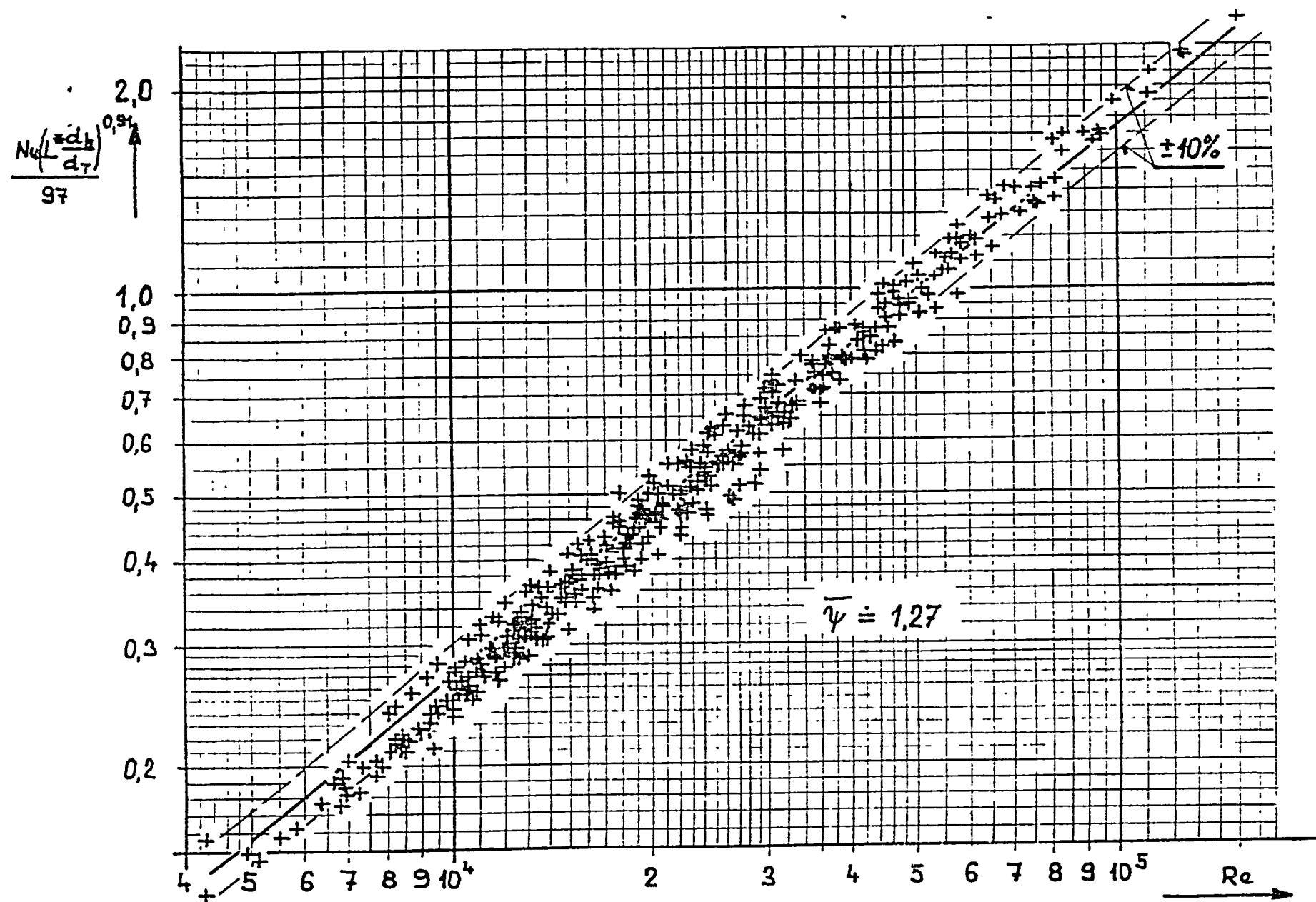
Fig. 30. Processing of the results of thermokinetic experiments on geometry A into the dependence form $\frac{1}{97}(L^* \frac{dh}{dT})^{0.91}$. $Nu = \int (Re)$.
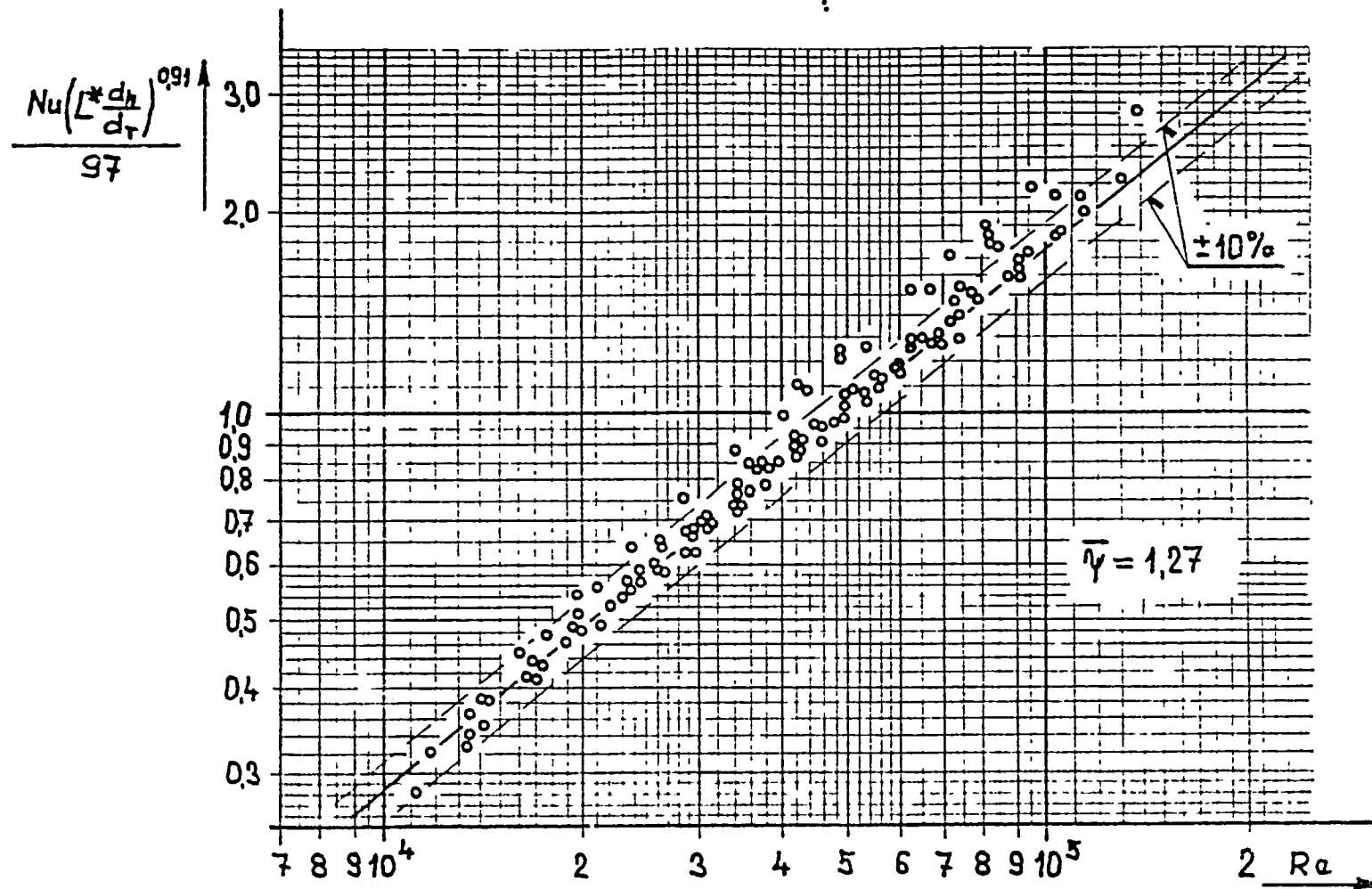
Fig. 31 Processing the results of thermokinetic experiments on geometry B into the dependence form $\frac{1}{97}(L^* \frac{d_h}{d_T})^{0.91}$. $Nu = \delta \, (\hbar e)$.
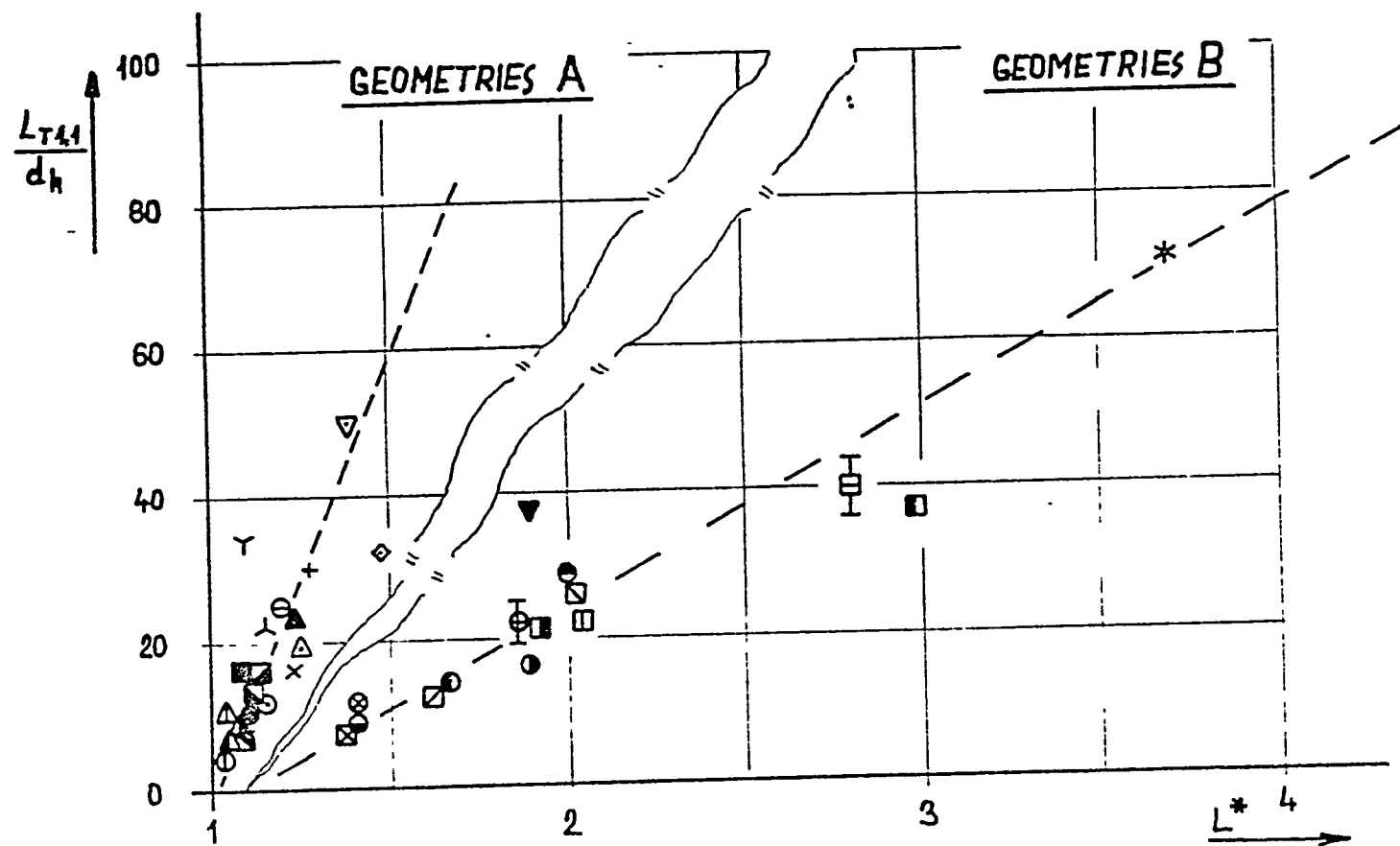
Fig. 32. Experimental values of $\frac{L_{T1,11}}{d_h}$ and their dependence on L^*.
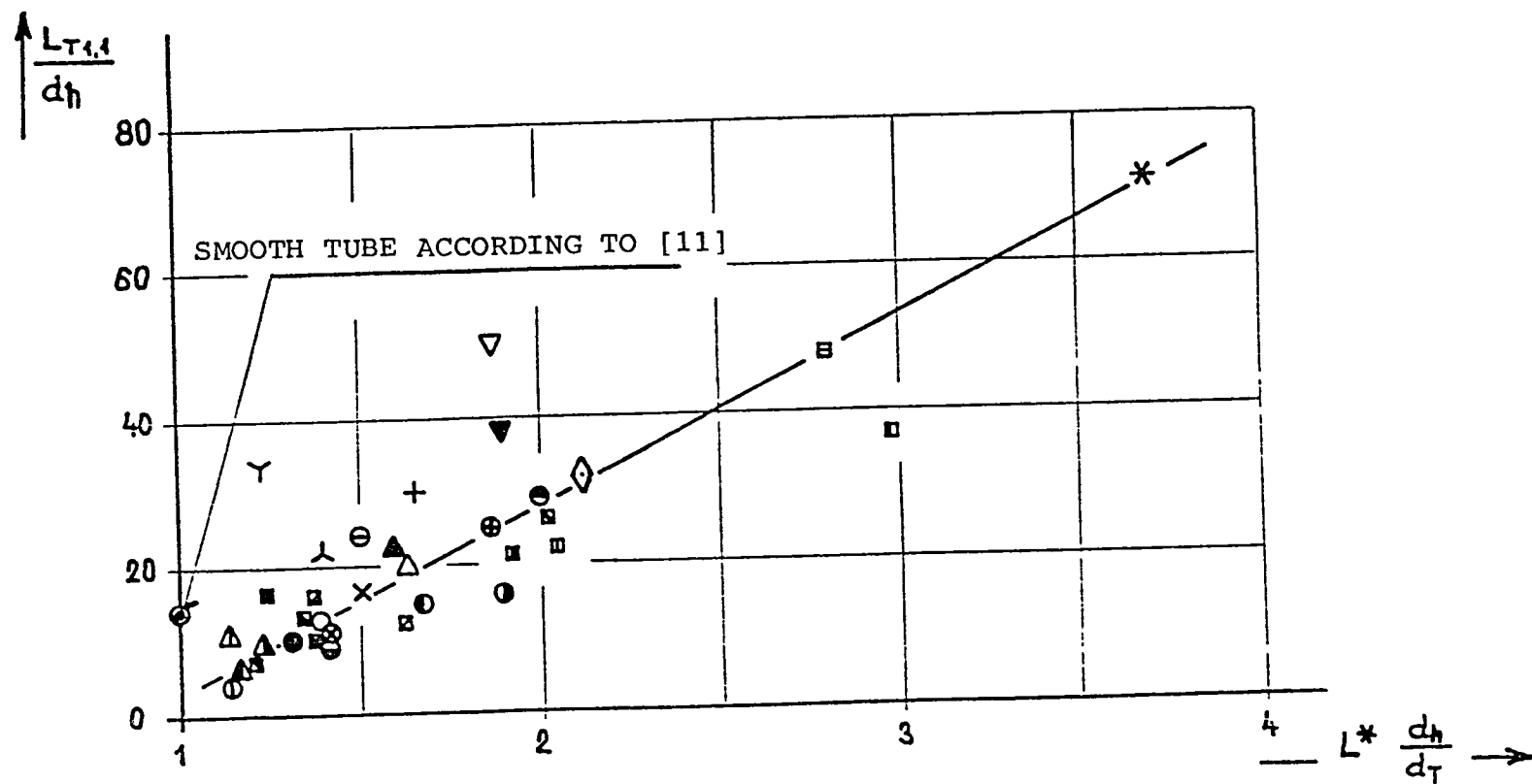
Fig. 33. Experimental values of $\frac{L_{T,11}}{d_h}$ and their dependence on $\left(L^* \frac{d_h}{d_T}\right)$.
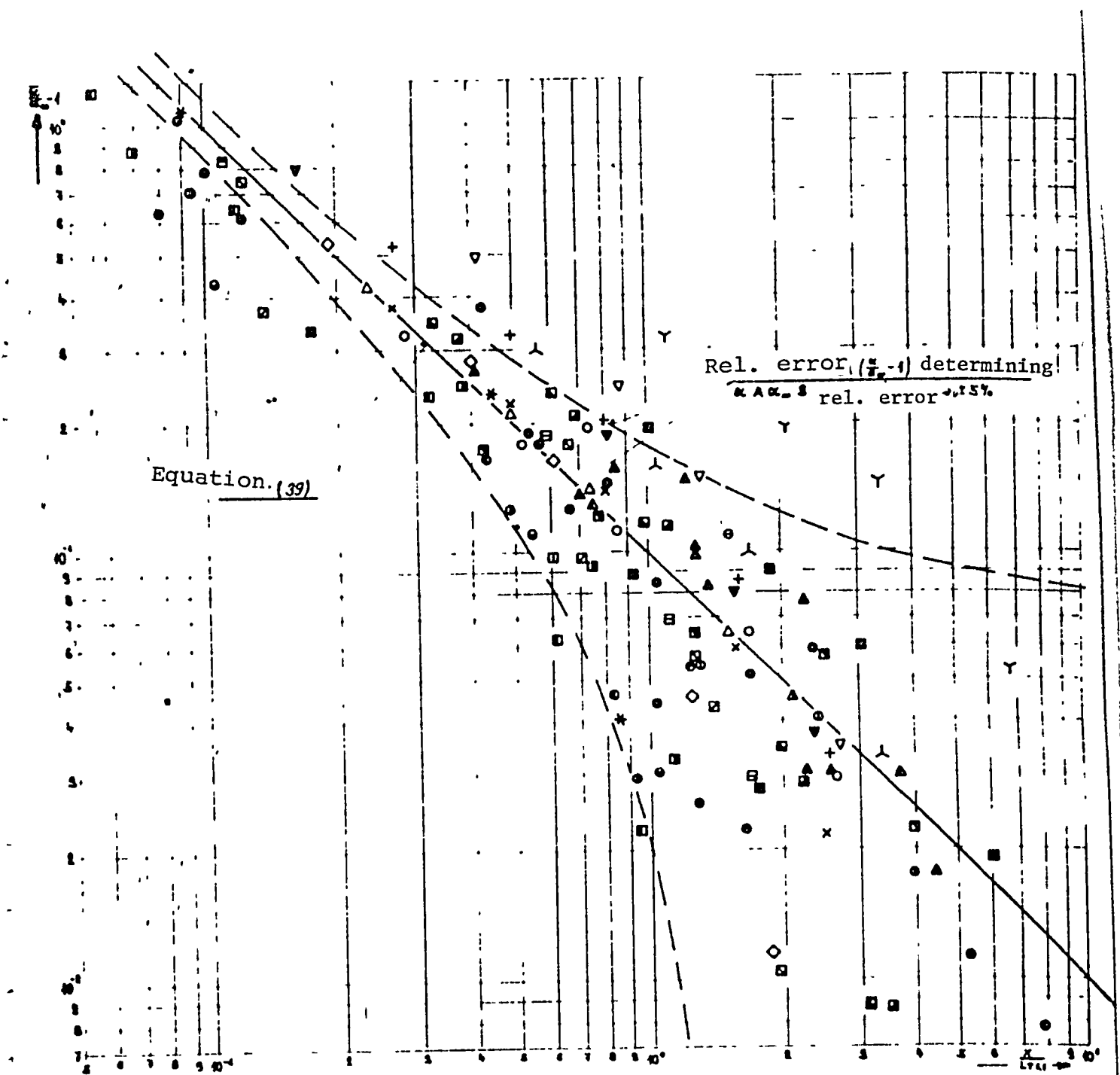
Fig. 34. Distribution of $\bar{\alpha}$ along the length of the model in the form of dependence $\frac{\bar{\alpha}}{\alpha_\infty} - 1 = \phi\left(\frac{x}{L_{T1.1}}\right)$. Values of $L_{T1.1}$ for individual variants were computed from equation (42).
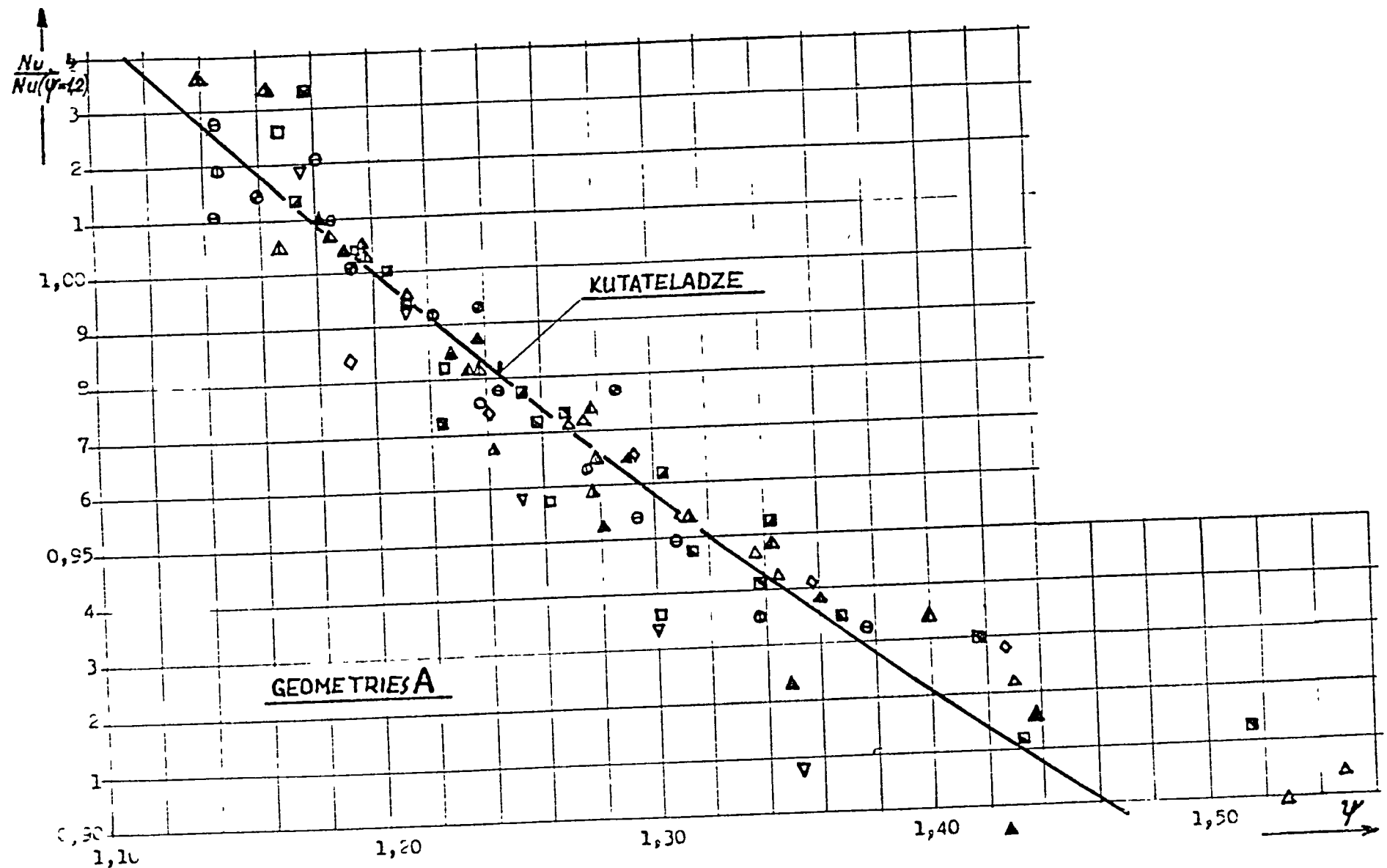
Fig. 35. Effects of the thermal factor on Nusselt's criterion at constant flow-through (with no consideration given to change in Reynold's number due to thermal effects and effects of the latter change on Nu).
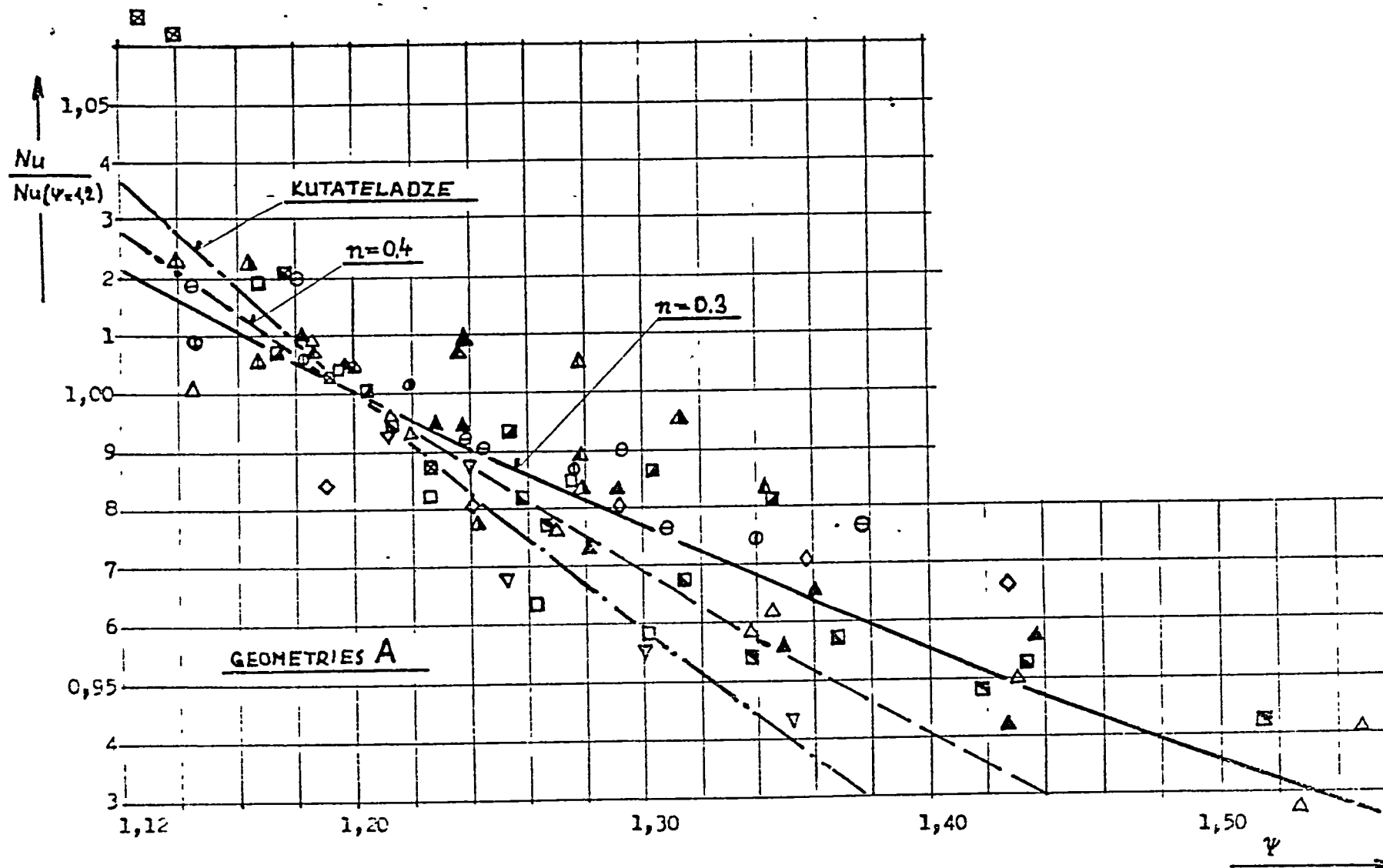
Fig. 36. Effects of the thermal factor on Nusselt's criterion at constant values of Re.
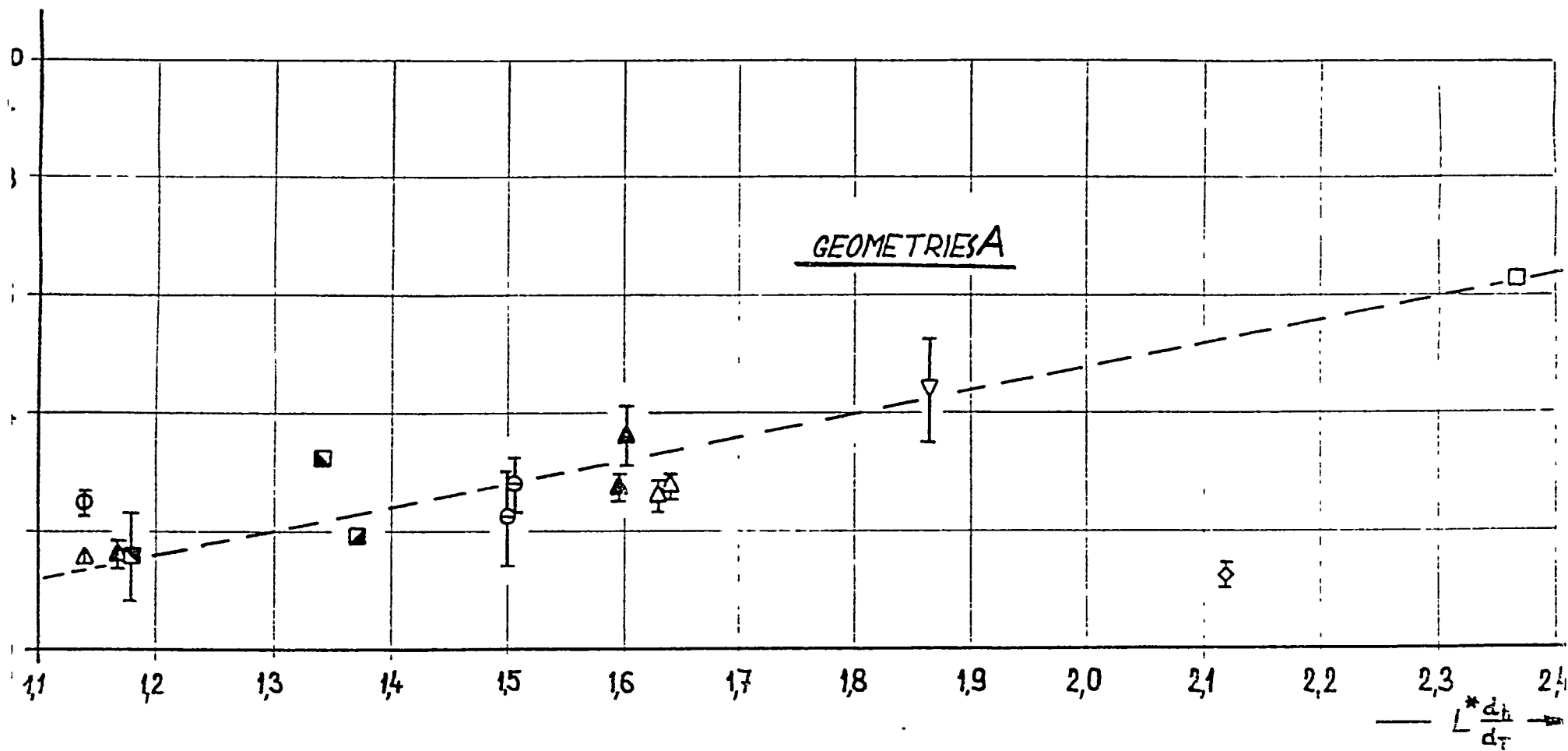
Fig. 37. Experimental values of exponent n as a function of criterion $(L^* \frac{d_h}{d_T})$.
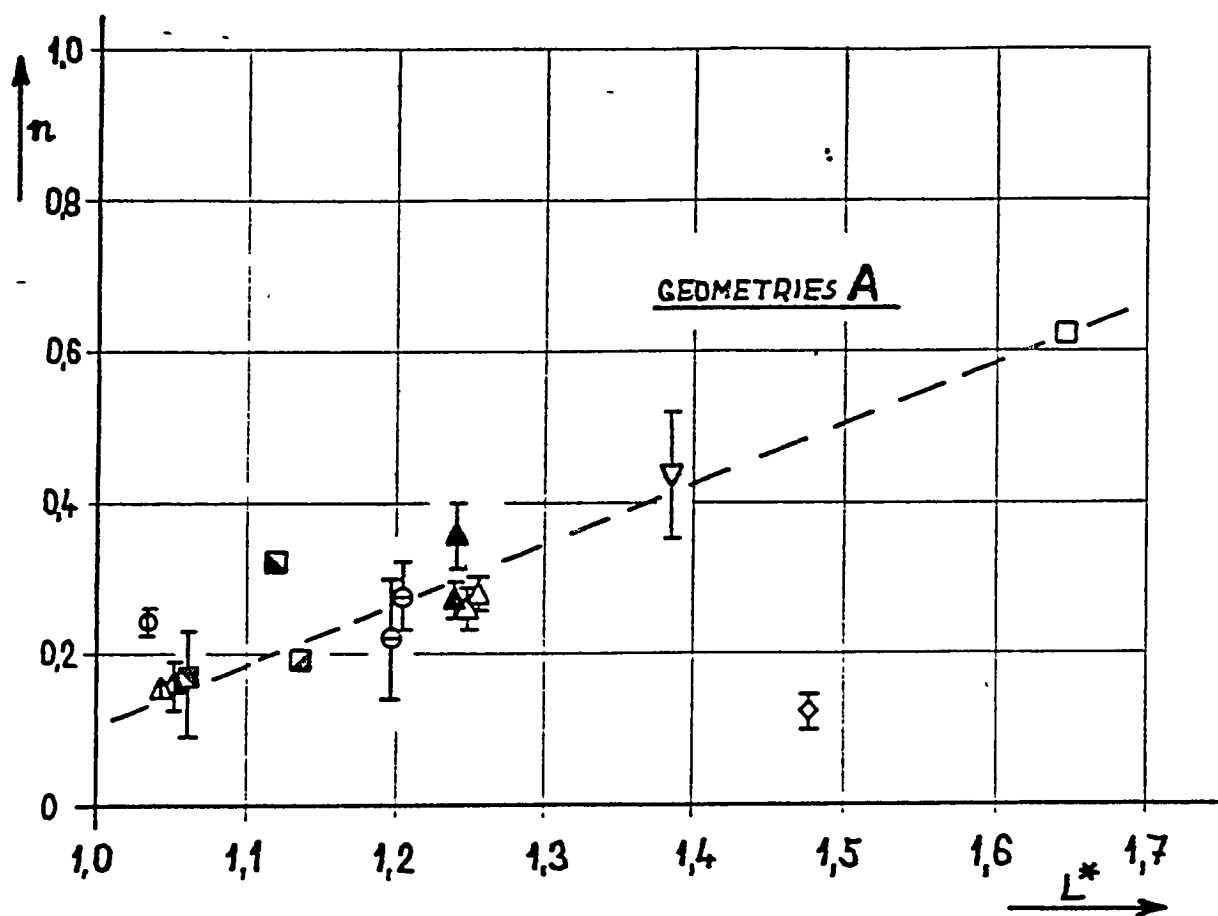
Fig. 38. Experimental values of exponent n as a function of criterion L^*.
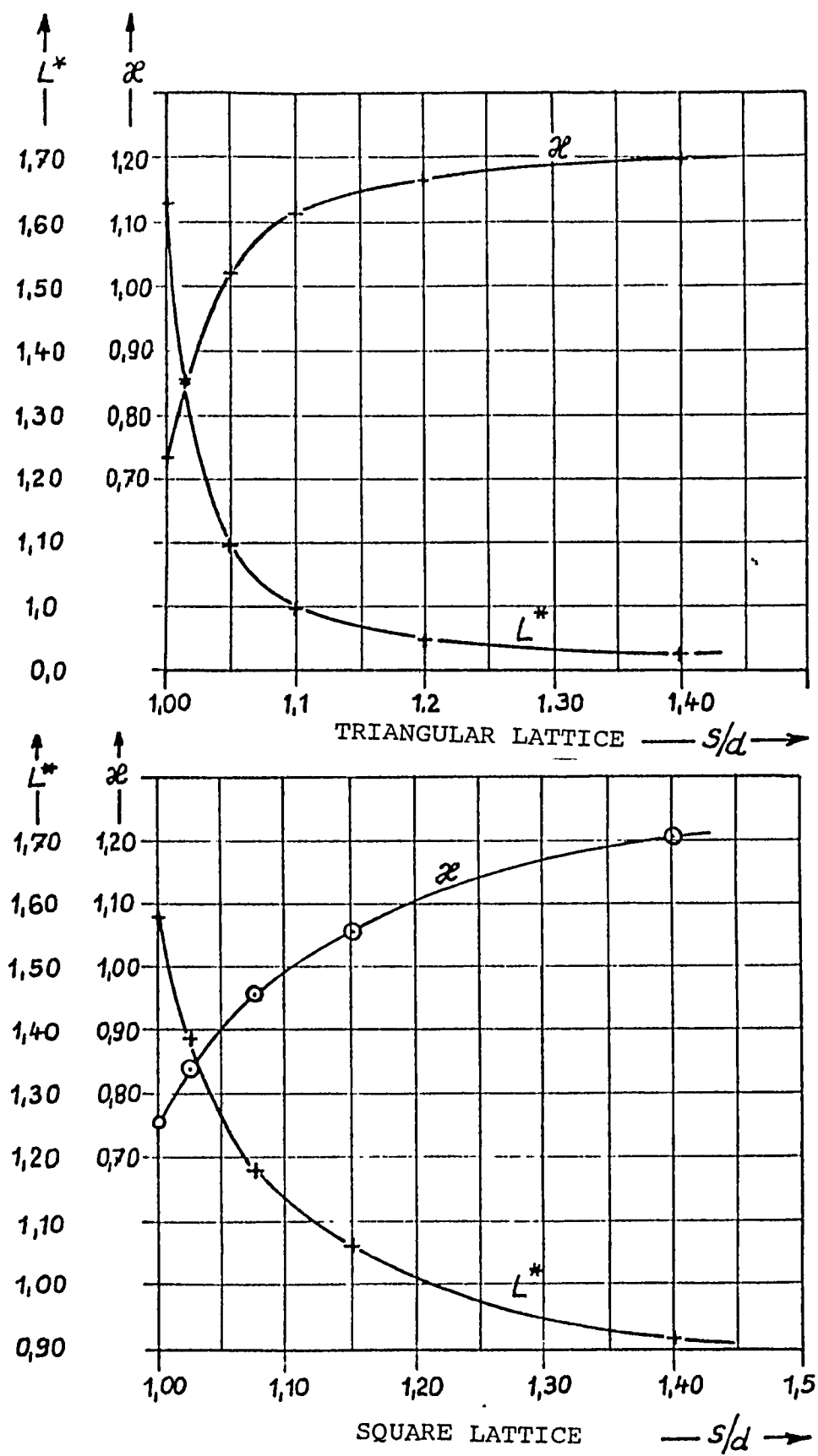
Fig. 39. Dependence of the geometrical criterion L^* and the grometrical factor H on the density of triangulat and square lattices.
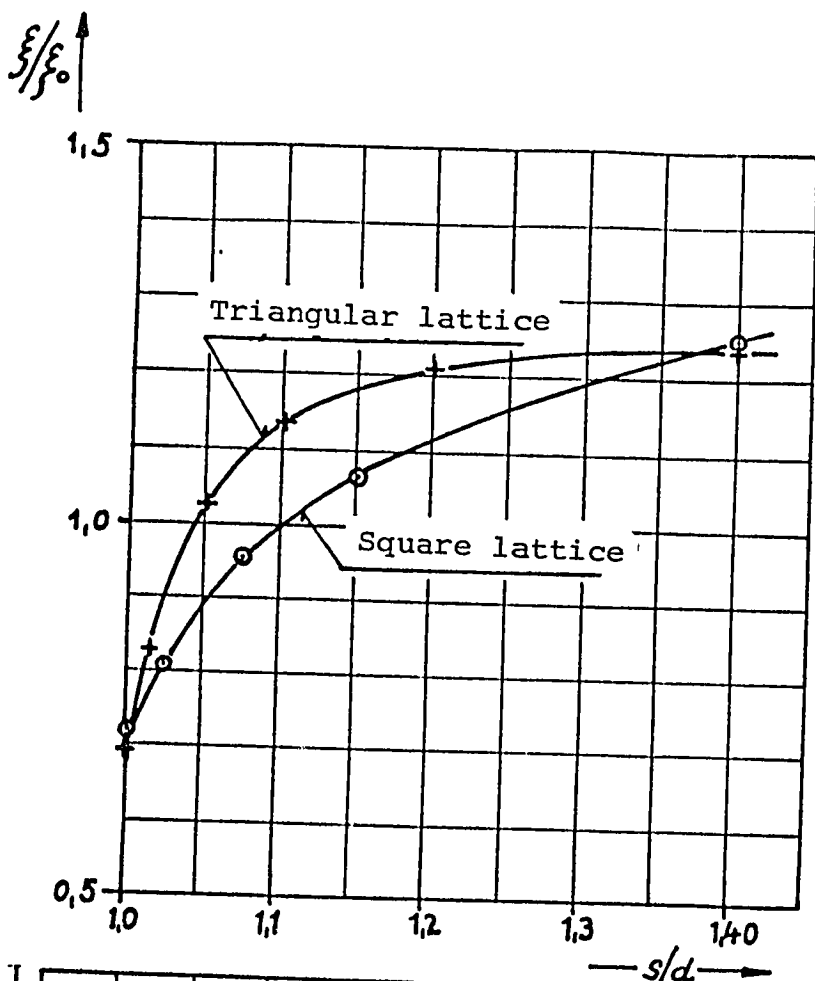
←Fig. 40. Computed progress of $\frac{\xi}{\xi_0} = f(\frac{s}{d})$ for a triangular and a square lattice.
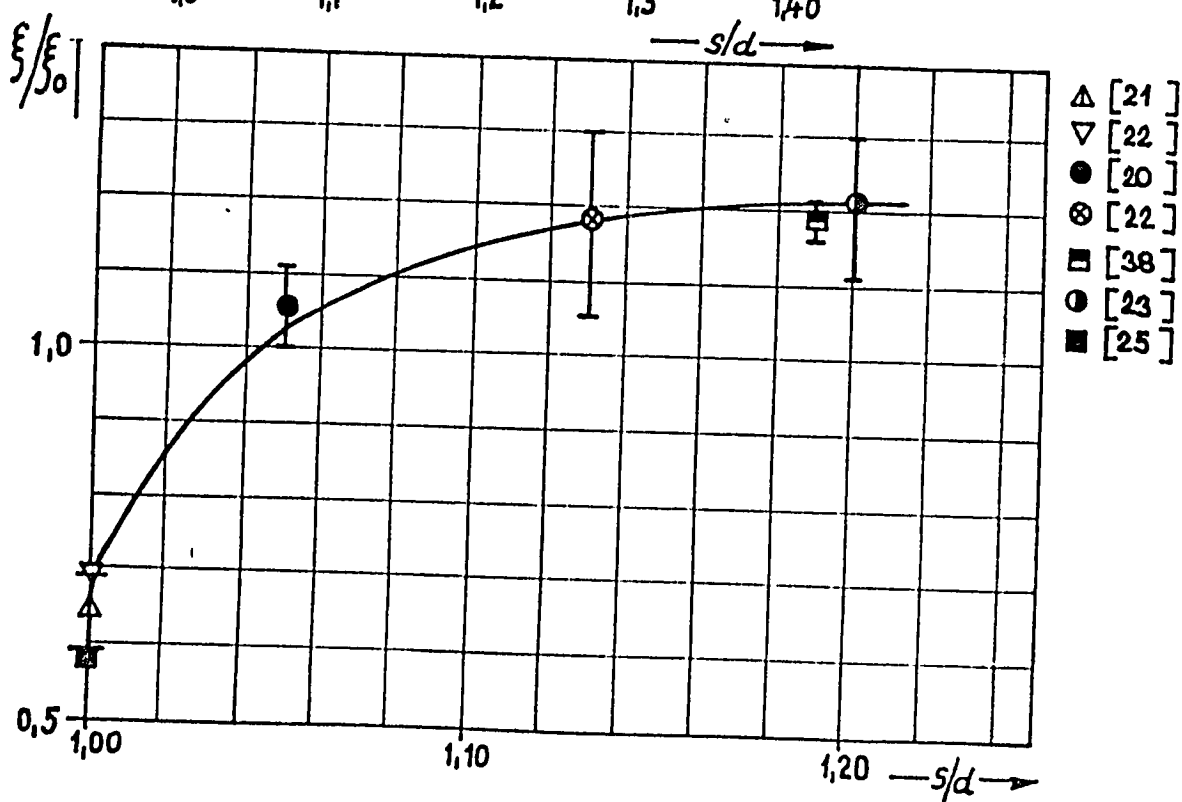
Fig. 41. Change in coefficient of friction losses with the density of a triangular lattice; comparison of criterial relation (21) with experiments.
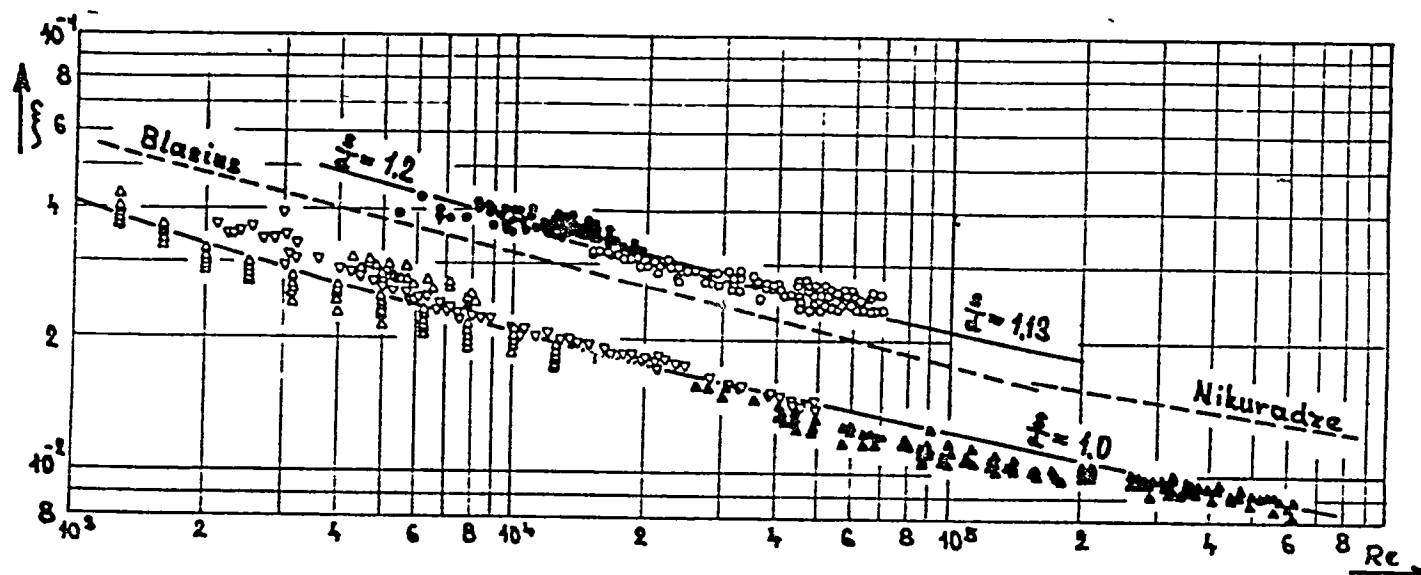
74
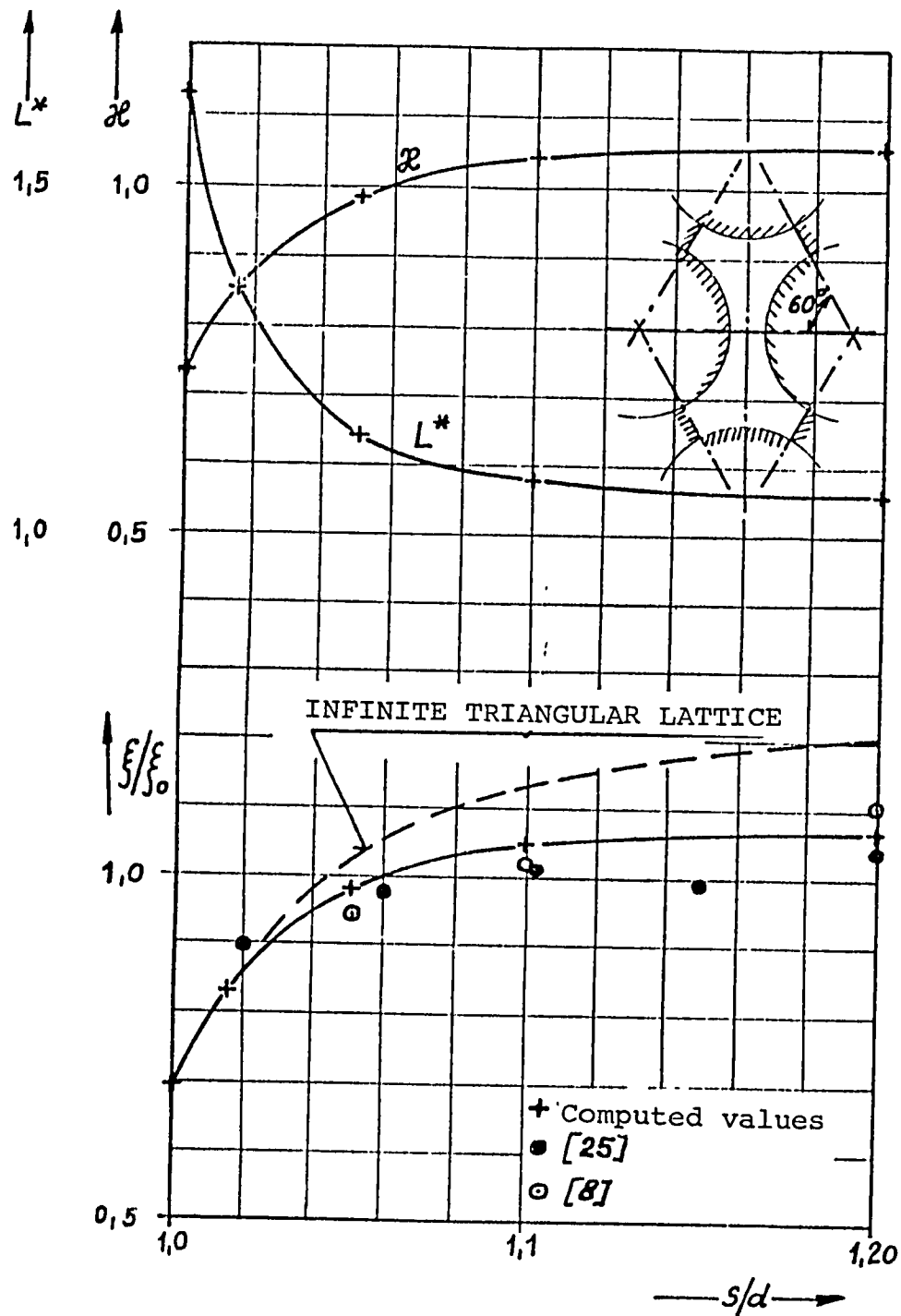
Fig. 42. Comparison of computed and experimental
values of ξ/ξ_0 for the used cell models of an infi-
nite triangular lattice.

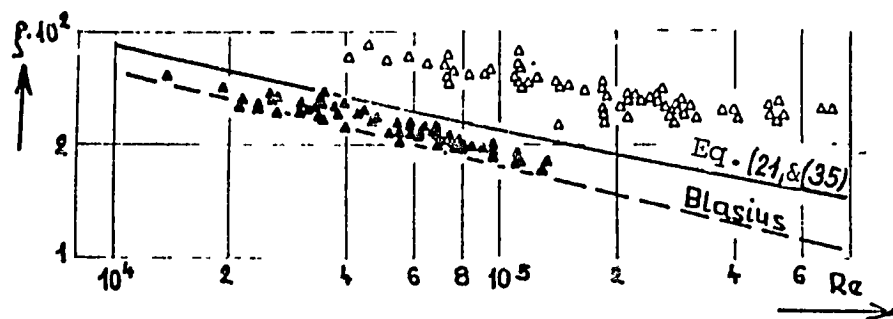| Ref. no:	$\frac{s}{d}$	N	d	$d_{h\infty}$	d_h	L	Oper. medium	Range $Re \cdot 10^3$	Symbol	Model section
22	1,0	19	17,6	1,81	1,81	700	water	1-20	△▽	
21	1,0		205	20,9		1800	water	8-630	▲	
22	1,13	19	12,0	4,8	5,0	980	water	14-70	○	
23	1,2	7	22,0	12,94	14,43	1050	water	5-20	●	

Fig. 43. Comparison of experiments and computations for a triangular lattice (in cases when it can be considered to be infinite).
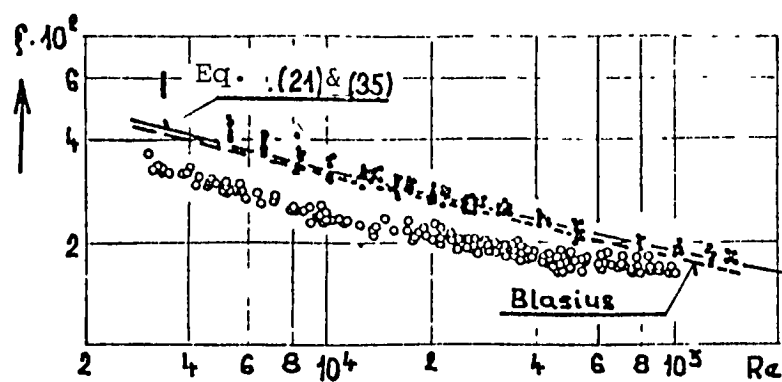
$$\frac{s}{d} = 1{,}05$$

$$\frac{s}{d} = 1{,}4 \; ; \; 1{,}46$$

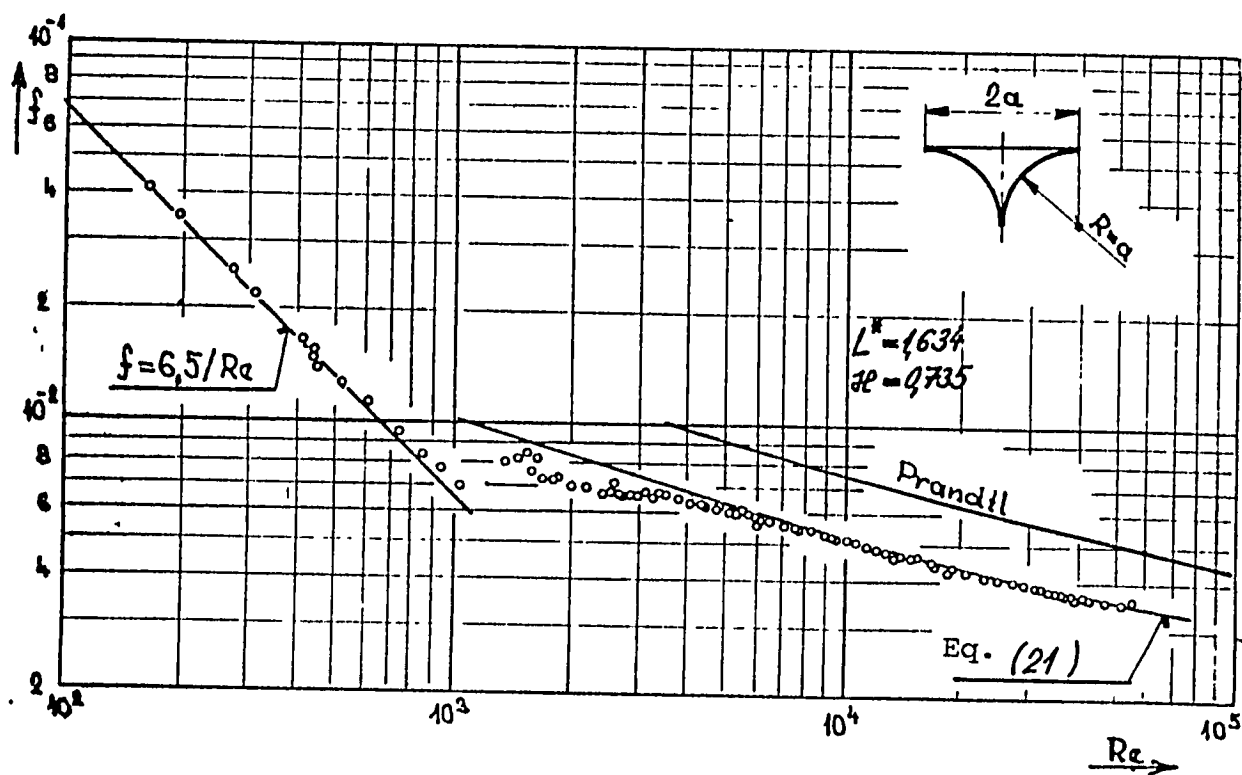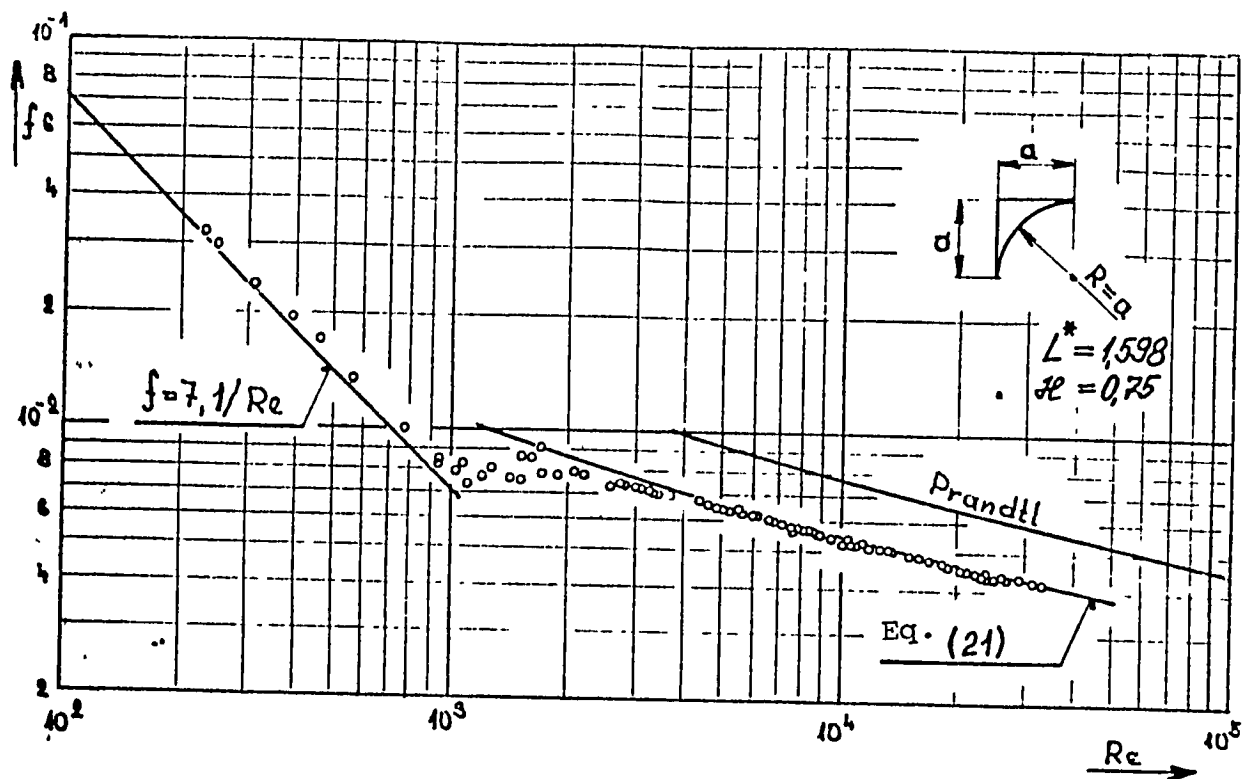| Litera-tura	$\frac{s}{d}$	N	d	$d_{h\infty}$	d_h	L	Oper. medium	range $Re \cdot 10^{-3}$	Sym-bol	Model section
20	1,05	37	14,0	3,02	3,00	1000	water	3–120	●	
20	1,05	37	10,0	2,16	2,16	840	water	3–100	○	
20	1,4	37	10,0	11,62	11,53	840	water	12–120	▲	
24	1,46	37	15,9	19,5	21,5	1220	water	40–800	△	

Fig. 44. Continuation of Fig. 43.
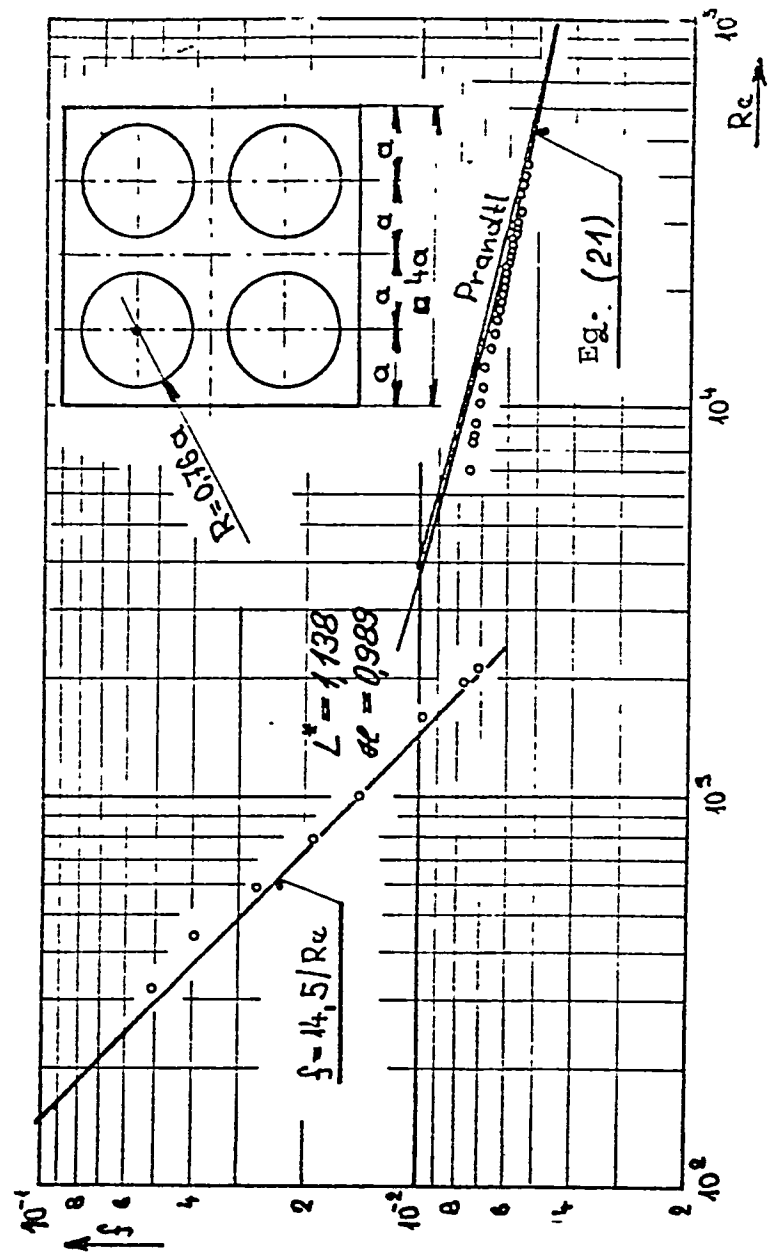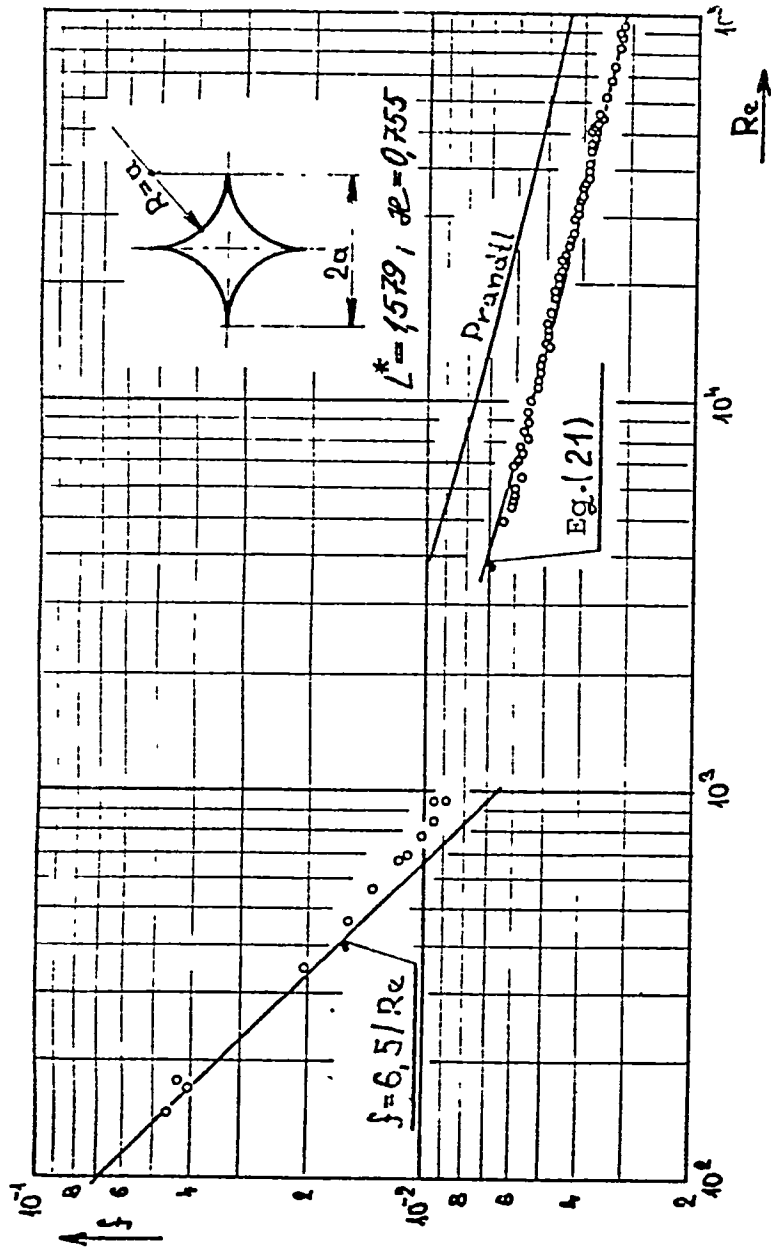
Fig. 45. Comparison of experiments and computations for elements
of a square lattice [27].

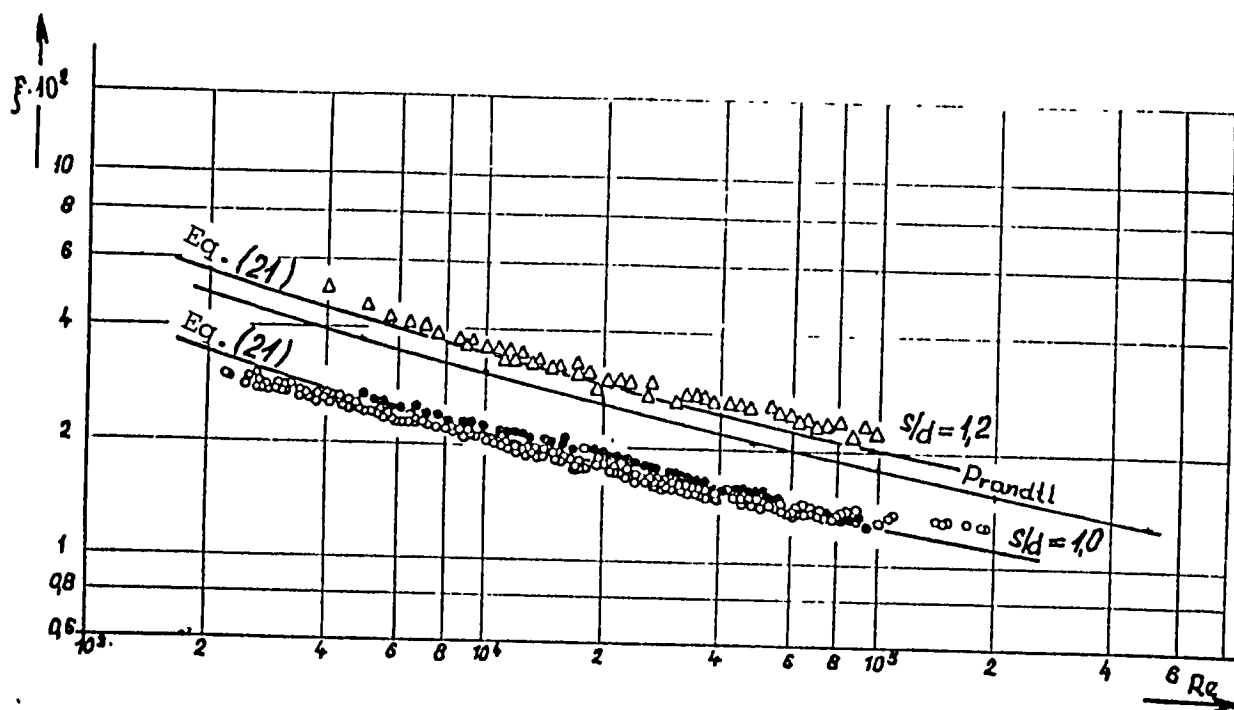Fig. 46. Continuation of Fig. 45.
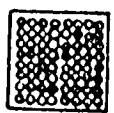
Litera-tura	$\frac{s}{d}$	N	d	dh_∞	dh	L	Oper. Medium	Range $Re \cdot 10^{-3}$	Symbol	Model section
[28]	1,0	25	11,4	3,12	3,12	600	water	2-200	o	
[27]	1,0		48,2	13,2	13,2	3400	water	5-100	•	
[26]	1,2	64	7,92	6,6	5,6			5-100	Δ	

Fig. 47. Comparison of computations and experiments for a square lattice.
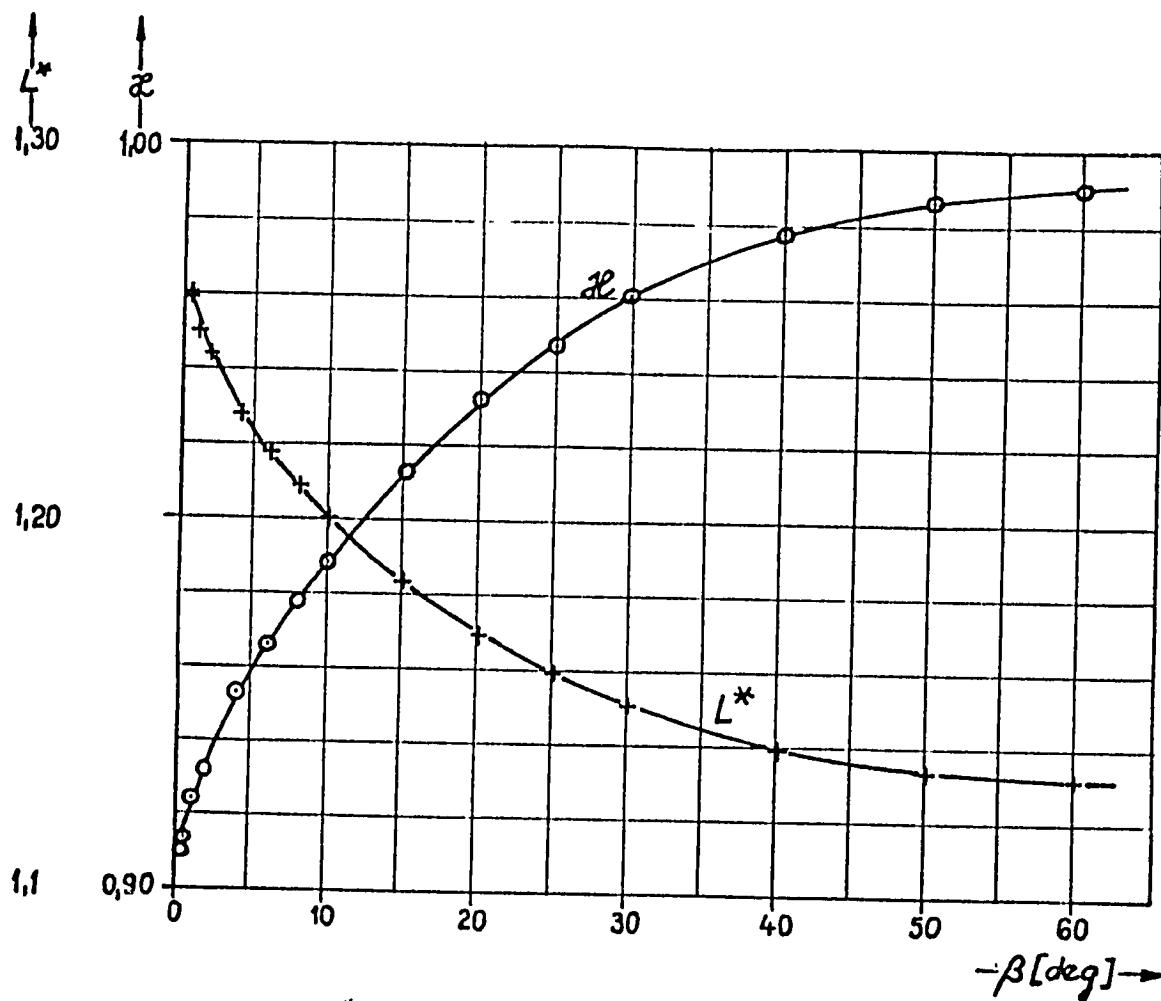
Fig. 48. Dependence of L^* and H on the apex angle of an isosceles triangle.
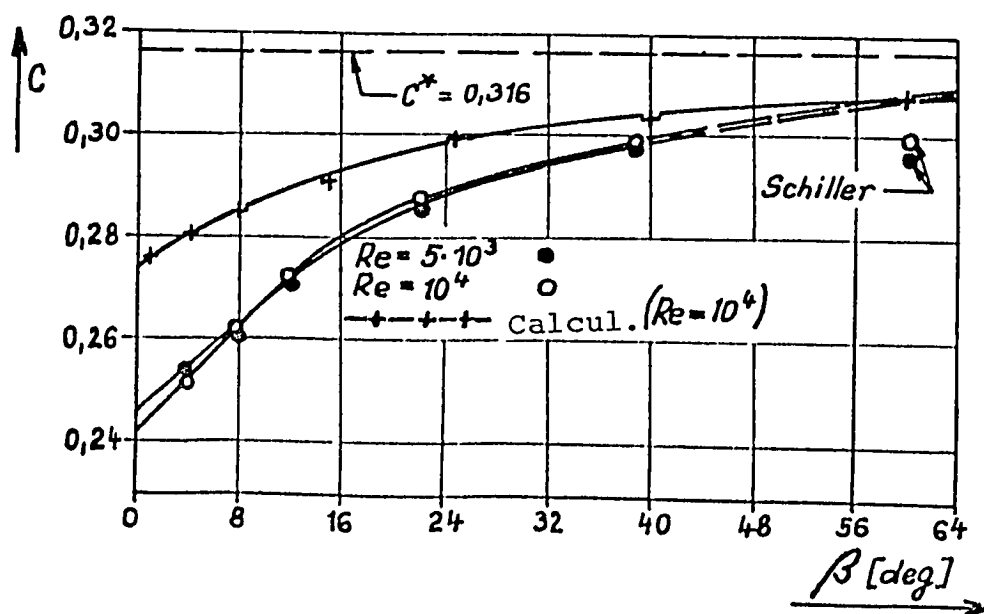
Fig. 49. Comparison of computed and experimental values [32] for a channel with a cross section in the shape of an isoscles triangle.
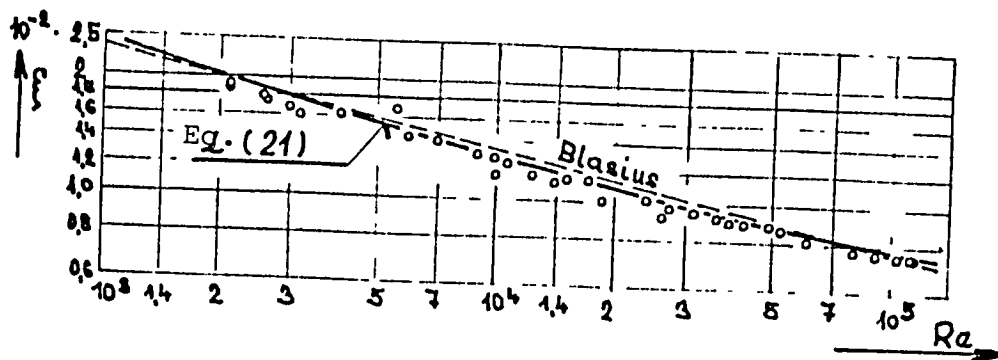
Fig. 50. Coefficient of friction losses
in an isosceles triangle [29].
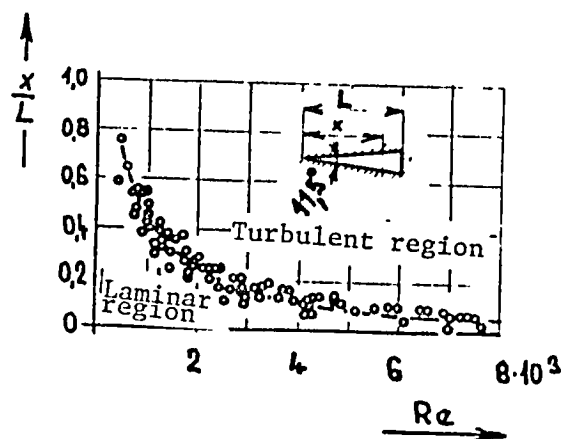
Fig. 51. Extent of the laminar region in a channel with an isosceles
triangle cross section with an apex angle of 11.5° [30].
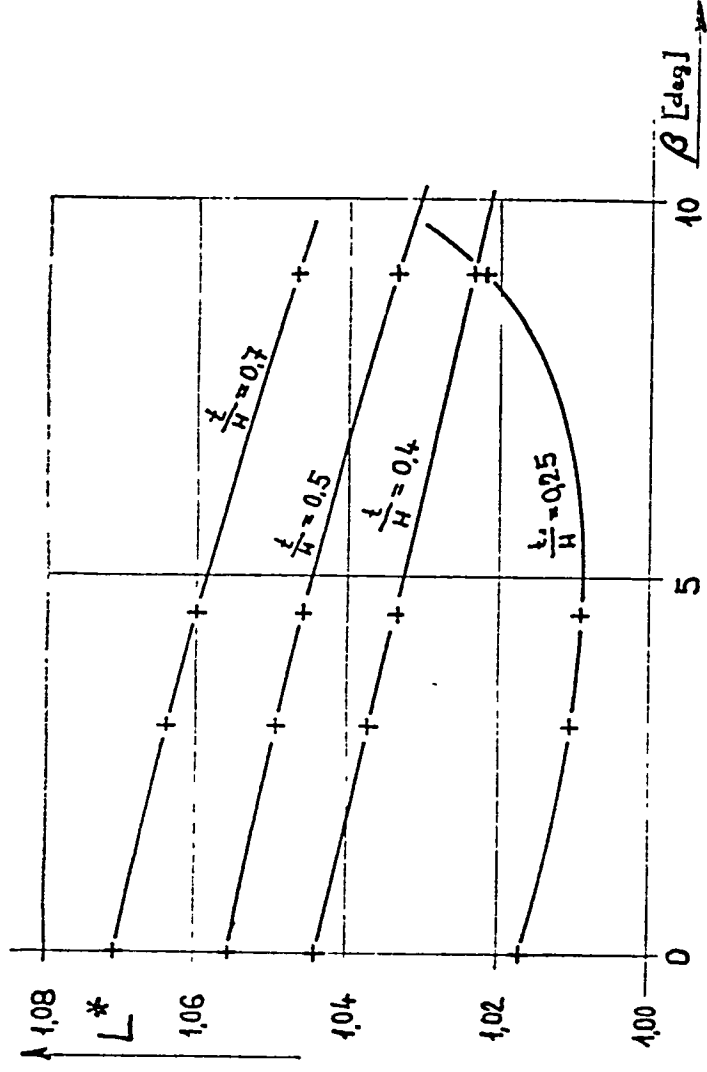
←Fig. 52. Values of L^* for a regular trapezoid.
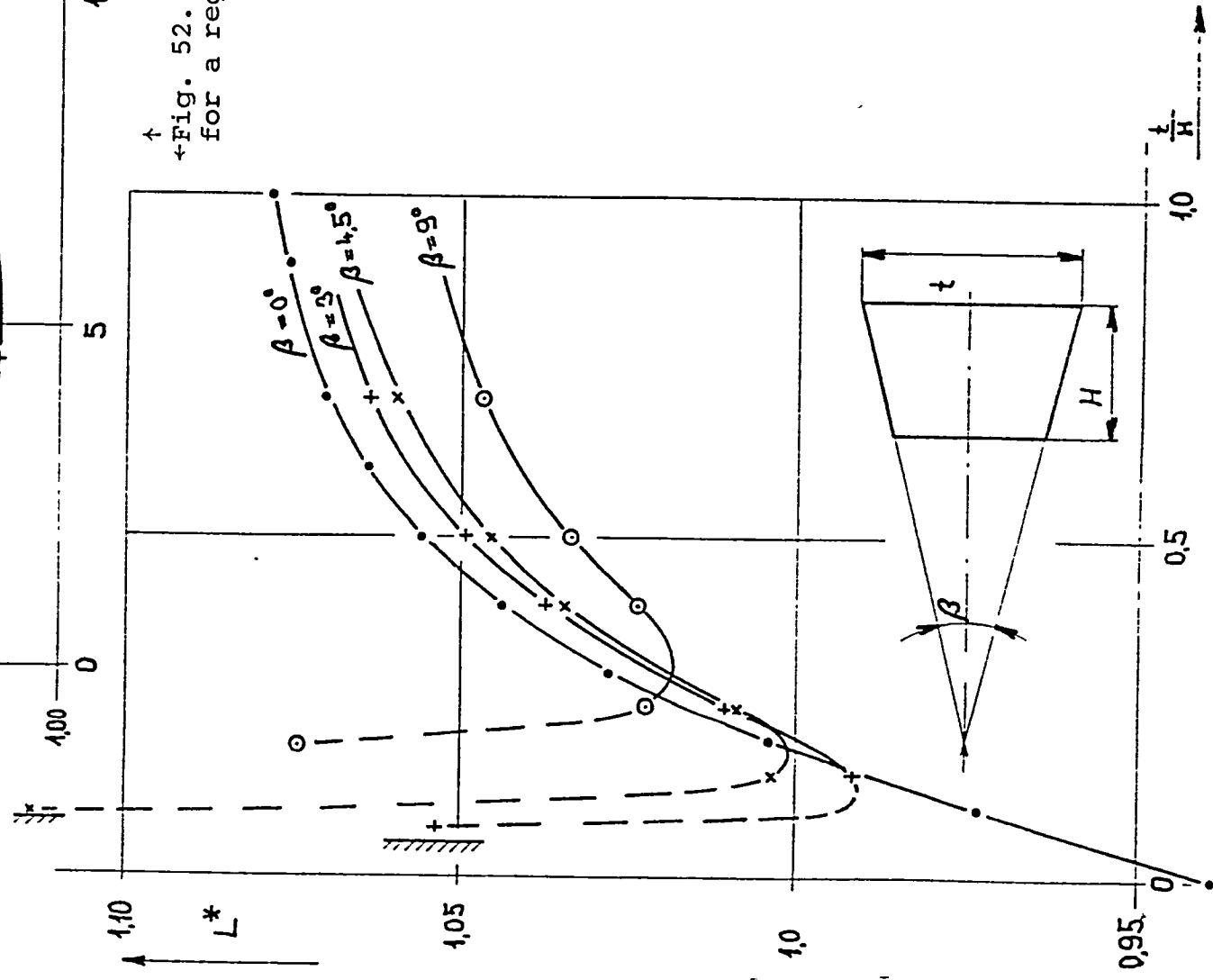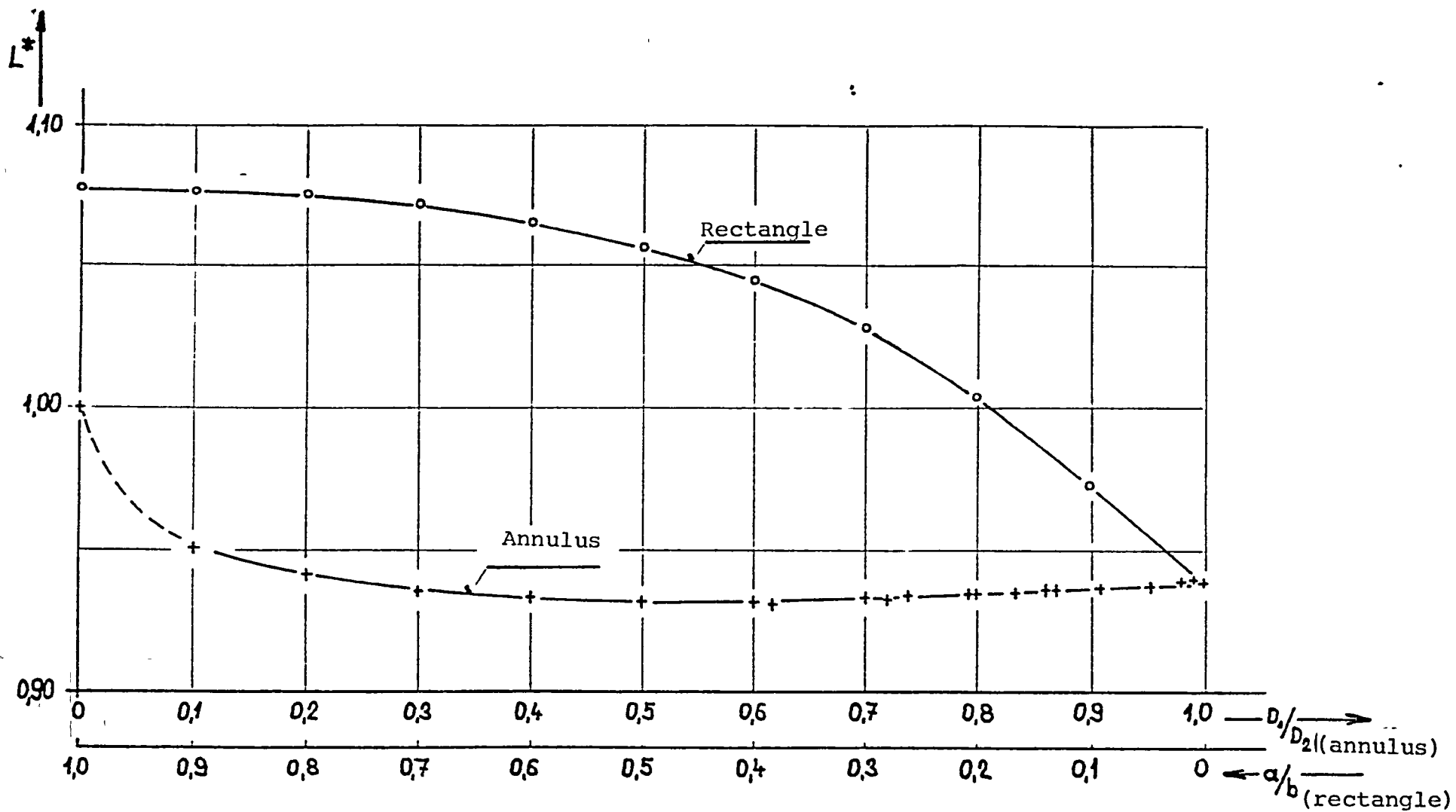
Fig. 53   Values of L^* for a rectangle and an annulus.
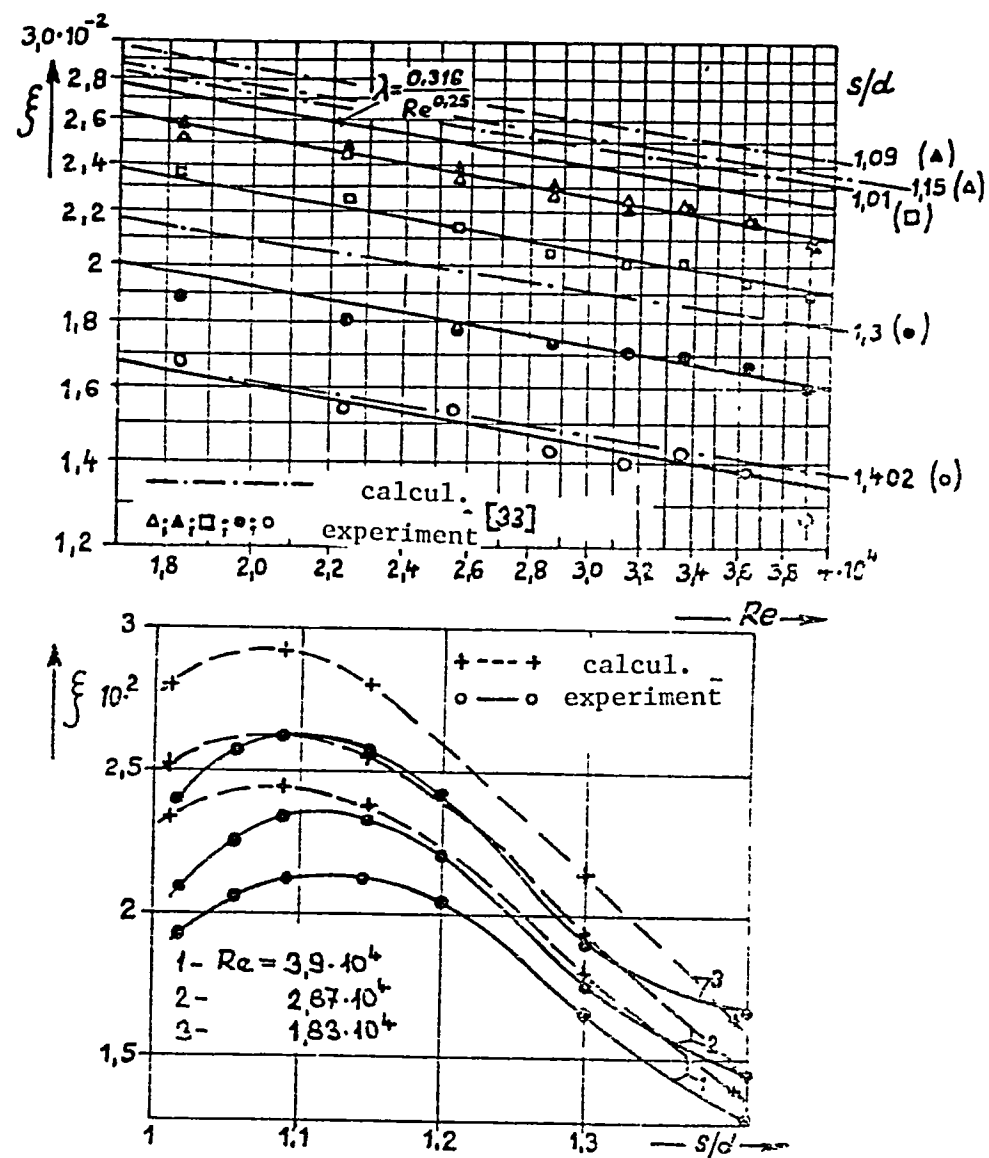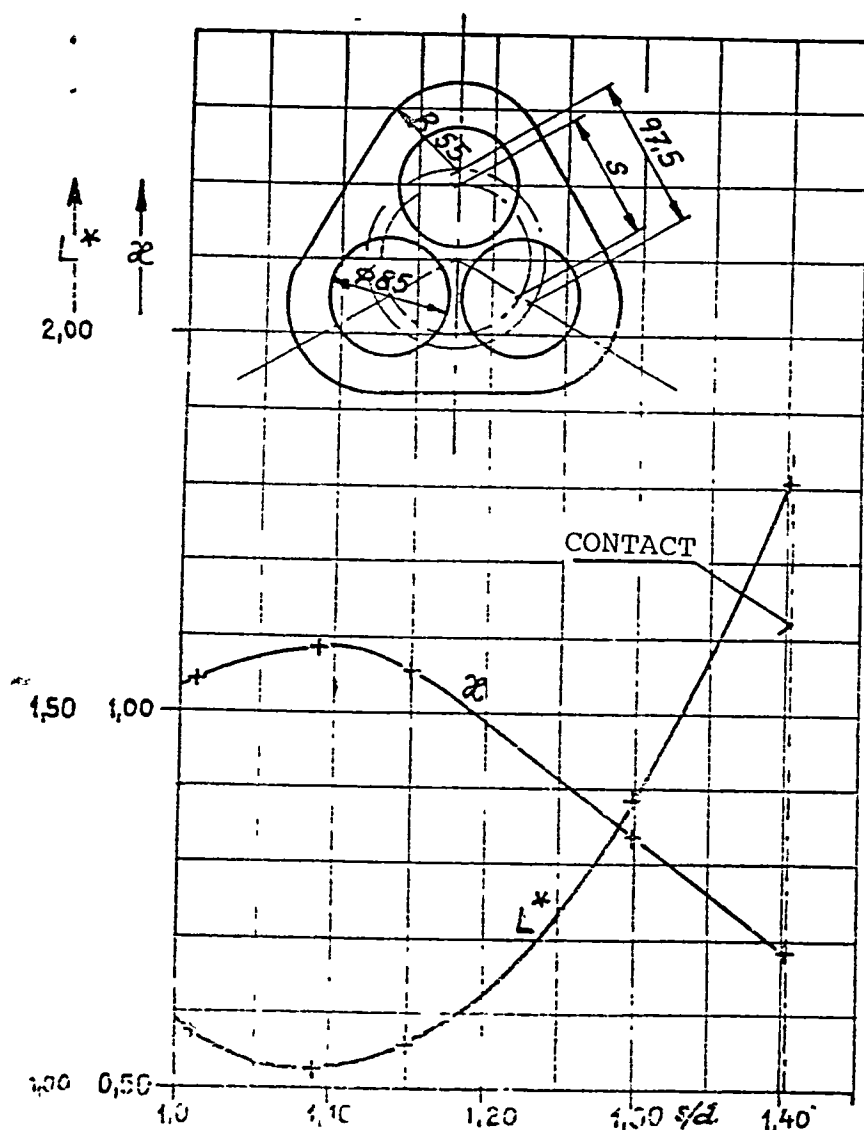
Fig. 54. Comparison of computed and experimental data of study [33].

$\dfrac{1}{\sqrt{\xi}}$

10

9

8

7

6

5

10^3 2 3 4 5 6 7 8 9 10^4

$Re\sqrt{\xi}$

s/d

▲   1,09

□   1,01

●   1,3

○   1,41

Fig. 55. Results of study [33] recomputed into form $1/\sqrt{\xi} = f(Re\sqrt{\xi})$.
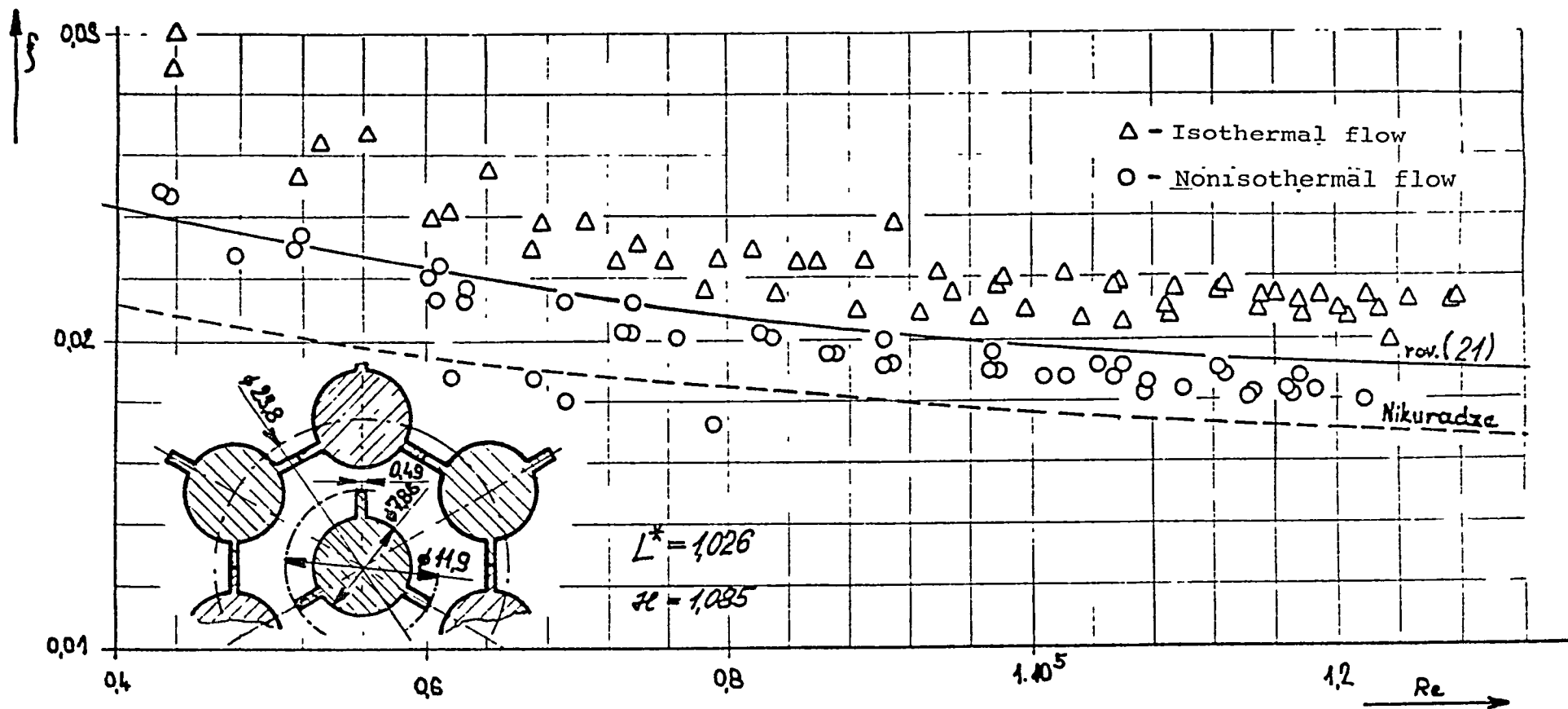
Fig. 56. Coefficient of friction losses in a sheaf of rods with longitudinal fins [37].
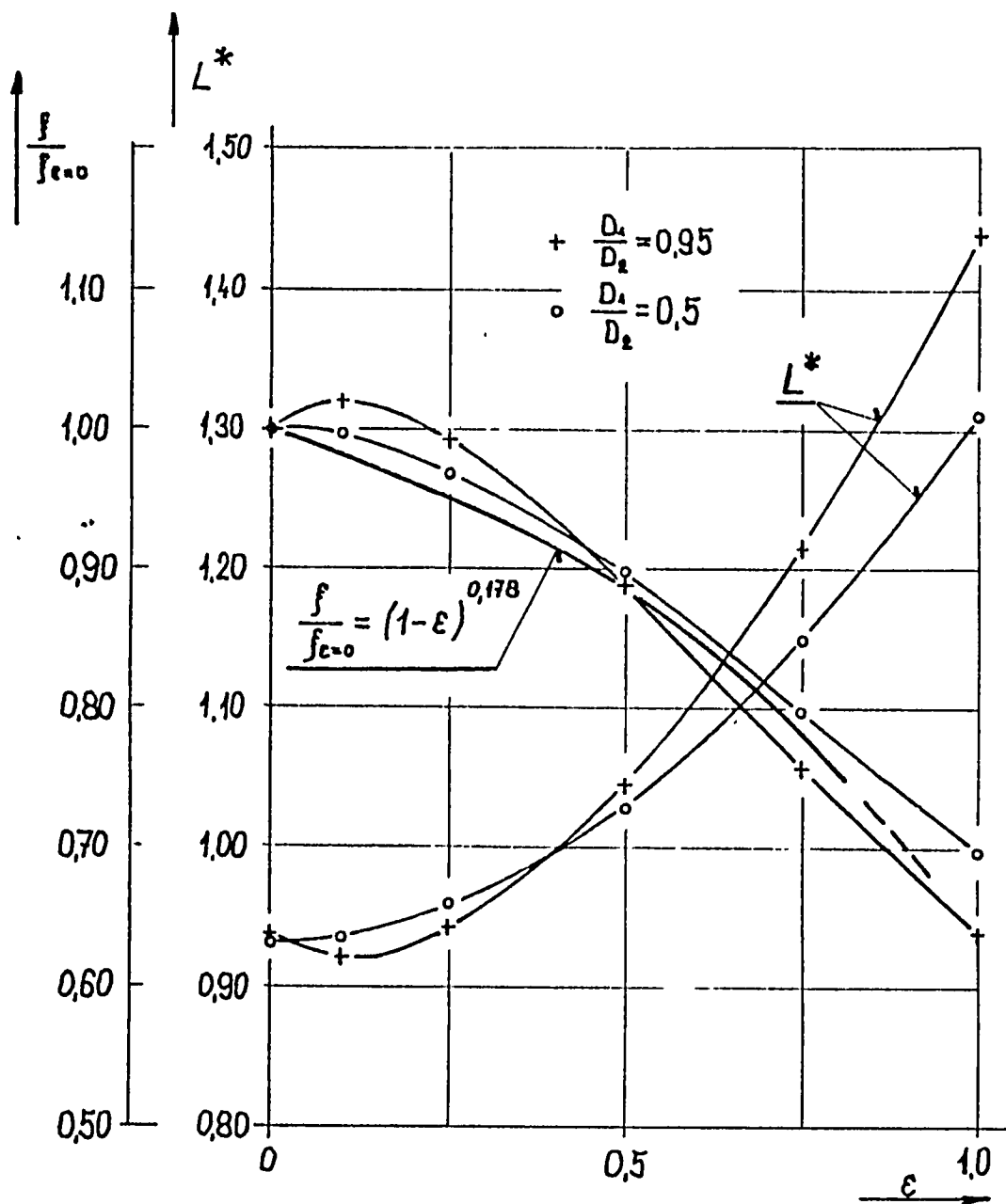
Fig. 57. Dependence of the coefficient of friction losses
on eccentricity of an annular channel. Comparison
of computations with the relation from study [34].
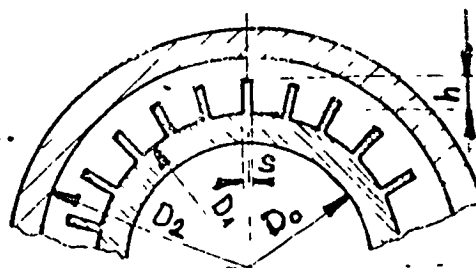
TABLE I.

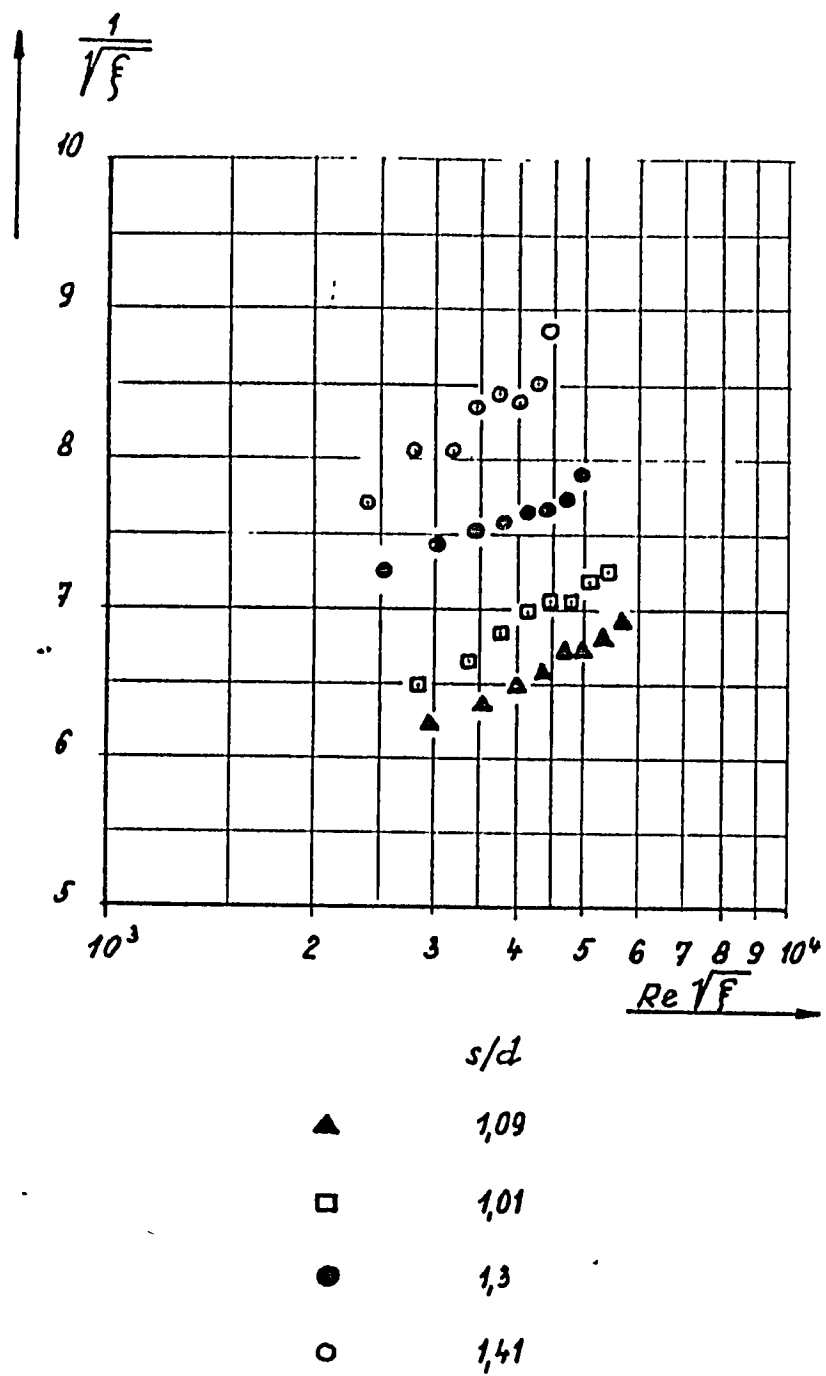| Variant # & symbol _oznočení_	No. of fins n	Main channel ∅ D_2	Outer dia of model D_1	Inner dia of model tube D_0	Height of fins h	Thickness of fins B
		mm	mm	mm	mm	m.m.
1 ▧	24	$81,0^{+}_{-}0,1$	$50,25^{+0,03}_{-0,09}$	$41,25^{+0,03}_{-0,03}$	$4,73^{+0,3}_{-0,25}$	$1,15^{+0,15}_{-0,3}$
2 ◩	"	— " —	— " —	— " —	$3,02^{+0,1}_{-0,02}$	— " —
3 ◪	"	— " —	— " —	— " —	$1,52^{+0,08}_{-0,2}$	— " —
4 +	36	— " —	$50,70^{+0,08}_{-0,03}$	$41,80^{+0,17}_{-0,25}$	$5,24^{+0,16}_{-0,14}$	$1,29^{+0,11}_{-0,09}$
5 ×	"	— " —	— " —	— " —	$2,91^{+0,25}_{-0,25}$	— " —
6 ○	"	— " —	— " —	— " —	$1,57^{+0,03}_{-0,07}$	— " —
7 □	60	— " —	$50,85^{+0,1}_{-0,05}$	$41,95^{+0,05}_{-0,1}$	$5,34^{+0,2}_{-0,2}$	$1,34^{+0,15}_{-0,15}$
8 ◇	"	— " —	— " —	— " —	$2,94^{+0,15}_{-0,15}$	— " —
9 △	"	— " —	— " —	— " —	$1,45^{+0,1}_{-0,15}$	— " —
10 ▲	24	$70,3^{+}_{-}0,04$	$50,25^{+0,03}_{-0,09}$	$41,25^{+0,03}_{-0,03}$	$4,73^{+0,3}_{-0,25}$	$1,15^{+0,15}_{-0,3}$
11 ▲	"	— " —	— " —	— " —	$3,02^{+0,1}_{-0,02}$	— " —
12 ▲	"	— " —	— " —	— " —	$1,52^{+0,08}_{-0,02}$	— " —
13 Y	36	— " —	$50,70^{+0,08}_{-0,03}$	$41,80^{+0,17}_{-0,25}$	$5,24^{+0,16}_{-0,14}$	$1,29^{+0,11}_{-0,09}$
14 ⅄	"	— " —	— " —	— " —	$2,91^{+0,25}_{-0,25}$	— " —
15 ●	"	— " —	— " —	— " —	$1,57^{+0,03}_{-0,07}$	— " —

GEOMETRICAL CHARACTERISTICS OF MODELS A.

TABLE II.

Variant number	Flow-thru surface $F \cdot 10^3$ m^2	Wetted circuit $S \cdot 10$ m	Heated circuit $S_T \cdot 10$ m	$d_h \cdot 10^2$ m	L^*	$\frac{d_h}{d_T}$
1	3,037	6,334	3,849	1,900	1,136	1,205
2	3,084	5,577	3,028	2,214	1,120	1,195
3	3,126	4,853	2,309	2,576	1,056	1,116
4	2,887	7,908	5,363	1,460	1,281	1,286
5	2,995	6,236	3,692	1,921	1,233	1,215
6	3,057	5,265	2,721	2,323	1,136	1,192
7	2,691	10,549	8,004	1,020	1,646	1,438
8	2,884	7,671	5,127	1,504	1,478	1,436
9	3,005	5,792	3,338	2,043	1,249	1,304
10	1,767	6,058	3,849	1,16"	1,047	1,091
11	1,815	5,236	3,028	1,386	1,076	1,141"
12	1,856	4,517	2,309	1,643	1,049	1,118
13	1,617	7,572	5,363	0,854	1,098	1,119
14	1,725	5,900	3,692	1,169	1,160	1,210
15	1,788	4,929	2,721	1,450	1,111	1,179
16	1,421	10,212	8,004	0,557	1,309	1,243
17	1,614	7,335	5,127	0,880	1,386	1,347
18	1,735	5,546	3,338	1,251	1,240	1,285
19	1,103	5,860	3,849	0,758	1,012	0,992

GEOMETRICAL CHARACTERISTICS OF MODELS B.

(1) Číslo variant α schéma	(2) Počet žeber n	(3) Vnější průměr D	(4) Vnitřní průměr d	(5) Výška žeber h	(6) Tloušťka žeber s	(7) Průtočná plocha $y \cdot 10^2$ m^2	(8) Omočený obvod $y \cdot 10$	$d_h \cdot 10^2$ m	L^*	(9) Poznámka
1 ▢	44	38,16 +0,04 −0,03	48,14 +0,08 −0,14	1,48 +0,05 −0,06	1,26 +0,03 −0,06	1,0615	2,499	1,6999	2,0196	
2 ▣	44	38,24 +0,03 −0,04	48,14 +0,08 −0,14	2,82 +0,06 −0,05	1,25 −0,14	0,9916	3,6045	1,0712	2,7945	
3	44	38,00	48,00	5,00	2,20					mají (10) vyčteny
4 ▱	77	38,24 +0,03 −0,05	48,14 +0,08 −0,14	1,47 +0,04 −0,05	1,20 +0,06 −0,03	1,0165	1,9961	2,1973	1,6226	
5 ◿	77	38,24 +0,08 −0,07	48,14 +0,08 −0,14	2,74 +0,06 −0,04	1,21 +0,05 −0,05	1,0592	2,6825	1,5794	2,0215	−(10)
6	77	38,00	48,00	5,00	1,20					mají vyčteny
7 ⊠	16	38,22 +0,05 −0,03	48,14 +0,08 −0,14	1,34 +0,06 −0,06	1,30 +0,05 −0,05	1,1165	1,6834	2,6530	1,3037	
8 ▷	15	38,26 +0,02 −0,03	48,14 +0,08 −0,08	2,75 +0,15 −0,15	1,23 +0,02 −0,06	1,0975	2,0168	2,1852	1,5956	
9 ▶	15	38,09 +0,03 −0,14	48,14 +0,08 −0,14	4,65 +0,15 −0,22	1,10 +0,05 −0,05	1,0474	2,0706	1,4595	1,8930	
10 ●	57	38,92 +0,12 −0,15	58,86 +0,22 −0,18	1,21 +0,11 −0,11	1,35 +0,05 −0,06	1,7865	2,9103	2,4564	1,8863	
11 ◆	57	49,62 +0,17 −0,19		2,92 +0,13 −0,07	1,32 +0,07 −0,07	1,6676	4,8699	1,3766	2,9726	
12 ✳	57	48,99 +0,12 −0,17		4,40 +0,15 −0,20	1,25 +0,06 −0,06	1,5715	6,5552	0,9589	3,6915	
13 ◇	34	48,62 +0,03 −0,07		1,52 +0,06 −0,07	1,19 +0,04 −0,04	1,8296	2,5736	2,0377	1,6472	
14 ◆	34	48,44 +0,03 −0,03		2,74 +0,06 −0,14	1,04 +0,11 −0,09	1,7766	3,1976	2,0916	2,0677	
15 ◆	34	48,67 +0,05 −0,08		4,51 +0,17 −0,21	1,44 +0,08 −0,05	1,7010	4,5961	1,4564	2,4993	
16 ⊗	23	48,26 +0,03 −0,08		1,45 +0,05 −0,06	1,09 +0,04 −0,04	1,8455	2,2046	3,3482	1,4108	
17 ◈	23	49,10 +0,03 −0,07		2,71 +0,04 −0,07	1,11 +0,07 −0,04	1,8243	2,7491	2,6163	1,7694	
18 ⊕	23	48,95 +0,04 −0,04		3,54 +0,16 −0,14	0,98 +0,07 −0,03	1,8021	3,1662	2,7767	1,8593	
19 ⊡	70	60,06 +0,12 −0,15	69,77 +0,13 −0,27	1,24 +0,09 −0,11	1,19 +0,11 −0,09	2,7291	3,6220	3,0146	1,9156	
20 ▣	70	60,44 +0,06 −0,42		2,71 +0,07 −0,13	1,17 +0,07 −0,07	2,6362	5,974	1,7611	2,9316	
21	70	60,00	70,00	5,00	1,20					mají vyčteny (10), tvar laboru je −(11)
22 ◕	42	60,23 +0,05 −0,16	69,97 +0,13 −0,27	1,54 +0,06 −0,07	1,25	2,7684	3,1841	3,4770	1,6654	
23 ▽	42	60,02 +0,04 −0,02		2,94 +0,06 −0,06	1,15	2,6476	4,3507	2,4664	2,1838	as sporeoble by
24 ▣	42	60,07 +0,03 −0,14		4,67 +0,11 −0,16	1,21 +0,04 −0,12	2,5593	5,8077	1,7063	2,6818	
25 ◑	28	60,00 +0,06 −0,06		1,43 +0,02 −0,03	1,12 +0,03 −0,07	2,7045	2,6364	4,14611	1,4063	
26 ▽	28	60,12 +0,06 −0,06		2,85 +0,06 −0,10	1,11 +0,09 −0,08	2,7502	3,4448	3,1568	1,7567	
27 ◐	28	59,91 +0,02 −0,03		4,11 +0,04 −0,11	1,12 +0,08 −0,07	2,6961	4,1838	2,5719	2,0624	

Key: (1) Variant #, & symbol; (2) Number of fins; (3) Inner diameter; (4) Outer diameter; (5) Height of fins; (6) Tickness of fins; (7) Flow-through area; (8) Wetted circuit; (9) Remark; (10) Not investigated; (11) Shape of fins considerably irregular.

Designation	D_2 [mm]	D_1 [mm]	$d_h \cdot 10^2$ [m]	$\frac{D_1}{D_2}$
M1	80,98	50,65	3,033	0,625
M2	80,98	60,55	2,043	0,748
M3	70,3	50,65	1,965	0,72
M4	70,3	60,55	0,975	0,861
M5	63,99	50,65	1,334	0,792
M6	63,99	60,55	0,344	0,946

Geometrical Characteristics of Models from study [3].

SMOOTH ANNULAR CHANNELS

D_2	D_1	D_2/D_1	Length of model	d_h	L^*	Type of cooling	d_h/d_T
mm	mm		m	mm			.
38	16	2,376	2,0	22	0,932	cooled core	0,882
38	25	1,52	2,0	13	0,932	--"--	0,967
38	32	1,188	2,0	6	0,935	--"--	0,943
38	16	2,376	2,0	22	0,932	bilateral cooling	$\frac{dh}{d_{T1}}=0,882$ $\frac{dh}{d_{T2}}=1,06$
38	16	2,376	2,0	22	0,932	cooled sleeve	1,06

ANNULAR CHANNELS WITH A LONGITUDINALLY FINNED CORE (GEOMETRY A)

n	D_2	D_1	h	s	Length of model	d_h	L^*	d_h/d_T
	mm	mm	mm	mm	m	mm		
12	45,8	16	6,22	1,26	1,996	15,75	1,108	1,186
12	45,8	25	5,73	1,05	1,998	12,05	1,008	1,035
12	38	16	6,22	1,26	1,996	10,52	1,036	1,074
12	38	25	5,73	1,05	1,998	6,81	1,074	0,976
12	32	16	6,22	1,26	1,996	6,79	1,019	0,967

End of Document